CALIFORNIA CURRENT INTEGRATED ECOSYSTEM ASSESSMENT (CCIEA) CALIFORNIA CURRENT ECOSYSTEM STATUS REPORT, 2019

A report of the NOAA CCIEA Team to the Pacific Fishery Management Council, March 7, 2019.

Editors: Dr. Chris Harvey (NWFSC), Dr. Toby Garfield (SWFSC), Mr. Greg Williams (PSMFC), and Dr. Nick Tolimieri (NWFSC)

1 INTRODUCTION

Section 1.4 of the 2013 Fishery Ecosystem Plan (FEP) established a reporting process wherein NOAA provides the Pacific Fishery Management Council (Council) with a yearly update on the status of the California Current Ecosystem (CCE), as derived from environmental, biological, economic and social indicators. NOAA's California Current Integrated Ecosystem Assessment (CCIEA) team is responsible for this report. This marks our 7th report, with prior reports in 2012 and 2014-2018.

This report summarizes CCE status based on data and analyses that generally run through 2018, with some projections for 2019 as well. Highlights are summarized in Box 1.1. Appendices provide additional information or clarification, as requested by the Council, the Scientific and Statistical Committee (SSC), or other advisory bodies.

Box 1.1: Highlights of this report

- **Climate, oceanographic and streamflow indicators were fairly near average in 2018, though indices suggest weakening circulation and emerging mild El Niño conditions**
- **Several ecological indicators in 2018 reflect average or improving conditions:**
  - The copepod community off Newport was predominately cool-water, lipid-rich species
  - Krill lengths off northern California have increased
  - Anchovy densities continued to increase
  - Several indicators of juvenile and adult salmon survival increased slightly, particularly for coho salmon in the northern part of the system
  - Sea lion pup numbers, sea lion pup growth, and piscivorous seabird densities were high
- **However, there was lingering evidence of unfavorable conditions in 2018:**
  - Warmer than average subsurface water in the southern portion of the system
  - Strong hypoxia on the shelf in the northern part of the system
  - Pyrosomes (warm-water tunicates) remained abundant in northern and central waters
  - Reports of whale entanglements in fixed fishing gear were high for the fifth straight year
- **West Coast fishery landings in 2017 increased by 27.4% over 2016; revenues increased by 12.3%. Increases were driven by Pacific hake, Dungeness crab and market squid**
- **Fishery diversification remains relatively low on average across all vessel classes**
  - We introduce estimates of shifting annual availability of groundfish to different ports
- **Forecasts for 2019 include:**
  - A 65% chance of a weak El Niño through at least the spring
  - Average coho returns to Oregon coast, below-average Chinook returns to the Columbia R.
  - Extensive hypoxia and acidified bottom waters over the shelf off Washington and Oregon

Throughout this report, most indicator plots follow the formats illustrated in Figure 1.1.

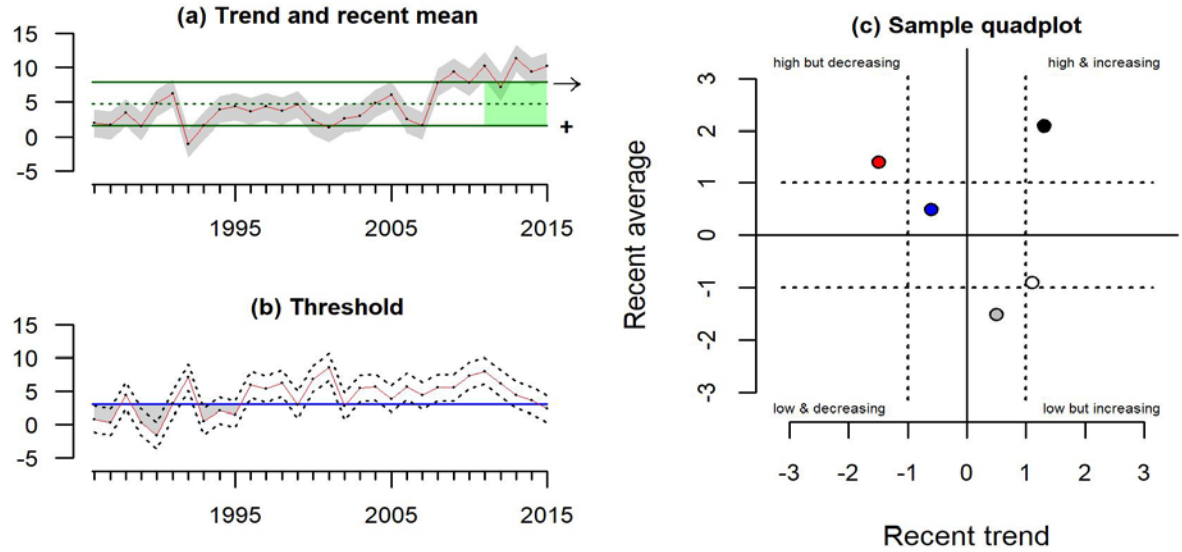

Figure 1.1 (a) Sample time-series plot, with indicator data relative to the mean (dashed line) and 1.0 s.d. (solid lines) of the full time series. Arrow at the right indicates if the trend over the evaluation period (shaded green) was positive, negative or neutral. Symbol at the lower right indicates if the recent mean was greater than, less than, or within 1.0 s.d. of the long-term mean. When possible, times series indicate observation error (grey envelope), defined for each plot (e.g., s.d, s.e., 95% confidence intervals). (b) Sample time-series plot with the indicator plotted relative to a threshold value (blue line). Dashed lines indicate upper and lower observation error, again defined for each plot. (c) Sample quadplot. Each point represents one normalized time series. The position of a point indicates if the times series was increasing or decreasing over the evaluation period and whether the mean recent years of the time series (recent trend) was above or below the long-term average (recent mean). Dashed lines represent 1.0 s.d. of the full time series.

2 SAMPLING LOCATIONS

Figure 2.1a shows the CCE and headlands that define key biogeographic boundaries. We generally consider areas north of Cape Mendocino to be the "Northern CCE," areas between Cape Mendocino and Point Conception the "Central CCE," and areas south of Point Conception the "Southern CCE." Figure 2.1a also shows sampling locations for most regional oceanographic data (Sections 3.2 and 3.3). Key transects are the Newport Line off Oregon, the Trinidad Line off northern California, and the CalCOFI grid further south. This sampling is complemented by basin-scale observations and models.

Freshwater ecoregions in the CCE are shown in Figure 2.1b, and are the basis by which we summarize indicators for snowpack, streamflow and stream temperature (Section 3.5).

Figure 2.1c indicates sampling locations for most biological indicators, including zooplankton (Section 4.1), forage species (Section 4.2), juvenile salmon (Section 4.3), California sea lions (Section 4.6) and seabirds (Section 4.7). The blue and green areas in Figure 2.1c also approximate the areal extent of the groundfish bottom trawl survey (Section 4.4), which covers trawlable habitat on the shelf and upper slope (55–1280 m depths). Indicators of highly migratory species (HMS, Section 4.5) are derived from data collected at scales far larger than pictured in Figure. 2.1c.

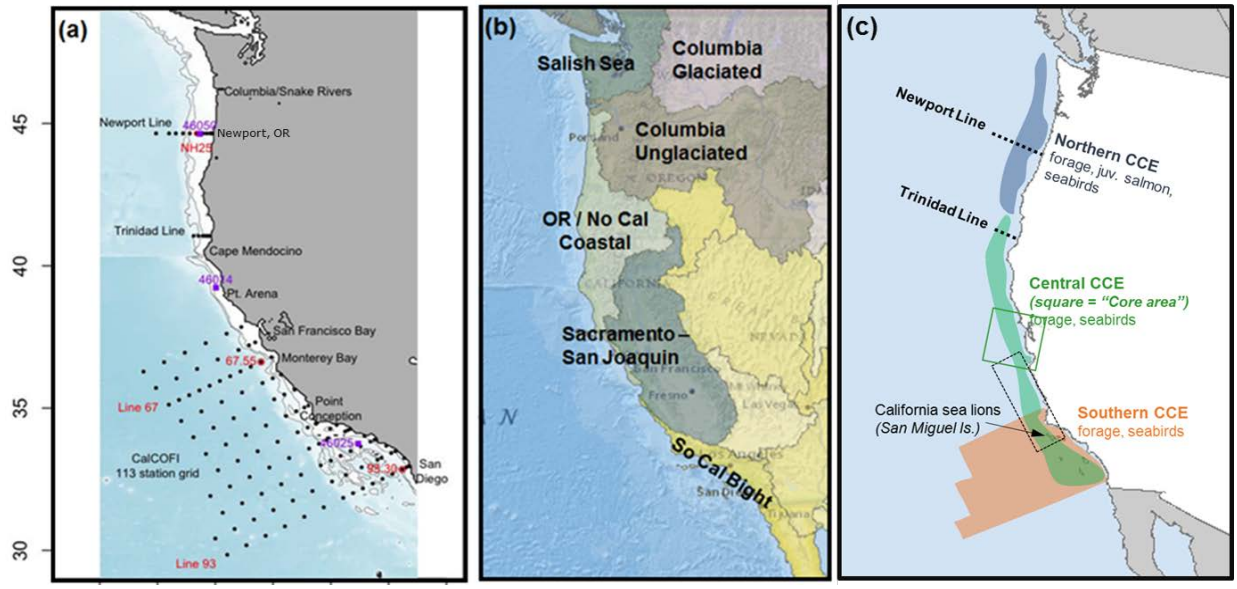

Figure 2.1 Map of the California Current Ecosystem (CCE) and sampling areas: (a) key geographic features and oceanographic sampling locations; (b) freshwater ecoregions, where snowpack and streamflow indicators are measured; and (c) biological sampling areas for zooplankton (Newport Line, Trinidad Line), pelagic forage, juvenile salmon, seabirds, and California sea lions. Solid box = core sampling area for forage in the Central CCE. Dotted box approximates foraging area for adult female California sea lions from the San Miguel colony.

3 Climate and Ocean Drivers

Climate and ocean indicators in the CCE in 2018 reveal a physical system that remains in transition following the historically unprecedented marine heat wave from 2014-2015 and the strong El Niño event in 2015-2016. The transition is visible in Figure 3.1, where ocean temperature anomalies appear milder over the last two years than the years preceding. In 2018, nearshore sampling stations in the northern and southern CCE began the year with temperature anomalies near the long-term mean. Temperature anomalies in the north (station NH25) were less than 0.5°C, and progressively cooled near the surface to neutral or small negative anomalies (~-0.5°C). The southern station (CalCOFI 93.30) had the opposite temperature progression, with temperatures in the upper 100 m increasing and reaching the largest warm anomalies for the year by October 2018. This temperature increase was attributed to an influx of warm offshore waters (Thompson et al. 2018). This reverses a pattern described in last year's report, when subsurface anomalies in late 2016-2017 were slightly positive in the north and cooler in the south.

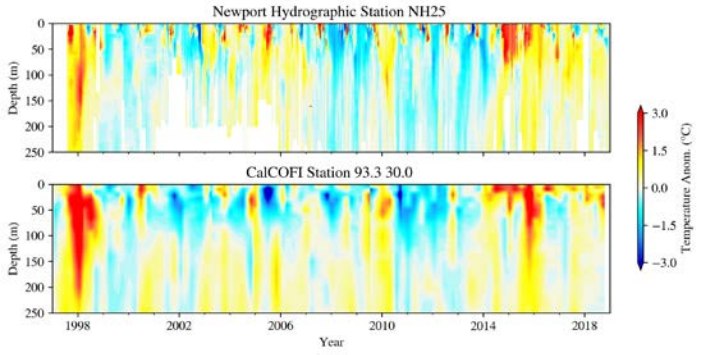

Figure 3.1 Time-depth temperature anomaly contours for nearshore stations NH25 (August 1998 to September 2018) and CalCOFI 93.30 (January 1998 to August 2018). For location of these stations see Fig. 2.1a. Extreme warm anomalies occurred throughout the water column during El Niño events in 1998 and 2016 and at the surface in the marine heat wave of 2014-2015. Off Newport, surface waters cooled in 2018, while water below 50 m remained above the long-term average. In the south, water throughout the water column remained above average..

3.1 Basin-Scale Indicators

To describe a wide range of large-scale physical ecosystem states, we report three independently varying indices. The Oceanic Niño Index (ONI) describes the equatorial El Niño Southern Oscillation (ENSO). A positive ONI indicates El Niño conditions, which usually mean lower primary productivity, weaker upwelling, poleward transport of equatorial waters and species, and more storms to the south in the CCE. A negative ONI means La Niña conditions, which usually lead to higher productivity. The Pacific Decadal Oscillation (PDO) describes Northeast Pacific sea surface temperature anomalies (SSTa) that may persist for many years. Positive PDOs are associated with warmer waters and lower productivity in the CCE, while negative PDOs indicate cooler waters and higher productivity. The North Pacific Gyre Oscillation (NPGO) is a signal of sea surface height, indicating changes in ocean circulation that affect source waters for the CCE. Positive NPGOs are associated with increased equatorward flow and higher surface salinities, nutrients, and chlorophyll-*a*. Negative NPGOs are associated with decreases in such values, less subarctic source water, and lower CCE productivity.

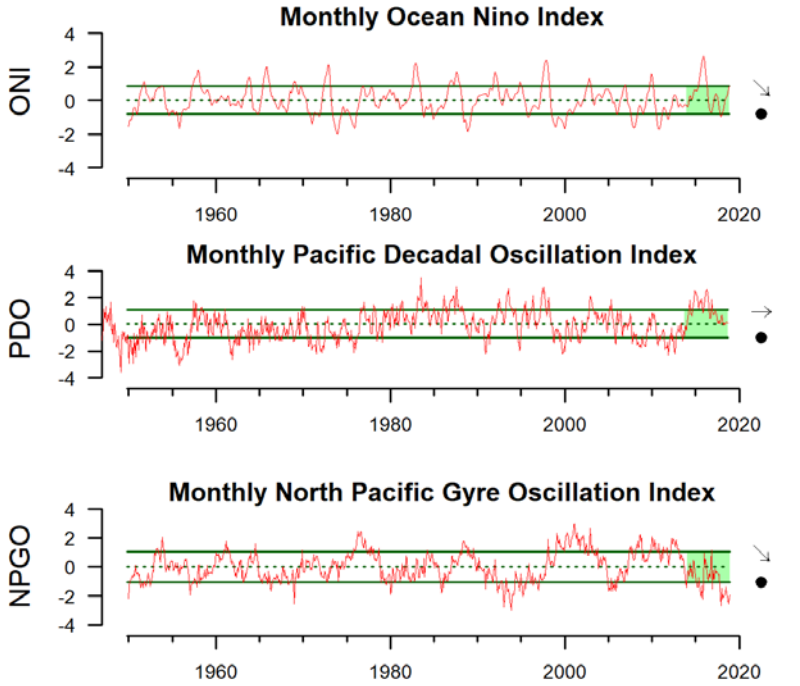

Figure 3.1.1 Monthly values of the Oceanic Niño Index (ONI), Pacific Decadal Oscillation (PDO), and the North Pacific Gyre Oscillation (NPGO) from 1950-2018. Lines, colors, and symbols are as in Fig.1.

In 2018, the ONI transitioned from the negative values of 2017 to neutral or weak El Niño conditions in the equatorial Pacific as of January 2019 (Figure 3.1.1, top). The Climate Prediction Center forecasts a ~65% chance for a weak El Niño to develop in spring 2019. The PDO has experienced a downward trend from high positive values over the last five years, reaching the long-term mean in 2018 (Figure 3.1.1, middle). This indicates that sea surface temperatures have steadily decreased from the extremes of the marine heat wave (Bond et al. 2015). However, the NPGO has declined to near historic lows over the last five years (Figure 3.1.1, bottom). This indicates an ongoing weak influx of nutrient-rich water from the North Pacific; the negative NPGO and a possible weak El Niño could represent a constraint on productivity in the CCE. Seasonal values for basin-scale indices are in Appendix D.1.

In 2018, large positive SSTa were mostly seen within the Southern California Bight during winter and summer (Figure 3.1.2, left). Average SSTa from 2014-2018 were positive for the majority of the eastern North Pacific, with means above 1 s.d. occurring over large areas including the Gulf of Alaska and the Southern California Bight (Figure 3.1.2, middle). These elevated 5-year mean SSTa are driven primarily by the 2014-2015 marine heat wave and the 2016 El Niño event (Jacox et al. 2016). SST cooled during 2017 and 2018; the widespread cooling trends (Figure 3.1.2, right) reflect the return to more average conditions after the extreme heating.

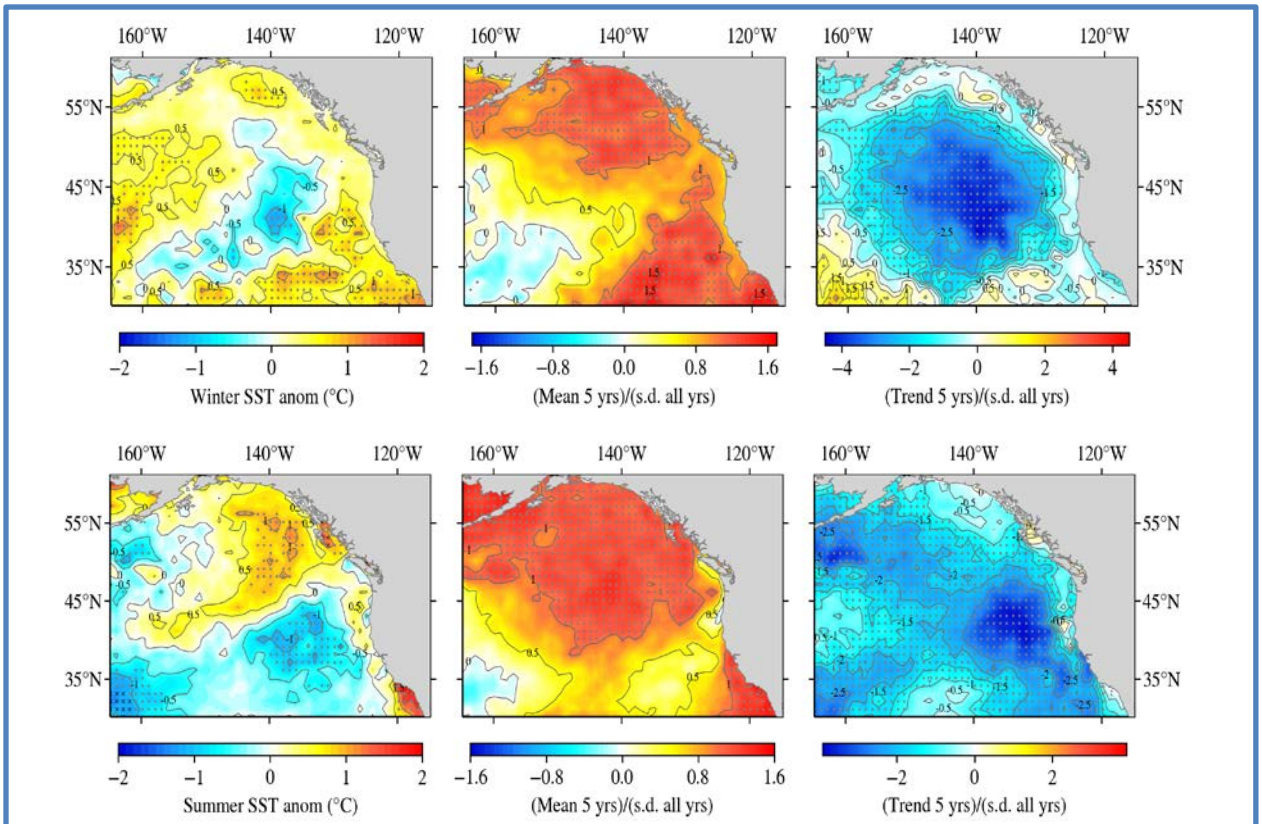

Figure 3.1.2 Left: Sea surface temperature (SST) anomalies in 2018, based on 1982-present satellite time series in winter (Jan-Mar; top) and summer (July-Sept; bottom); the 2018 summer warming of the Southern California Bight is evident. Center: Mean SST anomalies for 2014-2018. Right: trends in SST anomalies from 2014-2018, which are mostly negative because the marine heat wave of 2014-2015 and major El Niño of 2016 have subsided. Black circles mark cells where the anomaly was > 1 s.d. above the long-term mean. Black x's mark cells where the anomaly was the highest in the time series.

In late 2018, news media reported that, based on satellite imagery of SSTa, a marine heatwave similar to the "Blob" of 2014-2015 may be reforming in the northeast Pacific. Based on an analysis of SSTa from 1985-2016 (Leising, in prep), a marine heatwave has the potential to cause coastal impacts similar to those from the 2014-2015 event if the anomalous feature: (1) has SSTa >2 s.d. of the long-term SSTa time series at a particular location; (2) is greater than 500,000 km^2 in area; and (3) lasts for > 60 days. The feature in late 2018 (Figure 3.1.3) surpassed the area threshold, but did not surpass

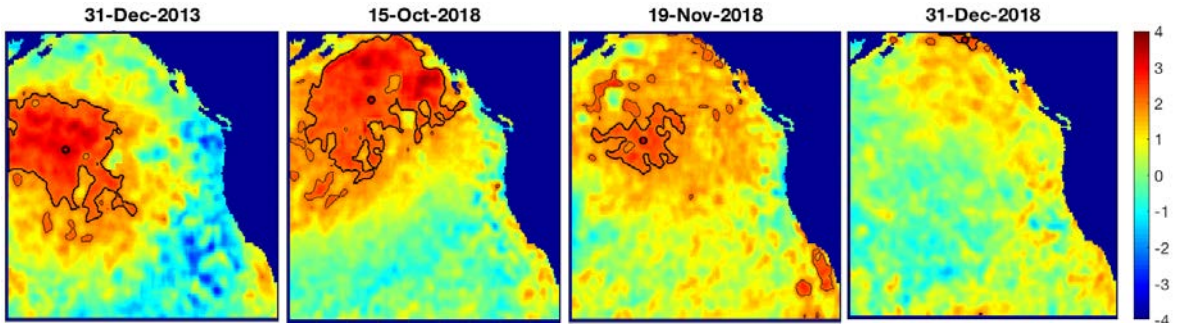

Figure 3.1.3 Standardized SSTa across the Pacific Northeast for the past three months of 2018, and December 2013. Dark contours denote regions that meet the criteria of a marine heat wave (see text and Appendix D.2). Multiple features can evolve at any time; e.g. the small feature outlined near the Southern California Bight in November 2018. The standardized SSTa is defined as SSTa divided by the standard deviation of SSTa at each location calculated over 1985-2016, thus taking into account spatial variance in the normal fluctuation of SSTa.

the duration threshold (see Appendix D.2). Moreover, it largely dissipated by December 2018 (unlike December 2013, prior to the 2014-2015 "Blob" event; Figure 3.1.3, left). The CCIEA team believes that a large-scale marine heatwave is not currently affecting the northeast Pacific or the CCE, although SSTa currently remains positive and conditions may change. Additional information on this analysis is in Appendix D.2.

3.2 Regional Climate Indicators

Upwelling, driven by variation in wind stress, is a physical process that moves cold, nutrient-rich water from deep in the ocean to the surface layer, which fuels the high seasonal primary production at the base of the CCE food web. The most common metric of upwelling is the Bakun Upwelling Index (UI), reported at a spatial scale of 1° latitude x 1° longitude. However, the Bakun UI does not take into consideration the underlying ocean structure (e.g. ocean stratification), which can have considerable influence on the volume and the nutrient content of the upwelled water. Jacox et al. (2018) developed new estimates of coastal upwelling using ocean models to improve upon the Bakun UI by estimating the vertical transport (Cumulative Upwelling Transport Index; CUTI) and nitrate flux (Biologically Effective Upwelling Transport Index; BEUTI).

The magnitude of vertical nitrate flux in the CCE varies greatly by latitude (Figure 3.2.1, left). The northern stations at 45°N (Newport, OR) and 39° (Point Arena, CA) undergo downwelling in the winter due to reversing winds. The nitrate flux at 39°N is much greater than at 33° (Southern California) and 45°N. The timing of peak upwelling varies by latitude, with northern latitudes having a later onset of maximum upwelling. This can be seen in the maximum climatological value of CUTI, which is at the end of April at 33°N, the middle of June at 39°N, and the end of July at 45°N (Figure 3.2.1;). During 2018, BEUTI and CUTI were generally average through most of the seasons, with strong periods of upwelling during the spring at 33° and 39°N. In general, CUTI and BEUTI show similar fluctuations in the north and less in the south. In the southern latitudes BEUTI is more influenced by subsurface nutrient concentration.

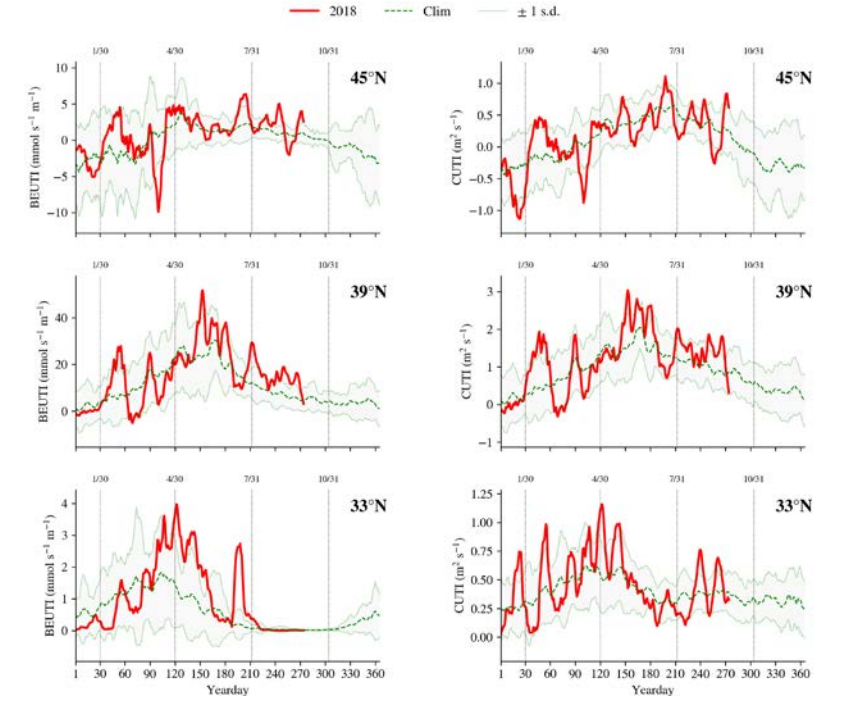

Figure 3.2.1 Daily 2018 values of Biologically Effective Upwelling Transport Index (BEUTI; left) and Coastal Upwelling Transport Index (CUTI; right) from Jan. 1–Sept. 1, relative to the 1988-2018 climatology average (green dashed line) ±1 s.d (shaded area), at latitudes 33°, 39°, and 45°N. Daily data are smoothed with a 10-day running mean. Vertical lines mark the end of January, April, July and October.

3.3 Hypoxia and Ocean Acidification

Dissolved oxygen (DO) is dependent on processes such as currents, upwelling, air-sea exchange, community-level production, and respiration. Low DO can compress habitat and cause stress or die-offs for sensitive species. Waters with DO levels <1.4 ml/L (2 mg/L) are considered hypoxic.

For the second consecutive year, low DO was a serious issue in the northern CCE. At station NH05 (5 km off of Newport, OR), water near bottom over the continental shelf was below the hypoxia threshold from June through September before its seasonal rebound in fall (Figure 3.3.1, top). Hypoxic DO levels were also observed during June further offshore at station NH25 (Figure 3.3.1, bottom). Seasonal trends for these stations and other stations off Southern California (where DO was well above the 1.4 ml/L threshold) are shown in Appendix D.3.

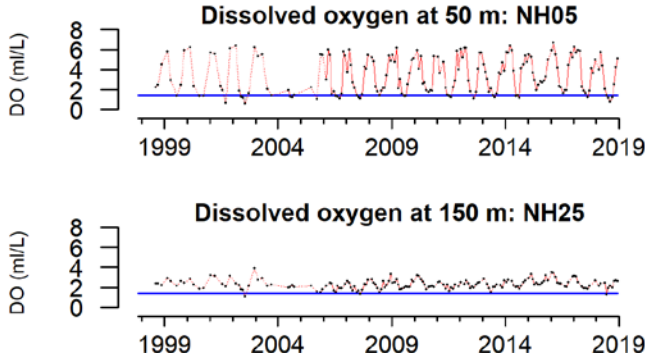

Figure 3.3.1 Dissolved oxygen at 50-m and 150-m depths off Oregon through 2018. Stations NH05 and NH25 are 5 and 25 km from shore, respectively. The blue line is the hypoxic threshold of 1.4 ml dissolved oxygen per liter. Dotted red line indicates missing data. Lines, colors, and symbols are as in Fig.1.

Ocean acidification (OA), caused by increased levels of atmospheric CO_2, lowers pH and carbonate in seawater. An indicator of OA is the saturation state of aragonite (a form of calcium carbonate). Aragonite saturation <1.0 indicates corrosive conditions that may be stressful to shell-forming organisms and other species. Upwelling transports hypoxic, acidified waters from offshore onto the continental shelf, where increased community-level metabolic activity can further exacerbate OA (Chan et al. 2008, Feely et al. 2008).

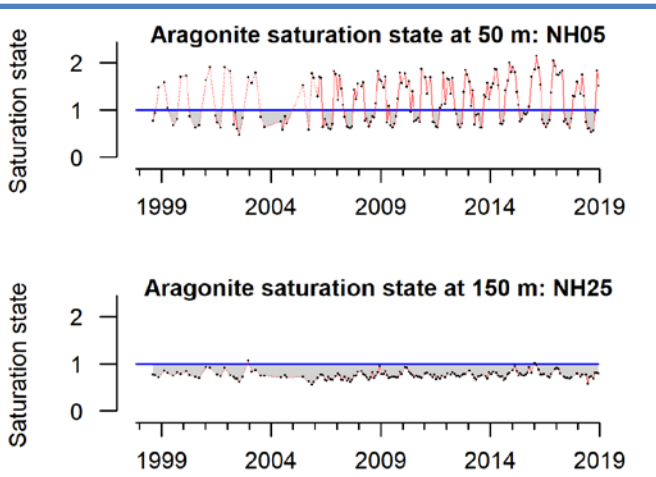

Figure 3.3.2 Monthly aragonite saturation values off Newport, Oregon, 1998-2018. The blue line indicates the threshold value of 1.0 for aragonite saturation state. Lines, colors, and symbols are as in Fig.1.

Aragonite saturation levels off Newport in 2018 had some of the lowest values over the last five years (Figure 3.3.2). At the nearshore station (NH05), aragonite levels at 50 m depth were saturated (>1.0) in winter and spring, then fell below 1.0 in the summer and fall, as is typical, although summer/fall values were lower than in the anomalous years of 2014-2016, implying greater extent of OA in 2018. At station NH25 at 150 m depth, aragonite saturation state followed the same seasonal cycle but across a narrower range; conditions at this site and depth were always corrosive (<1.0). Seasonal aragonite trends are in Appendix D.3.

3.4 Harmful Algal Blooms

In response to requests from various Council advisory bodies, this year we are introducing a new indicator of the occurrence of harmful algal blooms (HABs). Blooms of the diatom genus *Pseudo-nitzschia* can increase concentrations of the toxin domoic acid in coastal waters. Because domoic acid can cause amnesic shellfish poisoning in humans, shellfish fisheries (including the recreational razor clam and commercial Dungeness crab fisheries) are closed when concentrations exceed regulatory thresholds for human consumption. Razor clams provide an accurate record of the arrival and intensity of HAB events on beaches, and they can accumulate and retain domoic acid for up to a year following HABs of *Pseudo-nitzschia*. Extremely toxic HABs of *Pseudo-nitzschia* frequently coincide with warming events in the CCE (Appendix E).

Monthly maximum domoic acid concentrations in razor clams from six sites along the Washington coast from 1991 through 2018 are shown in Figure 3.4.1; site-specific trends are in Appendix E. Domoic acid levels at or exceeding 20 parts per million trigger closures of razor clam harvests; such events occurred most recently in 2015, 2016 and 2017, coincident with the anomalous warming events in the CCE. In 2018, the low levels of domoic acid detected in Washington razor clams and Dungeness crabs did not trigger fishery closures at any of the sites.

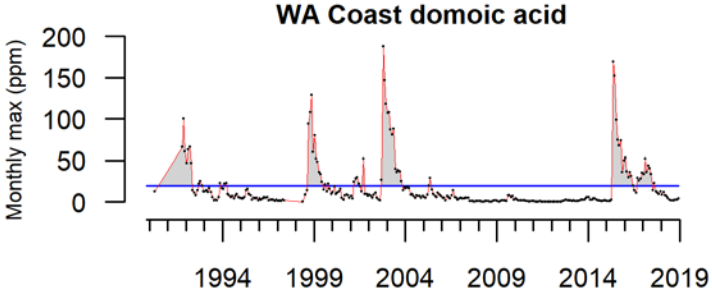

Figure 3.4.1 Monthly maximum domoic acid concentration (ppm) in razor clams through 2018 for the WA coast. The blue line is the managment threshhold of 20 ppm. Lines, colors, and symbols are as in Fig.1.

3.5 Hydrologic Indicators

Freshwater conditions are critical for salmon populations and estuaries that support many marine species. The indicators presented here include snowpack, streamflow and stream temperature, summarized by freshwater ecoregion (see Figure 2.1b) or by salmon evolutionarily significant units (ESUs, Waples 1995). Snow-water equivalent (SWE) is the water content in snowpack, which provides cool freshwater in the spring, summer and fall months. Maximum streamflow in winter and spring is important for habitat formation and removal of parasites, but extreme discharge relative to historic averages can scour salmon nests (redds). Minimum streamflow in summer and fall can restrict habitat for in-stream juveniles and migrating adults. High summer water temperatures can impair physiology and cause mortality to both juveniles and adults. All indicators are influenced by climate and weather patterns and will be affected as climate change intensifies.

In 2018, SWE anomalies were within 1 s.d. of long-term means, though the southerly ecoregions were relatively low (Figure 3.5.1). Even these ecoregions were well above the extremely low SWE

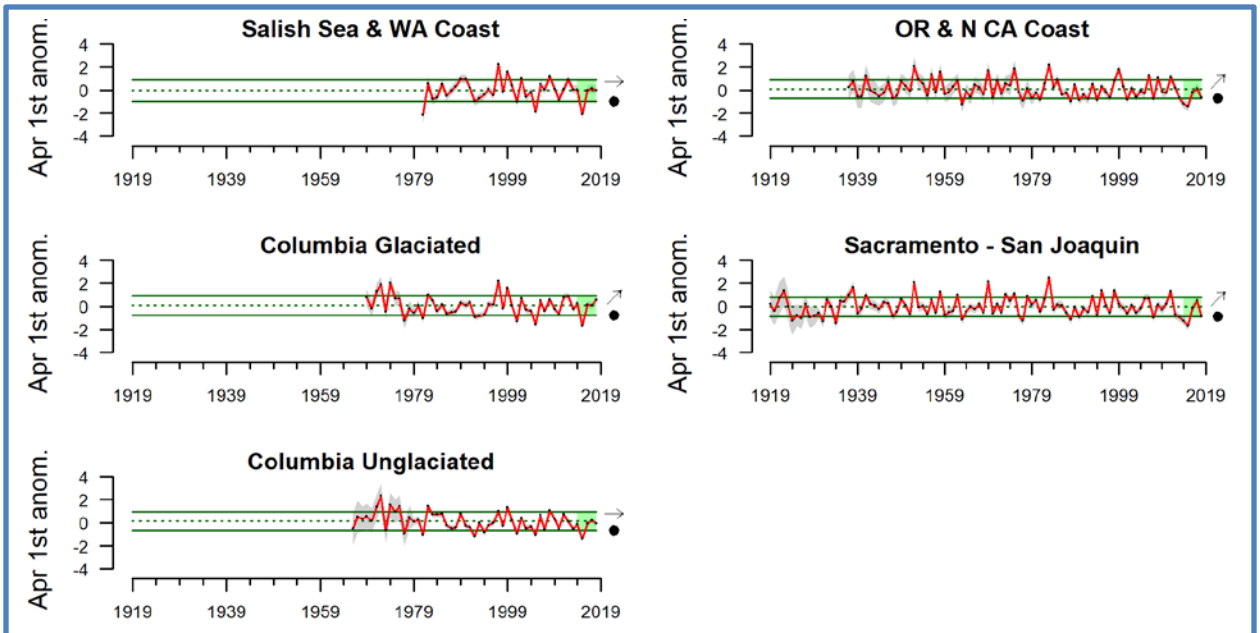

Figure 3.5.1 Anomalies of April 1st snow-water equivalent (SWE) in five freshwater ecoregions of the CCE through 2018. Lines, colors, and symbols are as in Fig.1. Ecoregions are mapped in Fig. 2.1.

measures of 2015. Corresponding to these precipitation patterns, minimum streamflows in 2018 were within 1 s.d. of long-term means in all ecoregions except the Southern California Bight, which was 1 s.d. below average (Appendix F). Maximum flows were at or above long-term means in the northerly ecoregions, but at or below average in the central and southerly ecoregions (Appendix F).

As of February 1st, SWE in 2019 is on pace to be below average in much of Washington, Oregon and Idaho, but above average in the Sierra Nevada range following high snow accumulation in January (Appendix F). Because SWE values do not typically peak until early spring, however, the peak measure of SWE for the year will not be until April 1, 2019.

We further summarized streamflows with quad plots that compile recent flow anomalies at the finer spatial scale of individual Chinook salmon ESUs. The error bars describe 95% credible intervals of flow, allowing us to determine which ESUs have significant short-term trends or recent averages that differ from long-term means. Maximum flow events were generally within range of long-term means, although the short-term trends of several ESUs were positive and some short term averages were greater than long-term means (Figure 3.5.2, left; Appendix F). The positive trends likely reflect short-term rebounds from the system-wide extremely low snowpack of 2015. Similarly, minimum flow anomalies had either positive or neutral short-term trends for all Chinook salmon ESUs that we evaluated (Figure 3.5.2, right). Recent averages of minimum flows were generally similar to long-term averages, except for below-average minimum flows for the Washington Coast ESU.

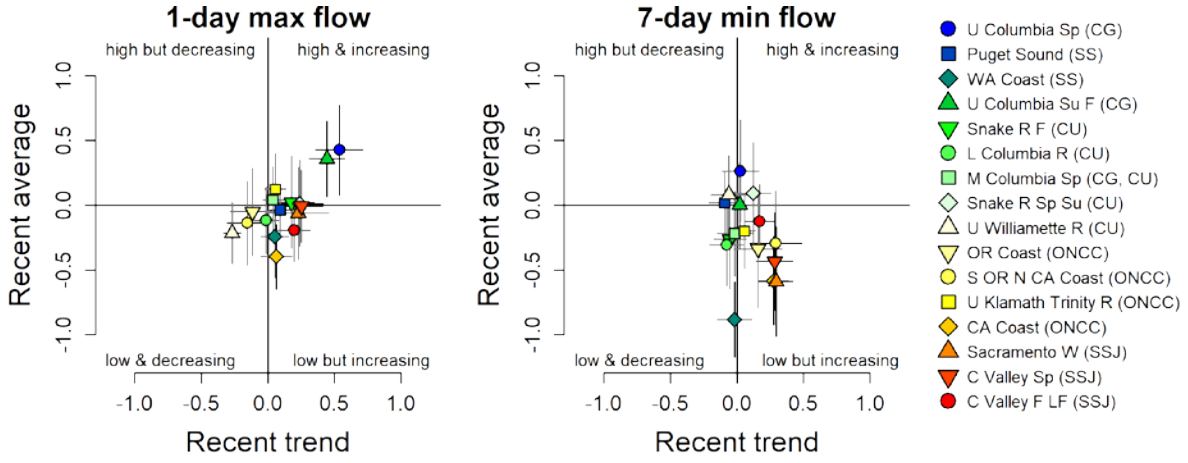

Figure 3.5.2 Recent (5-year) trend and average of maximum and minimum flow anomalies in 16 freshwater Chinook salmon ESUs through 2018. Symbols of ESUs are color-coded from north (blue) to south (red). Error bars represent the 2.5% and 97.5% upper and lower credible intervals. Grey error bars overlap zero, while heavy black error bars differ from zero. Abbreviations in the legend refer to the ESU's freshwater ecoregion shown in Fig. 2.1b (CG = Columbia Glaciated; SS = Salish Sea; CU = Columbia Unglaciated; ONCC = OR/No Cal Coastal; SSJ = Sacramento/San Joaquin).

Maximum August stream temperatures, which are summarized by ecoregion in Appendix F, have been above average recently in the Salish Sea and Washington Coast ecoregion, and have experienced short-term declines along the Oregon Coast and in California following peaks in 2014-2016.

4 Focal Components of Ecological Integrity

The CCIEA team examines many indicators related to the abundance and condition of key species and the dynamics of ecological interactions and community structure. Many CCE species and processes respond very quickly to changes in ocean and climate drivers, while other responses may not manifest for many years. These dynamics are challenging to predict. From 2014 to 2016, the marine heatwave and major El Niño event resulted in generally poor productivity at lower trophic levels and poor foraging conditions for many predators. In 2017-2018, the physical and ecological influence of

these anomalous warm events lingered, although some ecological integrity indicators suggested a return toward average conditions, particularly in the southern CCE.

4.1 Copepod Biomass Anomalies and Krill Size

Copepod biomass anomalies represent inter-annual variation for two groups of copepod taxa: northern copepods, which are cold-water species rich in wax esters and fatty acids that appear to be essential for pelagic fishes; and southern copepods, which are warm-water species that are smaller and have lower fat content and nutritional quality. In summer, northern copepods usually dominate the coastal zooplankton community observed along the Newport Line (Figure 2.1a,c), while southern copepods dominate in winter. El Niño events and positive PDO regimes can promote higher biomass of southern copepods (Keister et al. 2011, Fisher et al. 2015). Positive values of northern copepods in summer are correlated with stronger returns of Chinook salmon to Bonneville Dam, and values >0.2 are associated with better survival of coho salmon (Peterson et al. 2014).

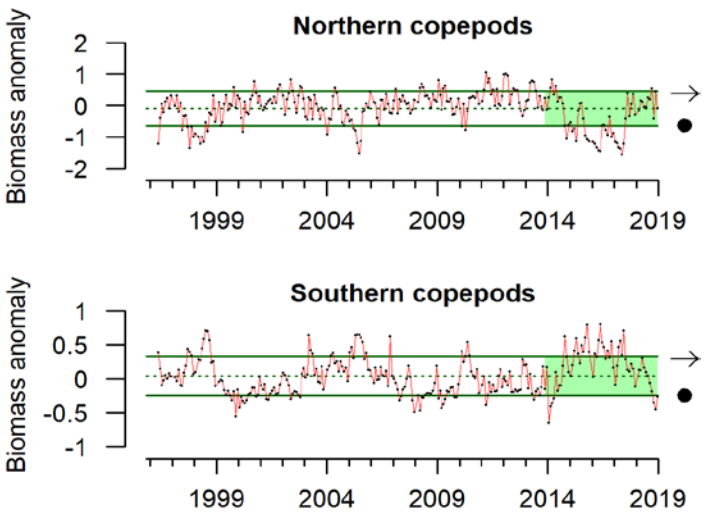

Figure 4.1.1 Monthly northern and southern copepod biomass anomalies from 1996-2018. Lines, colors, and symbols are as in Fig.1.

From the onset of the anomalous warm period in fall 2014 until mid 2017, copepod anomaly trends strongly favored southern copepods. However, in July 2017 the northern copepod anomaly shifted from negative to neutral, and has oscillated around neutral values ever since, while the southern copepod anomaly declined from positive to neutral values in 2017 and negative values by the end of 2018 (Figure 4.1.1). These changes seem to signal improving foraging conditions for pelagic fishes in this region of the CCE, relative to the anomalous period of 2014-2016.

We added an additional indicator of lower trophic level productivity—the length of krill sampled on the Trinidad transect off northern California (41°N; Figure 2.1a,c). Zooplankton data at Trinidad indicated a shift in 2017-2018 toward species assemblages and conditions last observed prior to the 2014-2016 anomalies. One indicator of this is mean lengths of the cool-water krill *Euphausia pacifica*, an important prey item. Krill lengths were >1 s.d. below average for much of 2014-2016, but increased in the 2017 upwelling season and remained near or above the time series mean throughout much of 2017 and 2018 (Figure 4.1.2). Krill size naturally decreases in winter, but wintertime lengths in 2017 and 2018 were typical of pre-heat wave conditions. As with copepod community composition off Newport, these results imply more productive conditions for predators of zooplankton over the last two years.

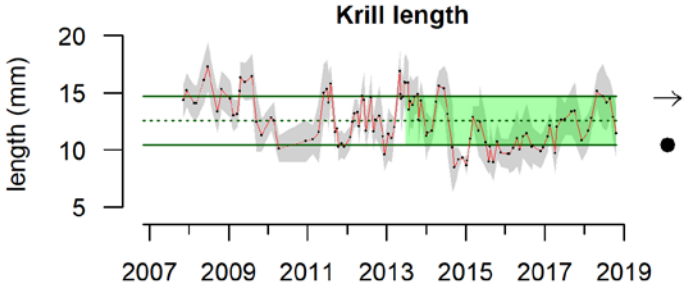

Figure 4.1.2 Mean krill length from 1996-2018. Grey envelope indicates ±1.0 s.d. Lines, colors, and symbols are as in Fig.1.

4.2 Regional Forage Availability

The CCE forage community is a diverse portfolio of species and life history stages, varying in behavior, energy content, and availability to predators. The species summarized here represent a substantial portion of the available forage in the CCE. *We consider these regional indices of relative forage availability and variability, not indices of abundance of coastal pelagic species (CPS).*

The regional surveys that produce CCE forage data use different methods (e.g., gear, timing, survey design), which makes comparisons across regions difficult. The CCIEA team has adopted new methods to identify and compare regional shifts in forage community composition. The new plots are shown here, with related time series plots in Appendix G. Clusters of co-occuring species are grouped on the y-axis and their regional abundances are indicated by color (red = abundant, blue = rare); significant temporal shifts in a region's forage community composition are marked by vertical lines.

Northern CCE: The northern CCE survey off Washington and Oregon (Figure 2.1c) targets juvenile salmon in surface waters, but also effectively catches surface-oriented juvenile groundfish and squid. Since the major shift in the forage assemblage between 2013 and 2014, the assemblage has been variable, with minor shifts in each of the past 3 years (Figure 4.2.1). Market squid have been consistently present since 2014, while pelagic juvenile groundfish and salmon have been present intermittently. This departs from the 2006-2013 assemblage that was characterized by abundant salmon and very few market squid.

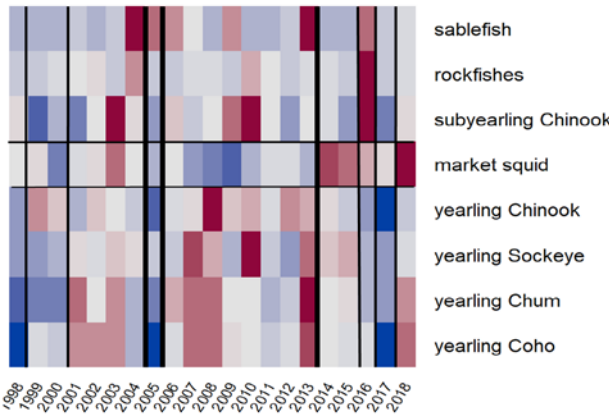

Figure 4.2.1 Cluster analysis of key forage species in the northern CCE through 2018. Horizontal lines indicate clusters of typically co-occurring species. Vertical lines indicate temporal shifts in community structure. Colors indicate relative abundance (red = abundant, blue = rare).

Central CCE: Data presented here are from the "Core area" of a survey (Figure 2.1c) that targets young-of-the-year (YOY) rockfishes, but also effectively samples pelagic fish and squid. This forage community last underwent a major shift before 2010, driven by the steep decline of adult sardines (Figure 4.2.2; see also Appendix G.2). A minor shift occurred between 2012 and 2013, as YOY rockfishes, YOY sanddabs, market squid, and many mesopelagic schooling fishes greatly increased and remained high through 2018. Other forage groups have occasionally been abundant during the 2013-2018 phase, including juvenile sardine, juvenile anchovy and adult anchovy in 2018.

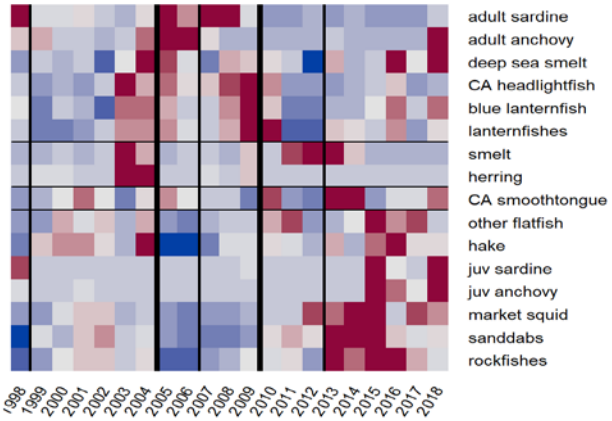

Figure 4.2.2 Cluster analysis of key forage species in the central CCE through 2018. Horizontal lines indicate clusters of typically co-occurring species. Vertical lines indicate temporal shifts in community structure. Colors indicate relative abundance (red = abundant, blue = rare).

Southern CCE: Forage data for the Southern CCE (Figure 2.1c) come from CalCOFI larval fish surveys. Larval biomass of forage species is assumed to correlate with regional abundance of adult forage species. The southern forage assemblage is the most variable over time, with 9 substantial breaks from 1998-

2018. The last major change was between 2011 and 2012, when sardine became very rare and larval rockfishes, flatfishes, squid and certain mesopelagic species became abundant (Figure 4.2.3; see also Appendix G.3). The assemblage was dynamic from 2014-2018, with spikes in mackerels in some years, squid and groundfishes in some years, and the recent increase in larval anchovy.

Many of these forage surveys have captured high numbers of pyrosomes, a type of warm-water gelatinous tunicate, ever since the anomalous warm years (Brodeur et al. 2018). Preliminary information from 2018 (data not shown) indicates that pyrosomes remained abundant in central and northern waters of the CCE, particularly earlier in the spring and summer, although densities in many areas appeared to be lower than in 2017.

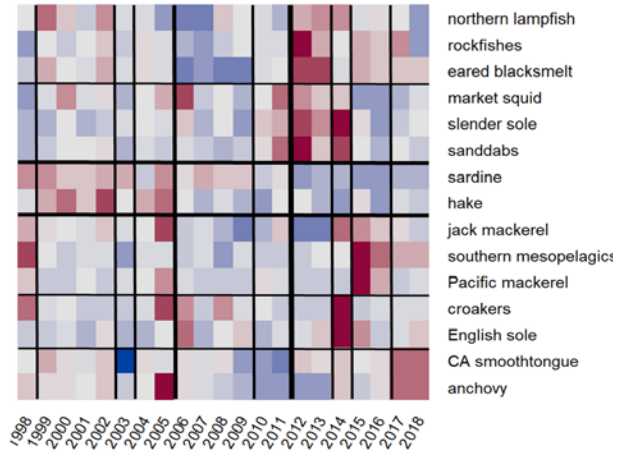

Figure 4.2.3 Cluster analysis of key forage species in the southern CCE through 2018. Horizontal lines indicate clusters of typically co-occurring species. Vertical lines indicate temporal shifts in community structure. Colors indicate relative abundance (red = abundant, blue = rare).

4.3 SALMON

For indicators of the abundance of adult Chinook salmon, we examine trends in natural spawning escapement from different populations to compare status and coherency in production dynamics across their range. We summarize escapement trends in quad plots; time series are shown in Appendix H. For juvenile salmon, we include time series of juvenile coho and Chinook salmon catches from surveys in the Northern CCE (Figure 2.1c).

Most Chinook salmon escapement data are updated through 2017. Generally, escapements of California Chinook salmon ESUs over the last decade of available data were within 1 s.d. of long-term averages (Figure 4.3.1), although 2017 escapements were among the lowest on record in several ESUs (Appendix H.1). California Chinook salmon stocks had neutral trends over the last decade, and annual variation was generally high (Appendix H.1). In Washington, Oregon and Idaho, most escapements were within 1 s.d. of average for the past decade; the exception was Snake River Fall Chinook after a series of large escapements since 2009 (Appendix H.2). Escapements in 2017 ranged from relatively high (Willamette Spring) to relatively low (Upper Columbia Spring, Lower Columbia; Appendix H.2). Escapement trends for northern stocks were mostly neutral, but Willamette Spring and Snake River Fall Chinook had significantly positive trends over the most recent decade of data.

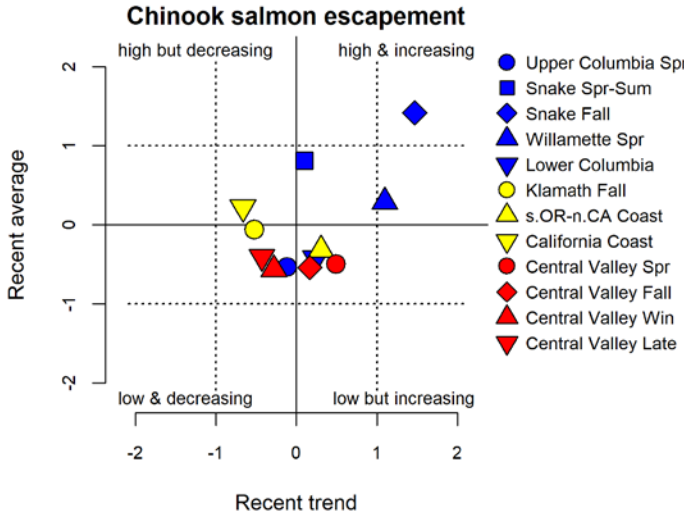

Figure 4.3.1 Recent (10-year) trend and average of Chinook salmon escapement through 2017. Recent trend indicates the escapement trend from 2007-2017. Recent average is mean natural escapement (includes hatchery strays) from 2007-2017. Lines, colors, and symbols are as in Fig.1.

Catches of juvenile Chinook and coho salmon in June off the coasts of Washington and Oregon can serve as indicators of survival during their first few weeks at sea, and are correlated to later years' returns of adults to Bonneville Dam. Catches of subyearling Chinook and yearling Chinook salmon were close to long-term averages in 2018, one year removed from near-historic lows; catches of yearling coho in 2018 were among the highest observed (Figure 4.3.2). These data suggest that the direct negative impacts of the marine heatwave on salmon survival have subsided. However, other aspects of the ecosystem have not completely returned to normal, suggesting that indirect impacts on survival may still occur. The recent catch trend for yearling Chinook in this region remains negative, while trends for subyearling Chinook and yearling coho salmon are neutral and more variable.

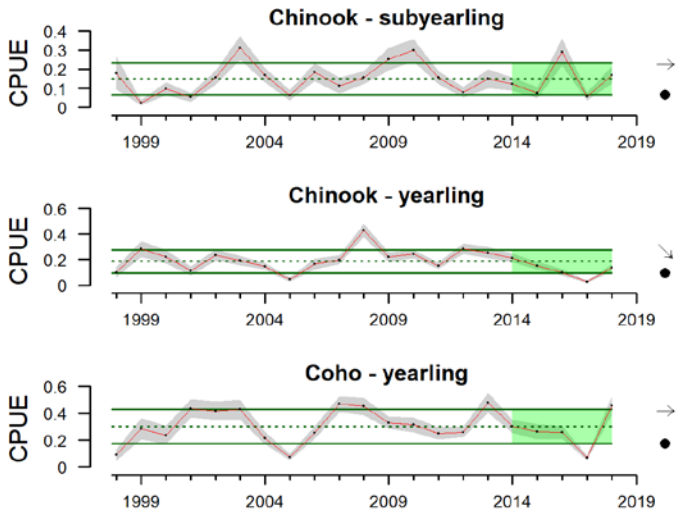

Figure 4.3.2 At sea juvenile salmon catch (Log10(no/km + 1)) from 1998 to 2018 for Chinook and coho salmon. Lines, colors, and symbols are as in Fig.1.

A suite of relevant indicators suggests some improvements in returns of salmon to the Columbia Basin in 2019. Long-term associations between oceanographic conditions, food web structure, and salmon productivity (Burke et al. 2013, Peterson et al. 2014) support forecasts of returns of Chinook salmon to Bonneville Dam and smolt-to-adult survival of Oregon Coast coho salmon. Indicators of conditions for smolts that went to sea between 2015 and 2018 are generally consistent with below-average returns of Chinook and average returns of coho salmon in 2019, as depicted in the "stoplight chart" in Table 4.3.1; this includes many indicators in this report, such as PDO, ONI, Copepod Biomass Anomalies and Juvenile Salmon Catch. A related quantitative model predicts a reasonable probability

Table 4.3.1"Stoplight" table of basin-scale and local-regional conditions for smolt years 2015-2018 and projected adult returns in 2019 for coho and Chinook salmon that inhabit coastal Oregon and Washington waters during their marine phase. Green/circle = "good," yellow/square = "intermediate," and red/diamond = "poor," relative to long-term time series. Courtesy of Dr. Brian Burke (NOAA).

	Smolt year				Adult return outlook	
Scale of indicators	2015	2016	2017	2018	Coho, 2019	Chinook, 2019
Basin-scale						
PDO (May-Sept)	◆	◆	◆	■	■	◆
ONI (Jan-Jun)	◆	◆	■	●	●	■
Local and regional						
SST anomalies	◆	◆	●	◆	◆	●
Deep water temp	◆	■	◆	◆	◆	◆
Deep water salinity	◆	■	●	●	●	●
Copepod biodiversity	◆	◆	◆	■	■	◆
Northern copepod anomaly	◆	◆	◆	●	●	◆
Biological spring transition	◆	◆	◆	◆	◆	◆
Winter ichthyoplankton biomass	●	●	●	●	●	●
Winter ichthyoplankton community	◆	◆	◆	◆	◆	◆
Juvenile Chinook catch (Jun)	■	◆	◆	■	■	◆

of modest increases in returns of Fall Chinook and coho relative to 2018, but comparable returns of Spring Chinook (Appendix H.3).

4.4 Groundfish: Stock Abundance and Community Structure

Because no assessments were conducted in 2018, this year's groundfish stock indicators are identical to last year's (updated through the 2017 assessment year). All groundfish assessed from 2007-2017 were above biomass limit reference points (LRPs); thus, no stocks were considered "overfished" (Figure 4.4.1, x-axis), although previously overfished yelloweye rockfish and cowcod were still rebuilding toward target reference points. Stocks of black rockfish (in CA and WA) and China rockfish (in CA) were being fished above the fishing rate proxy in their most recent assessments from 2015 (Figure 4.4.1, y-axis). These three stocks' fishing rates appear to be over the targets due to recent changes in how the targets are calculated in the assessments, not because of changes in management or fishery practices.

This figure will be updated with the assessments done in 2019.

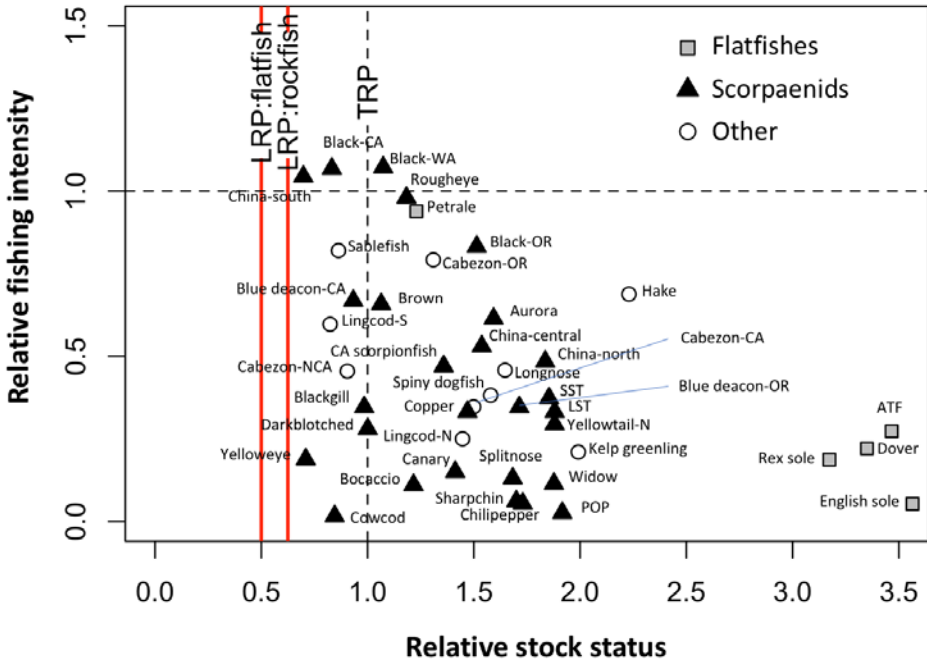

Figure 4.4.1 Stock status of CCE groundfish. X-axis: Relative stock status is the ratio of spawning output (in millions of eggs) of the last to the first years in the assessment. Y-axis: Relative fishing intensity uses the Spawner Potential Ratio (SPR) and is defined as (1-SPR)/1-(SPRMSY proxy), where the SPRFMSY proxy is stock specific. Horizontal line = fishing intensity rate reference. Above the line would be above the reference level. Vertical lines = biomass target reference point (dashed line) and limit reference point (solid line; left of this line indicates overfished status). Symbols indicate taxonomic group. All points represent values from the most recent Council-adopted stock assessment.

4.5 Highly Migratory Species

For highly migratory species (HMS), we present quad plots of recent averages and trends of biomass and recruitment from the most up-to-date stock assessment, including several species that are managed by the Council; time series and supporting documentation are found in Appendix I. The most recent assessments range from 2015-2018. Average biomass of two stocks (eastern Pacific swordfish and skipjack) over the most recent 5 years was >1 s.d. above the long-term mean, while blue marlin and bigeye tuna were >1 s.d. below their long-term means (Figure 4.5.1, left). Bigeye tuna, bluefin tuna, and blue marlin biomasses appeared to be near historic lows. Only bluefin tuna are thought to be overfished and experiencing overfishing at the scale of their full range, although uncertainty exists for other stocks, particularly bigeye tuna (Appendix I). Biomass trends were neutral for all species except skipjack, which were increasing. Recruitment indicators varied widely: recruitment appears to be increasing for skipjack and yellowfin tuna and neutral for other stocks (Figure 4.5.1, right). There was an apparent increase in age-0 bluefin in 2016 (Appendix I).

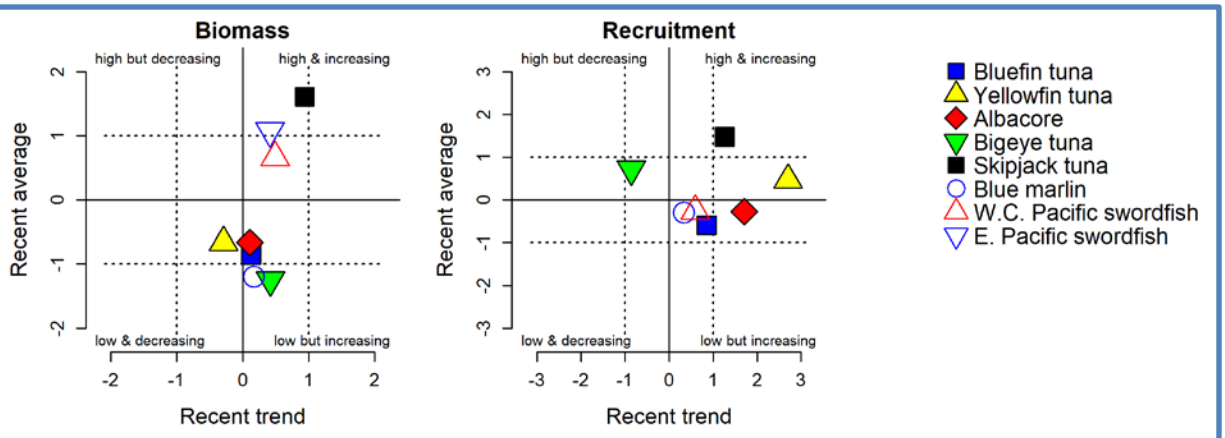

Figure 4.5.1 Recent trend and average of biomass and recruitment for highly migratory species (HMS) in the California current from the 2014-2016 stock assessments. Data are total biomass for swordfish, relative biomass for skipjack, spawning biomass for bluefin, and female spawning biomass for all other species. Lines, colors, and symbols are as in Fig.1.

4.6 Marine Mammals

Sea lion production: California sea lions are sensitive indicators of prey availability in the central and southern CCE (Melin et al. 2012): sea lion pup count at San Miguel Island relates to prey availability to gestating females from October to June, while pup growth at San Miguel from birth to age 7 months is related to prey availability to lactating females from June to February.

In 2017, pup births and growth rates showed significant improvement over 2016. Births were >1 s.d. above the long-term mean for the first time since 2012 and contrasting a declining trend in recent cohorts (Figure 4.6.1, top). The increase in births indicates that low numbers of births in 2015 and 2016 were due to the poor foraging conditions during gestation and fewer successful pregnancies, rather than a decline in survival of reproductive females. Pup growth rate was the third highest observed since 1997, and has increased since record lows in the 2014 and 2015 cohorts (Figure 4.6.1, bottom). The return of anchovy to the community and to the diet of sea lion females coincided with improved pup condition. However, the fattest pups in the time series occurred in the mid-2000s when sardine and anchovy dominated the diet, suggesting that a diverse diet with anchovy and sardine or other high-quality species like mackerel is key to supporting reproductive efforts of California sea lion females.

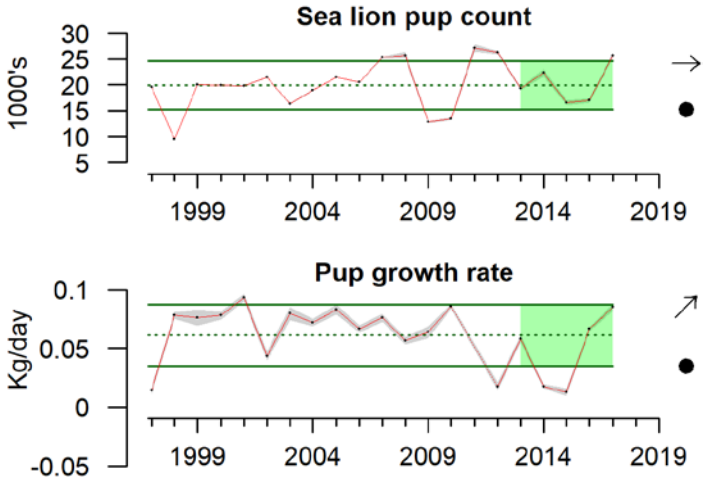

Figure 4.6.2 California sea lion pup counts, and estimated mean daily growth rate of female pups between 4-7 months on San Miguel Island for the 1997-2017 cohorts. Lines, colors, and symbols are as in Fig.1.

Whale entanglement: Coincident with the anomalous warming in 2014-2016, observations of whales entangled in fishing gear occurred at levels far greater than in the preceding decade. Reported entanglements were most numerous in 2015 and 2016, the majority involving humpbacks. Most observations occurred in California waters, although entanglement reports in 2018 were more widely dispersed along the US West Coast than in previous years. Based on preliminary data, in 2018 the number of reported entanglements increased toward the record highs seen in 2015 and 2016

after a decrease in 2017 (Figure 4.6.2). The majority of reported entanglements occur in gear that cannot be identified visually. Most of the portion that can be identified is confirmed to be Dungeness crab gear. However, in both 2016 and 2017, sablefish fixed gear was identified in at least one entanglement, and gillnets have been observed in some entanglements in every year since 2012. Many interacting factors could be causing the increased numbers of observed entanglements, including shifts in oceanographic conditions and prey fields, changes in whale populations, changes in distribution and timing of fishing effort, and increased public awareness and improved reporting.

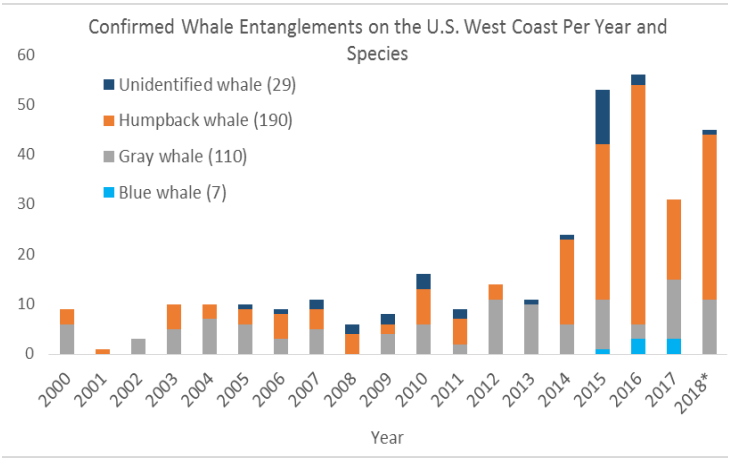

Figure 4.6.3 Numbers of whales reported as entangled in fishing gear along the West Coast from 2000-2018.

4.7 SEABIRDS

Seabird abundance indicators are assumed to reflect regional forage availability. The three bird species included here represent distinct foraging strategies and spatial ranges (Appendix J). We use a quad plot to summarize regional time series of at-sea density of these species in spring and early summer (Figure 4.7.1); time series updated through 2018 are in Appendix J.

Seabird density patterns varied by species and region. Though sooty shearwaters experienced short-term declines in both the northern and central CCE (Figure 4.7.1), their 2018 densities were substantially greater than in 2017 in all regions (Appendix J). Common murre spring densities increased in the central and southern CCE over the past 5 years, and were the highest ever recorded in the southern region in 2018. Cassin's auklet densities declined in the northern CCE over the past 5 years and were stable elsewhere; densities in 2018 were just below average in all regions.

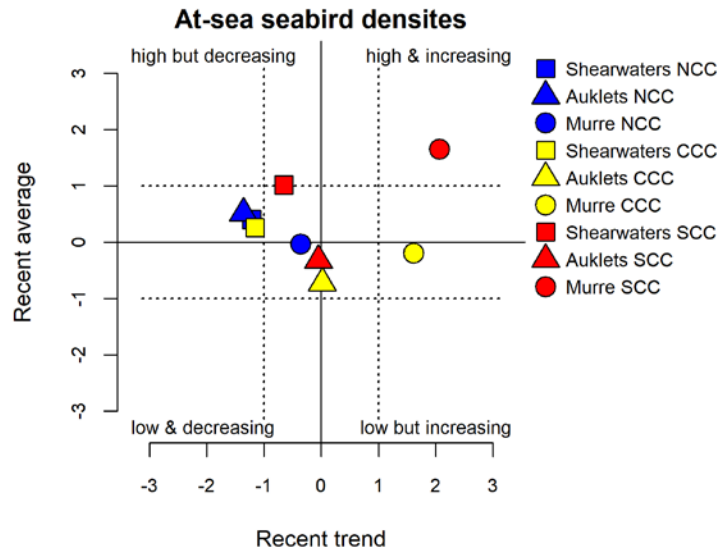

Figure 4.7.1 Recent (5-year) trend and average of seabird at-sea densities during the spring in the California Current in three regions through 2018. Lines, colors, and symbols are as in Fig.1.

In the warm and unproductive years of 2014-2016, there were major seabird mortality events ("wrecks") of Cassin's auklets in 2014, common murres in 2015 and rhinoceros auklets in 2016. In 2018, for the second year in a row, there were no widespread wrecks in the CCE (Appendix J.2).

5 HUMAN ACTIVITIES

5.1 COASTWIDE LANDINGS BY MAJOR FISHERIES

Data for fishery landings are available through 2017. Coastwide landings have been highly variable in recent years, driven by steep declines in landings of CPS finfish, market squid, shrimp and salmon, coupled with large Pacific hake landings in 2016 and especially 2017 (Figure 5.1.1). Total landings increased 27.4% from 2016 to 2017. Landings of groundfish (excluding hake) were near historic lows from 2013-2017, though a slight increase occurred in 2017. Landings of CPS finfish decreased to the lowest levels in recent decades. Shrimp landings have been above average for the most recent 5-year span, despite declines in 2016 and 2017. Commercial landings of salmon have declined sharply and remained low over the last several years. Landings of HMS and other species have been within ±1 s.d. of historic averages over the last 20+ years. State-by-state landings are presented in Appendix K.1.

Recreational landings (excluding salmon and Pacific halibut) were within historical averages for the last 5 years (Figure 5.1.1). A recent decline was due to a 70-80% decrease in yellowfin tuna and yellowtail landings in 2016. Recreational landings of Chinook and coho salmon were near the lowest levels observed in recent decades. State-by-state recreational landings are in Appendix K.1.

Total revenue for West Coast commercial fisheries in 2017 was ~1 s.d. above the long-term average, and 12.3% higher than 2016. The increase was driven by high revenues from Pacific hake, market squid and crab. Coastwide and state-by-state revenue data are presented in Appendix K.2.

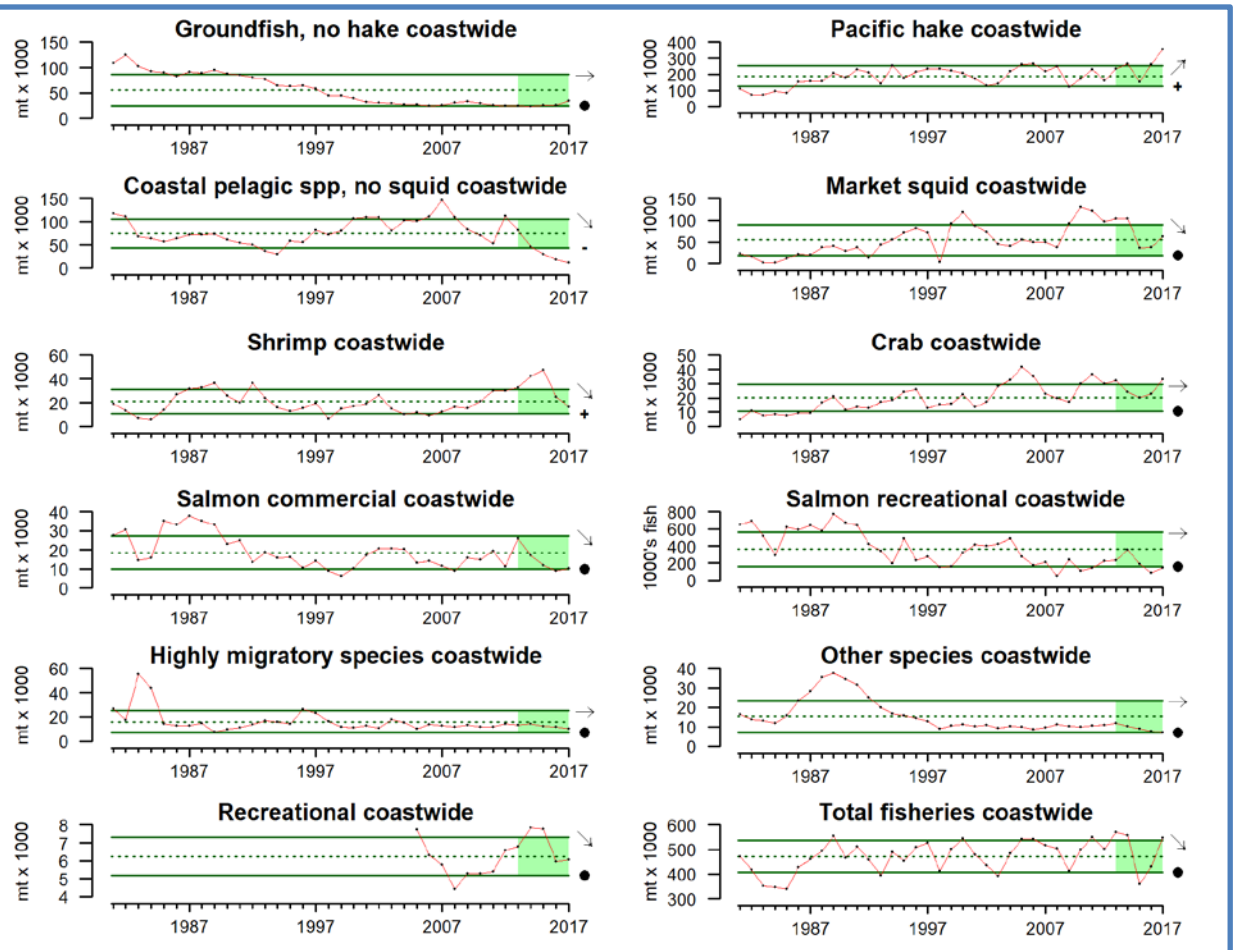

Figure 5.1.1 Annual landings of West Coast commercial (data from PacFIN) and recreational (data from RecFin) fisheries, including total landings across all fisheries from1981-2017. Lines, colors, and symbols are as in Fig.1.

5.2 Gear Contact with Seafloor

Benthic species, habitats and communities can be disturbed by natural processes, and also by human activities (e.g., fishing, mining, dredging). The impacts of these activities likely differ by seafloor habitat type, with hard, mixed and biogenic habitats needing longer to recover than soft sediment. Spatially explicit indicators may inform spatial management of specific human activities.

To illustrate spatial variation in bottom trawling activity, we estimated total distance trawled on a 2x2-km grid from 2002-2016. For each grid cell, we mapped the 2016 anomaly from the long-term mean, the most recent 5-year average and the most recent 5-year trend (Figure 5.2.1). Off Washington, cells where distance trawled was above average and increasing tended to be in central and southern waters (red cells), while northern cells mostly experienced below-average and decreasing trawl contact (blue cells). Off Oregon, red cells in 2016 and in the trend map were in several patches, the largest of which was off Newport, while blue cells in 2016 and the trend map were most concentrated to the north and south of Cape Blanco. Off California, the most notable patches of red cells in 2016 were just north of Cape Mendocino, while cells with increasing or decreasing trends from 2012-2016 were widespread. These spatial indicators are more informative than the coast-wide aggregated time series which showed bottom trawl contact at historically low levels and no trend from 2012 to 2016 (Appendix L).

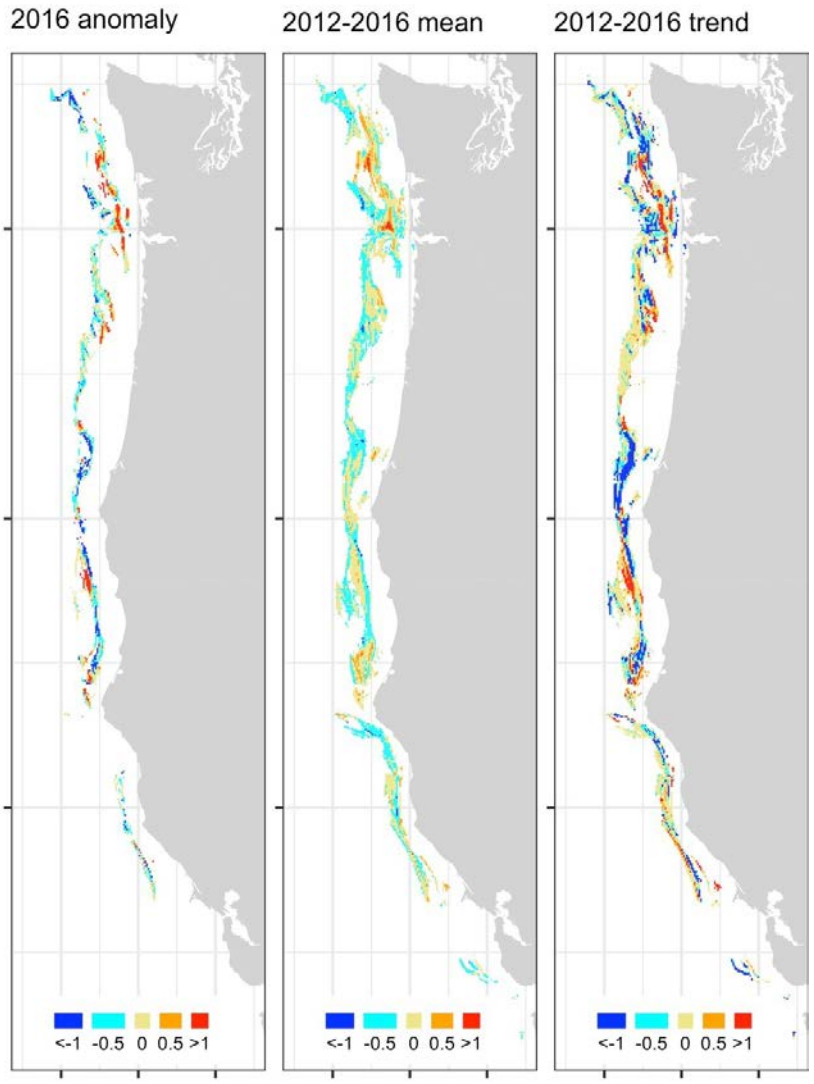

Figure 5.2.1 Values for each grid cell are relative to distances trawled using bottom trawl fishing gear in that grid cell from 2002 – 2016. Left: Annual bottom contact anomalies. Middle: Normalized mean values for the most recent five-year period. Right: Normalized trend values for the most recent five-year period. Grid cell values > 1 (red) or < -1 (blue) represent a cell in which the anomaly, 5-year mean or 5-year trend was at least 1 s.d. away from the long-term mean of that cell.

6 Human Wellbeing

6.1 Social Vulnerability

Coastal community vulnerability indices are generalized socioeconomic vulnerability metrics for communities. The Community Social Vulnerability Index (CSVI) is derived from social vulnerability data (demographics, personal disruption, poverty, housing, labor force structure, etc.; Jepson and

Colburn 2013). We monitor CSVI in communities highly reliant upon both commercial fishing (Figure 6.1.1) and recreational fishing (Figure 6.1.2).

The commercial fishing reliance index is based on an analysis of variables reflecting *per capita* engagement in commercial fishing (e.g., landings, revenues, permits, and processing) in 1140 West Coast communities. Figure 6.1.1 plots CSVI in 2016 against commercial fishery reliance for communities that are most reliant on commercial fishing in Washington, Oregon, and California. Communities above and to the right of the dashed lines are those with above average levels of CSVI (horizontal dashed line) and commercial fishing reliance (vertical dashed line). For example, Port Orford and Westport have high fishing reliance (4 and 9 s.d. above average) and high CSVI (6 and 4 s.d. above average) compared to other coastal communities. Outliers in both indices may be especially socially vulnerable to commercial fishery downturns.

The recreational fishing engagement index is a similar analysis of variables reflecting a community's *per capita* recreational fishing engagement (e.g., number of boat launches, number of charter boat and fishing guide license holders, number of charter boat trips, and a count of support businesses such as

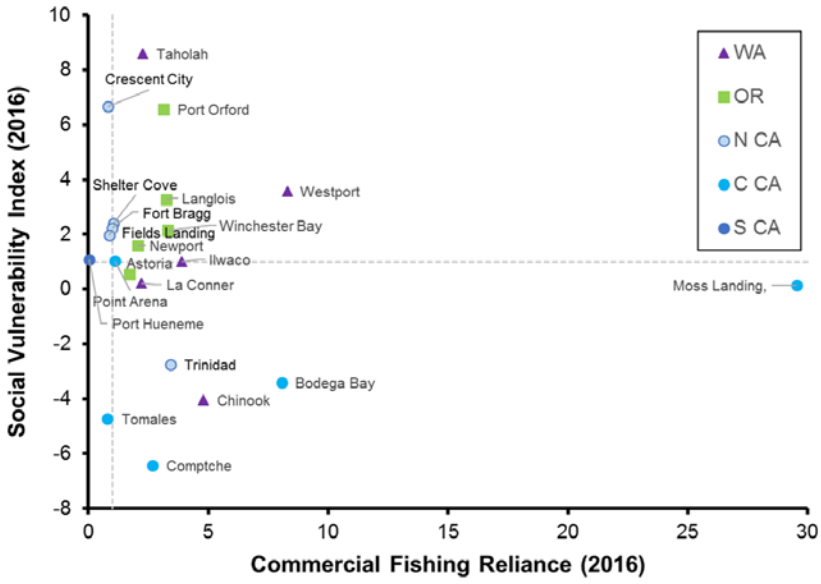

Figure 6.1.2 Commercial fishing reliance and social vulnerability scores plotted for twenty-five communities from each of the 5 regions of the California Current: WA, OR, Northern, Central, and Southern California. The top five highest scoring communities for fishing reliance were selected from each region.

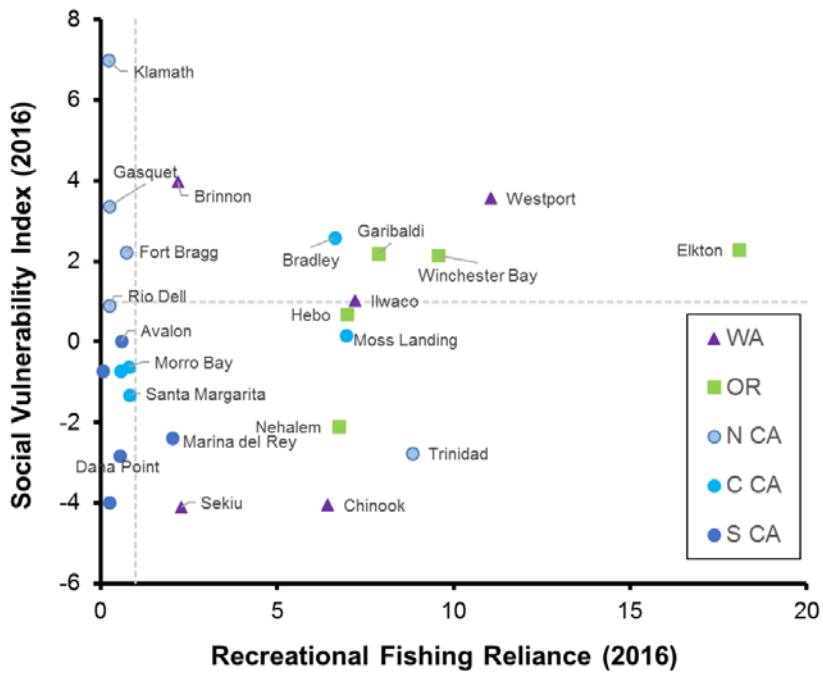

Figure 6.1.1 Recreational fishing reliance and social vulnerability scores plotted for twenty-five communities from each of the 5 regions of the California Current: WA, OR, Northern, Central, and Southern California. The top five highest scoring communities for fishing reliance were selected from each region.

bait and tackle shops). The analysis does not differentiate between marine recreational fishing and inland recreational fishing, which may include anadromous salmonids of coastal commercial and recreational interest. Figure 6.1.2 plots CSVI against recreational fishery reliance in 2016 for the five communities most reliant on recreational fishing in the same five geographic regions. Communities above and to the right of the dashed lines, such as Garibaldi and Westport, have higher-than-average recreational reliance and social vulnerability. Some communities (Westport, Ilwaco, Winchester Bay) are outliers on both axes in both the commercial and recreational plots, which may imply some potential for management-related tradeoffs in those communities.

This is an emerging area of work and more research will be required to understand the importance of these relationships. An effort to examine communities that may be particularly affected by ecosystem shifts, with respect to the Magnuson-Stevens Act's National Standard 8, is ongoing. Additional findings on these fishery engagement relationships are in Appendix M.

6.2 Diversification of Fishery Revenues

According to the effective Shannon index (ESI) metric that we use to measure diversification of revenues across different fisheries (see Appendix N), the fleet of 28,000 vessels that fished the West Coast and Alaska in 2017 was essentially unchanged from 2016 for most vessel classes, but was less diverse on average than at any time in the prior 36 years (Figure 6.2.1a). Most vessel categories have been trending down for several years, notably the California fleet and the largest vessels coastwide (Figure 6.2.1b, d). The long-term decline in fishery diversification is due both to entry and exit of vessels, and to changes for individual vessels. Less diversified vessels have been more likely to exit, vessels that remain in the fishery have become less diversified since the mid-1990s, and newer entrants have generally been less diversified than earlier entrants. Within the average trends, there are wide ranges of diversification levels and strategies, and some vessels remain highly diversified. Increased diversification from one year to the next may not always indicate an improvement. For example, if a class of vessels was heavily dependent on a single fishery with highly variable revenues (e.g., Dungeness crab), a decline in that fishery might force vessels into other fisheries, causing diversification to increase. Also an increase in a fleet's diversification may be due less diversified vessels exiting (Appendix N).

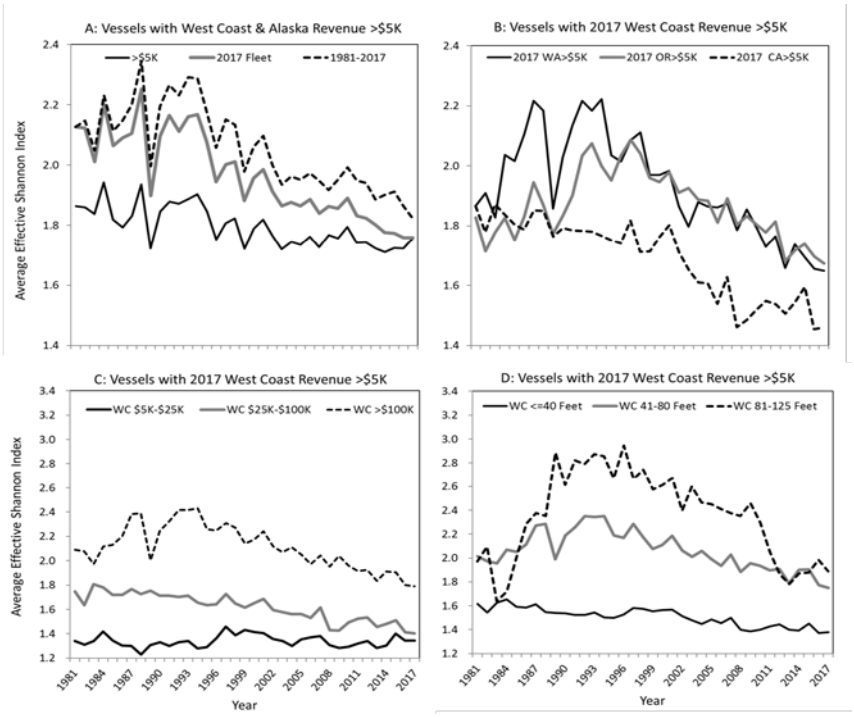

Figure 6.2.1 Trends in average diversification for US West Coast and Alaskan fishing vessels with over $5K in average revenues (top left) and for vessels in the 2016 West Coast Fleet with over $5K in average revenues, broken out by state (top right), by average gross revenue classes (bottom left) and by vessel length classes (bottom right)

6.3 Stock Spatial Distribution and Availability to Ports

Fishing communities must contend with changes in availability of important target stocks. Changes in availability may happen due to changes in the stock's population size, changes in its distribution, or both. To determine how fishing communities along the US West Coast experience changes in the distribution of fish stocks, we estimated fluctuations in the relative availability of two groundfish species (petrale sole and sablefish) to four communities (Astoria, Coos Bay, Fort Bragg, and Morro Bay) from 1980-2017 (Figure 6.3.1). This stock availability index represents the cumulative effects of changes in biomass (based on stock assessment output) and shifts in spatial distribution (based on VAST model output; methods details in Appendix O). While the qualitative trends in stock availability reflect trends in biomass reported in stock assessments, the four communities represented here experienced those trends quite differently depending on where they occur along the coast.

The coastwide biomass of sablefish declined more than 50% since 1980, but the distribution of sablefish is centered further south today than it was in the early 1990s. This change in the center of gravity of the stock has counteracted the decline in sablefish biomass for southern ports (Fort Bragg and Morro Bay) over the last 25 years, such that stock availability was relatively stable compared to Astoria and Coos Bay. In contrast, while the biomass of petrale sole has increased everywhere along the coast since the early 2000s, the center of gravity of this stock is now farther north than it was historically. Thus, relative stock availability has tripled for Astoria and Coos Bay but increased more modestly for Fort Bragg and Morro Bay.

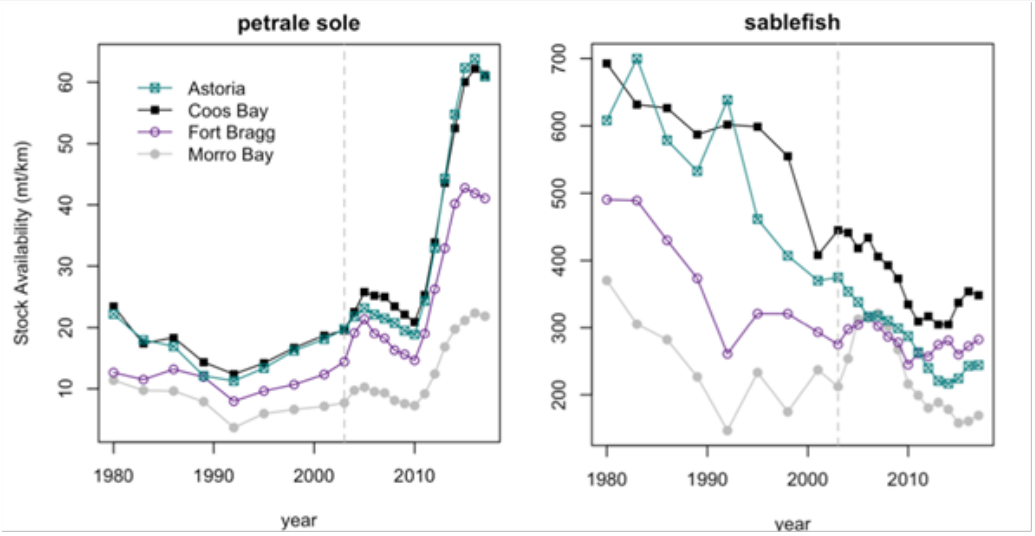

Figure 6.3.1. Stock availability of petrale sole (left) and sablefish (right) to four West Coast ports. Availability is a relative measure of fishable biomass per km of water over the shelf, in the region of each port. See Appendix O for methodological details.

Ecological, technological, management, economic, governance, and other social factors influence the availability of target species to fishing communities. This same set of considerations influences the capacity of these communities to respond to shifting availability of target species. Climate variability and change, in particular, challenge the capacities of fishing communities to keep pace with shifts in stock availability. Analyses like those presented here represent a first step toward evaluating the impacts of changing social and ecological conditions on the availability of target species and the individual fishing communities that depend upon them. In the future, this analysis can be updated annually for any west coast community and for groundfishes well-sampled by the trawl survey, and can focus on the attribution of potential causes underlying the shifts in availability observed here.

7 SYNTHESIS

7.1 SUMMARY OF RECENT CONDITIONS

Over the past two years, the CCE appears to have been in a slow transition away from the anomalous, warm, and relatively unproductive conditions of 2014-2016 (e.g., Thompson et al. 2018). Within our indicators, this slow transition is demonstrated by:

- Basin-scale climate indices, such as mostly neutral ONI and PDO values
- Regional environmental indicators (generally average upwelling, snowpack, stream flow)
- Indicators of productivity of lower trophic levels (relatively average copepod community composition off Newport and krill size off northern California, subtle improvements in salmon indicators, no evidence of recent HABs off Washington, increases in anchovy)
- Indicators of predator foraging (improving conditions for sea lion pups, average or increasing densities of piscivorous seabirds)
- Recent increases in landings and revenues in several FMPs

Furthermore, some variables that we had expected to be negatively affected by the warm conditions in 2014-2016 actually exceeded those expectations, notably the large numbers of juvenile groundfish caught in pelagic surveys, suggesting that some parts of the CCE were resilient to the direct influence of the anomalous conditions.

However, referring to the last few years as "a slow transition" begs the question: a transition to what? We do not know the answer to that, as there are neither definitive signs that the CCE will resume the productive conditions experienced for several years prior to 2014, nor definitive signs that the CCE will move back to a relatively unproductive state. Moreover, many indicators suggest lingering effects of the anomalies of 2014-2016, including persistence of subsurface warm water, high concentrations of pyrosomes, and whale entanglements in fishing gear. Other concerning signs include persistently low NPGO anomalies, widespread hypoxic events, episodes of northeast Pacific warming (see Figure 3.1.3), and loss of fishery diversification. Our uncertainty about where this "transition" is leading underscores the importance of continued careful monitoring, modeling and analysis of indicators at appropriate scales; refinement of forecasting tools (see below); and maintaining communication between scientists, managers, and stakeholders.

7.2 FORECASTS AND PREDICTIONS FOR 2019

In March 2015, the Council approved FEP Initiative 2, "Coordinated Ecosystem Indicator Review" (Agenda Item E.2.b), by which the Council, advisory bodies, the public, and the CCIEA team would work jointly to refine the indicators in the annual CCIEA Ecosystem Status Report to better meet Council objectives. Many of the recommendations of that 2-year process have already been implemented over the past several iterations of this report, including the current report for March 2019 (for examples, see Appendix C). One of the priorities identified by several advisory bodies was that the CCIEA team develop and evaluate leading indicators and analyses that support short-term forecasting. We therefore will conclude the main body of this year's report with information that may provide insight on conditions that will occur in 2019.

Some sections above have indicators and analyses that provide forecasting ability. These are:

- **El Niño forecast (Section 3.1).** The NOAA Climate Prediction Center predicts a 65% chance that a mild El Niño will form in the equatorial Pacific at least through spring 2019.
- **Salmon returns to the Columbia River and Oregon Production Index area (Section 4.3).** The indicator "stoplight chart" and related quantitative analyses predict below-average returns of Chinook salmon to Bonneville Dam in 2019, and moderate survival of coho salmon returning to Oregon coastal systems in 2019.

An additional set of forecasting tools has been developed in a partnership between academic scientists and CCIEA team members, and were reviewed in September 2018 by the SSC Ecosystem Subcommittee. The **J-SCOPE forecast system** (www.nanoos.org/products/j-scope) provides short-term skilled forecasts of ocean conditions off of Washington and Oregon, and these forecasts have been extended to include seasonal predictions of habitat quality for sardines (Siedlecki et al. 2016, Kaplan et al. 2016). Each January, the J-SCOPE modelers produce an ensemble of 3 forecasts that span January-September and include variables like temperature, dissolved oxygen, chlorophyll, aragonite saturation state (ocean acidification), and sardine habitat, in addition to other dynamics such as the timing and intensity of upwelling.

According to the J-SCOPE ensemble forecast of the 2019 summer upwelling season (May-August):

- Sea surface temperatures are expected to be higher than average, with warm anomalies extending below the surface (related to the El Niño forecast)
- Dissolved oxygen on the bottom declines over the course of the forecast, with hypoxia (<2 mg/L) prominent over the Oregon shelf in June and spreading to Washington by July (Figure 7.2.1, left). Compared to previous years, oxygen is expected to be lower than average in Washington and near average in Oregon. The relative uncertainty in the forecast remains low (10%) until the end of the upwelling season (July-August), when it increases to ~50%
- Aragonite on the bottom is expected to be undersaturated (i.e., more corrosive) throughout the upwelling season for most of the region except for shallow nearshore Washington shelves (Figure 7.2.1, right); surface waters are expected to be supersaturated throughout the season
- Chlorophyll-a concentrations are forecast to be below average early in the upwelling season; later, chlorophyll is forecast to be above average over the Washington shelf and Heceta Bank, but below average over the rest of the Oregon shelf
- Waters throughout the region are expected to be suitable for sardine (if they are present)

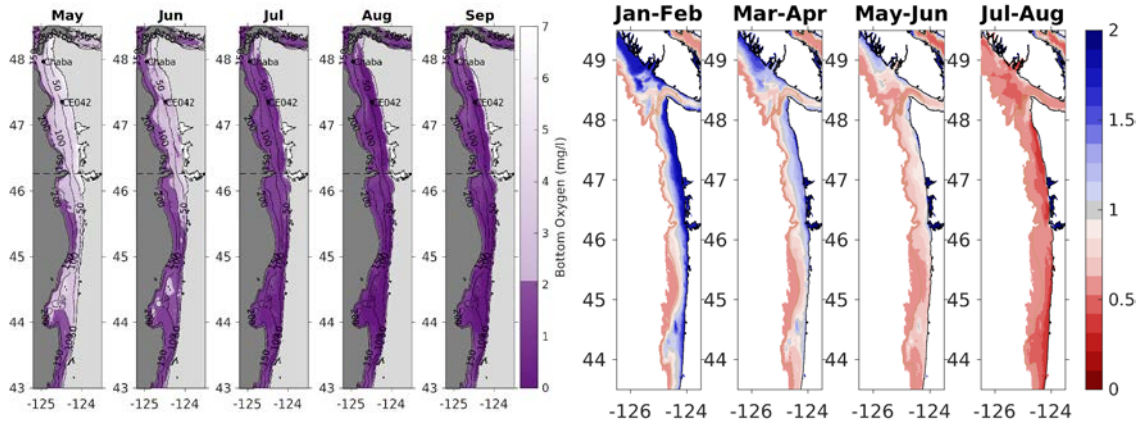

Figure 7.2.1. (Left) J-SCOPE forecasts of bottom dissolved oxygen (mg/l) for May-September 2019, averaged over all three ensemble members. Hypoxia (O_2 < 2 mg/l) is shown in dark purple and offshore areas are shaded dark gray. Black contours indicate bathymetry (m) on the shelf. (Right) J-SCOPE forecasts of bottom aragonite saturation state for January-August 2019, averaged over all three ensemble members. For reference, aragonite saturation state = 1 is broadly considered the boundary between undersaturated and saturated conditions, although stressful conditions for juvenile oysters begin to occur when saturation state is ≤ 1.3.

Forecasts for temperatures, chlorophyll and sardines can be viewed at the J-SCOPE website, http://www.nanoos.org/products/j-scope/forecasts.php. Additional species forecasts are being developed and will be available in future years.

SUPPLEMENTARY MATERIALS TO THE CALIFORNIA CURRENT INTEGRATED ECOSYSTEM ASSESSMENT (CCIEA) CALIFORNIA CURRENT ECOSYSTEM STATUS REPORT, 2019

Appendix A LIST OF CONTRIBUTORS TO THIS REPORT, BY AFFILIATION

NWFSC, NOAA Fisheries
Dr. Chris Harvey
(co-lead editor; Chris.Harvey@noaa.gov)

Mr. Kelly Andrews
Ms. Katie Barnas
Dr. Richard Brodeur
Dr. Brian Burke
Dr. Jason Cope
Dr. Correigh Greene
Dr. Thomas Good
Dr. Daniel Holland
Dr. Isaac Kaplan
Dr. Stephanie Moore
Dr. Stuart Munsch
Dr. Karma Norman
Dr. Jameal Samhouri
Dr. Nick Tolimieri (co-editor)
Dr. Vera Trainer
Ms. Margaret Williams
Dr. Jeannette Zamon

Pacific States Marine Fishery Commission
Mr. Gregory Williams (co-editor)
Ms. Anna Varney

University of Connecticut
Dr. Samantha Siedlecki

Rutgers University
Dr. Rebecca Selden

Washington Department of Health
Ms. Audrey Coyne

SWFSC, NOAA Fisheries
Dr. Newell (Toby) Garfield
(co-lead editor; Toby.Garfield@noaa.gov)

Dr. Eric Bjorkstedt
Dr. Steven Bograd
Ms. Lynn deWitt
Dr. John Field
Dr. Elliott Hazen
Dr. Michael Jacox
Dr. Andrew Leising
Dr. Barbara Muhling
Mr. Keith Sakuma
Dr. Isaac Schroeder
Dr. Andrew Thompson
Dr. Desiree Tommasi
Dr. Brian Wells
Dr. Thomas Williams

AFSC, NOAA Fisheries
Dr. Stephen Kasperski
Dr. Sharon Melin
Dr. Jim Thorson

NOAA Fisheries West Coast Region
Mr. Dan Lawson

Oregon State University
Ms. Jennifer Fisher
Ms. Cheryl Morgan

Humboldt State University
Ms. Roxanne Robertson

Farallon Institute
Dr. William Sydeman

Appendix B LIST OF FIGURE AND DATA SOURCES FOR THE MAIN REPORT

Figure 3.1: Newport Hydrographic (NH) line temperature data from J. Fisher, NMFS/NWFSC, OSU). CalCOFI hydrographic line data from https://calcofi.org. CalCOFI data before 2018 are from the bottle data database, while 2018 data are preliminary conductivity, temperature, and depth (CTD) data from the recent CTD database.

Figure 3.1.1: Oceanic Niño Index information and data are from the NOAA Climate Prediction Center (http://www.cpc.ncep.noaa.gov/products/analysis_monitoring/ensostuff/ONI_change.shtml). PDO data are from N. Mantua, NMFS/SWFSC, and are served by the University of Washington Joint Institute for the study of the Atmospheric and Ocean (JISAO; http://research.jisao.washington.edu/pdo/). North Pacific Gyre Oscillation data are from E. Di Lorenzo, Georgia Institute of Technology (http://www.o3d.org/npgo/).

Figure 3.1.2: Sea surface temperature maps are optimally interpolated remotely-sensed temperatures (Reynolds et al. 2007). The daily optimal interpolated AVHRR SST can be downloaded using ERDDAP (http://upwell.pfeg.noaa.gov/erddap/griddap/ncdcOisst2Agg.html).

Figure 3.2.1: Daily 2018 values of BEUTI and CUTI are derived from numerical model outputs described in Jacox et al. (2018); detailed information about these indices can be found at https://mjacox.com/upwelling-indices/.

Figure 3.3.1: Newport Hydrographic (NH) line dissolved oxygen data are from J. Fisher, NMFS/NWFSC, OSU. CalCOFI hydrographic line data from https://calcofi.org. CalCOFI data before 2018 are from the bottle data database, while 2018 data are preliminary conductivity, temperature, and depth (CTD) data from the recent CTD database.

Figure 3.3.2: Aragonite saturation state data from J. Fisher, NMFS/NWFSC, OSU.

Figure 3.4.1: Data on domoic acid concentrations in razor clams are from A. Coyne (Washington State Department of Health); these data are compiled from tests conducted by a variety of Tribal, State, and County partners on Washington beaches. Sample testing frequency is irregular as it depends on the timing of proposed recreational razor clamming digs by Washington State Department of Fish and Wildlife and prevalence of recent detections.

Figure 3.5.1: Snow-water equivalent data were derived from the California Department of Water Resources snow survey (http://cdec.water.ca.gov/) and the Natural Resources Conservation Service's SNOTEL sites in WA, OR, CA and ID (http://www.wcc.nrcs.usda.gov/snow/).

Figure 3.5.2: Minimum and maximum streamflow data were provided by the US Geological Survey (http://waterdata.usgs.gov/nwis/sw).

Figure 4.1.1: Copepod biomass anomaly data were provided by J. Fisher, NMFS/NWFSC, OSU).

Figure 4.1.2. Krill (Euphausia pacifica) data were provided by E. Bjorkstedt, NMFS/SWFSC and Humboldt State University (HSU), and R. Robertson, Cooperative Institute for Marine Ecosystems and Climate (CIMEC) at HSU. Krill were collected at monthly intervals from the Trinidad Head Line (Fig. 2.1b); krill body length (BL) was measured in mm from the back of the eye to base of the telson.

Figure 4.2.1: Pelagic forage data from the Northern CCE were provided by B.Burke, NMFS/NWFSC and C. Morgan, OSU/CIMRS. Data are derived from surface trawls taken during the NWFSC Juvenile Salmon & Ocean Ecosystem Survey (JSOES; https://www.nwfsc.noaa.gov/research/divisions/fe/estuarine/oeip/kb-juvenile-salmon-sampling.cfm).

Figure 4.2.2: Pelagic forage data from the Central CCE were provided by J. Field and K. Sakuma, NMFS/SWFSC, from the SWFSC Rockfish Recruitment and Ecosystem Assessment Survey (https://swfsc.noaa.gov/textblock.aspx?Division=FED&ParentMenuId=54&id=20615),

Figure 4.2.3: Pelagic forage larvae data from the Southern CCE were provided by A. Thompson, NMFS/SWFSC, and derived from spring CalCOFI surveys (https://calcofi.org/).

Figure 4.3.1: Chinook salmon escapement data were derived from the California Department of Fish and Wildlife (https://www.dfg.ca.gov/fish/Resources/Chinook/CValleyAssessment.asp), Pacific Fishery Management Council pre-season reports (https://www.pcouncil.org/salmon/stock-assessment-and-fishery-evaluation-safe-documents/review-of-2017-ocean-salmon-fisheries/), and the NOAA Northwest Fisheries Science Center's "Salmon Population Summary" database (https://www.webapps.nwfsc.noaa.gov/sps), with data provided directly from the Nez Perce Tribe, the Yakama Nation Tribe, and from Streamnet's Coordinated Assessments database (cax.streamnet.org), with data provided by the Oregon Department of Fish and Wildlife, Washington Department of Fish and Wildlife, Idaho Department of Fish and Game, Confederated Tribes and Bands of the Colville Reservation, Shoshone-Bannock Tribes, Confederated Tribes of the Umatilla Indian Reservation, and U.S. Fish and Wildlife Service.

Figure 4.3.2: Data for at sea juvenile salmon provided by B.Burke, NMFS/NWFSC, with additional calculations by C. Morgan, OSU/CIMRS. Derived from surface trawls taken during the NWFSC Juvenile Salmon and Ocean Ecosystem Survey (JSOES) cruises.

Figure 4.4.1: Groundfish stock status data provided by J. Cope, NMFS/NWFSC, derived from NOAA Fisheries stock assessments.

Figure 4.5.1: Highly migratory species data provided by B. Muhling, NMFS/SWFSC, and D. Tommasi, NMFS/SWFSC, UCSC. Data are derived from stock assessment reports completed through the International Scientific Committee for Tuna and Tuna-like Species in the North Pacific Ocean (ISC; (http://isc.fra.go.jp/reports/stock_assessments.html) or the Inter-American Tropical Tuna Commission (IATTC; https://www.iattc.org/PublicationsENG.htm).

Figure 4.6.1: California sea lion data provided by S. Melin, NMFS/AFSC.

Figure 4.6.2: Whale entanglement data provided by D. Lawson, NMFS/WCRO.

Figure 4.7.1: Seabird abundance data from the northern CCE were collected and provided by J. Zamon, NMFS/NWFSC. Seabird abundance data from central CCE (collected on the SWFSC Rockfish Recruitment and Ecosystem Assessment Survey) and southern CCE (collected on the CalCOFI surveys) courtesy of B. Sydeman, Farallon Institute. NCC data are from June surveys, CCC data are from May surveys, and SCC data are from April surveys, as no seabird data were collected during the summer survey.

Figure 5.1.1: Data for commercial landings are from PacFIN (http://pacfin.psmfc.org). Data for recreational landings are from RecFIN (http://www.recfin.org/).

Figure 5.2.1: Data for total benthic habitat distance disturbed by bottom-contact fishing gears were provided by J. McVeigh, NMFS/NWFSC, West Coast Groundfish Observer Program. Weightings for benthic habitat sensitivity values come from PFMC's Pacific Coast Groundfish 5-Year Review of Essential Fish Habitat.

Figure 6.1.1: Community social vulnerability index (CSVI) and commercial fishery reliance data provided by K. Norman, NMFS/NWFSC, and A. Varney, PSMFC, with data derived from the US Census Bureau's American Community Survey (ACS; https://www.census.gov/programs-surveys/acs/) and PacFIN (http://pacfin.psmfc.org), respectively.

Figure 6.1.2: Community social vulnerability index (CSVI) and recreational fishery reliance data provided by K. Norman, NMFS/NWFSC, and A. Varney, PSMFC, with data derived from the US Census Bureau's American Community Survey (ACS; https://www.census.gov/programs-surveys/acs/) and from PacFIN (https://pacfin.psmfc.org) and RecFIN (https://www.recfin.org/), respectively.

Figure 6.2.1: Fishery diversification estimates were provided by D. Holland, NMFS/NWFSC, and S. Kasperski, NMFS/AFSC.

Figure 6.3.1: Estimates of petrale sole and sablefish availability to ports were derived from catch data provided by PacFIN (http://pacfin.psmfc.org) and survey data and stock assessment outputs from the NOAA Northwest Fisheries Science Center; analyses provided by R. Selden (Rutgers University), J. Samhouri and N. Tolimieri (NMFS/NWFSC), and J. Thorson (NMFS/AFSC).

Table 4.3.1: Stoplight table of indicators and projected 2019 salmon returns courtesy of B. Burke, NMFS/NWFSC.

Appendix C CHANGES IN THIS YEAR'S REPORT

Below we summarize changes and improvements in the 2019 Ecosystem Status Report, in response to the requests and suggestions received from the Council and advisory bodies under FEP Initiative 2, "Coordinated Ecosystem Indicator Review" (March 2015, Agenda Item E.2.b). We also note other known data and information gaps that we have filled since last year's report. Finally, we note several instances where elements from past reports were streamlined or cut from this year's report, due to time constraints imposed by the partial federal government shutdown from December 22, 2018-January 25, 2019, during which NOAA line offices were closed.

Request/Need	Response/Location in document
The EAS previously noted that they "[a]ppreciated the report's current year information on unusual events like [the Warm] Blob" and also a "presentation slide showing N Pacific SST maps."	In response to this comment and to ongoing concern about marine heatwaves, including in recent media, we added an analysis (reviewed by the SSCES in September 2017) that measures and maps the magnitude, spatial extent and duration of warm SST events in the North Pacific and provides criteria for whether a marine heatwave is occurring. The analysis is depicted in Figure 3.1.3 and in Appendix D.2.
The EWG noted that "some effects of upwelling can be positive for some species, while other effects may be negative. [We] suggest more specific information in report on potential effects of upwelling on the biological environment." The SAS and GAS requested similar information on the characteristics of upwelled water in relation to hypoxia, ocean acidification, and other measures of water and habitat quality.	We have improved the upwelling indices to reflect total volume of upwelling (using new metrics that more accurately reflect upwelling magnitude at all latitudes along the west coast, published by Jacox et al. 2018) and that also reflect the amount of nutrients (specifically, nitrate) in the upwelled water. See Fig. 3.2.1. The JSCOPE seasonal forecasts (Section 7) also project hypoxia and ocean acidification on the seafloor off Washington and Oregon; both hypoxia and OA are driven in large part by upwelling. We will continue to build on these improvements. In Appendix E of last year's report, we included a time series of how shallow the OA threshold (aragonite saturation = 1.0) was off of Newport, OR. Due to the partial government shutdown we were unable to update this section of the report.
The EWG requested information on "the effects of shifting levels of phytoplankton blooms, domoic acid, and paralytic shellfish poisoning on fisheries"; similarly, the EAS requested "data on chlorophyll concentrations and harmful algal blooms."	This year we added time series of the concentrations of domoic acid in razor clams from 6 sites along the central and southern coast of Washington, including some information related to fishery closures (Figure 3.4.1 and Appendix E). We will continue to work with colleagues to identify time series of harmful algal blooms from elsewhere along the coast.
The SSC and SSCES requested that we include error bars around point estimates in quad plots to better distinguish significant averages and trends.	The models that calculate 95% credible intervals in the quad plots for maximum and minimum stream flows (Figure 3.5.2) have been improved. The models now account for spatial correlations, so that the credible intervals better reflect temporal variability.

Request/Need	Response/Location in document
The GMT stated, "We recommend that IEA scientists focus on improving and/or expanding those indicators that have shown promise in regards to correlations with fisheries productivity…. Copepod data is currently collected only off Newport, but effort could be expanded to other sites along the coast."	This year we have added a new time series of the length of the abundant krill species *Euphausia pacifica* off of Trinidad Head in northern California (Figure 4.1.2). This indicator reflects the condition of krill, an important prey species for small fishes, at another site along the coast, and thus extends our understanding of lower trophic level productivity. We hope to add copepod data from Trinidad Head in the future.
The EWG and other advisory bodies have requested improvements to regional forage time series.	This year we introduce a new statistical approach to analyze forage time series and improve comparability between regions. The analysis, which was reviewed by the SSCES in September 2018, identifies clusters of co-occurring forage species and also identifies years in which the forage composition changed significantly. This allows us to compare the synchrony of changes in forage among regions, and also to determine if forage changes coincide with oceanographic changes. The new analyses appear in Section 4.2.
The EWG and other advisory bodies have requested more information on highly migratory species.	Additional information to support interpretation of HMS biomass and recruitment estimates has been added to Appendix I. The information is derived from the most recent HMS stock assessments.
Seabird indicators have been limited to abundance estimates and less directly tied to mechanisms, except for reports of mass seabird mortality events	In last year's report, we included information on seabird diets in the Appendix. Due to the partial government shutdown we were unable to update this section of the report, and therefore removed it.
Updates of non-fishing human activities in the CCE (e.g., aquaculture, shipping, oil and energy activity, nutrient loading)	Due to the partial government shutdown we were unable to update this section of the report, and thus removed it from this year's report altogether.
The EWG asked, "Is there a way to assess longer-term fishing community stability, both in the past (How does distribution of target species catch by port change over time?) and, potentially, in the future (Are there shifts in species distribution in response to climate change and potential effects on coastal communities?).	In Section 6.3, we added a new analysis of shifts in availability of two valuable target stocks (petrale sole and sablefish) to four major ports; availability over time varies as a function of stock abundance and spatial distribution. Methods are described in Appendix O. This analysis can be expanded to additional assessed stocks or ports in the future.
In 2018, the EAS requested that the Human Wellbeing section include indicators of fishery participation and economic status of fishing communities, as relate to National Standard 8 of the Magnuson-Stevens Act	Due to the partial government shutdown we were unable to address this request and will attempt to include it in next year's report.
The Habitat Committee "encourages further efforts to define key indicators that can be used for forecasting.." Similarly, the EAS recommends that the report "provide projections of future ecosystem conditions."	In Section 7, we added a section that focuses on forecasts, in particular the J-SCOPE seasonal forecasts of ocean conditions off Washington and Oregon. In addition, we expanded the information on forecasts on salmon returns; text and plots are in Appendix H.3.

Appendix D CLIMATE AND OCEAN INDICATORS

Section 3 of the Main Body describes indicators of basin-scale and region-scale climate and ocean drivers. Here we present additional plots to allow a more complete picture of these indicators.

D.1 BASIN-SCALE CLIMATE/OCEAN INDICATORS AT SEASONAL TIME SCALES

These plots show seasonal averages, short-term trends, and short-term averages of the three basin-scale climate forcing indicators shown in the main report in Figure 3.1.1. Notable outcomes include: winter PDO has been above average over the past 5 years; summer PDO has exhibited a negative trend in the recent 5 years; and summer NPGO has been below average over the past 5 years.

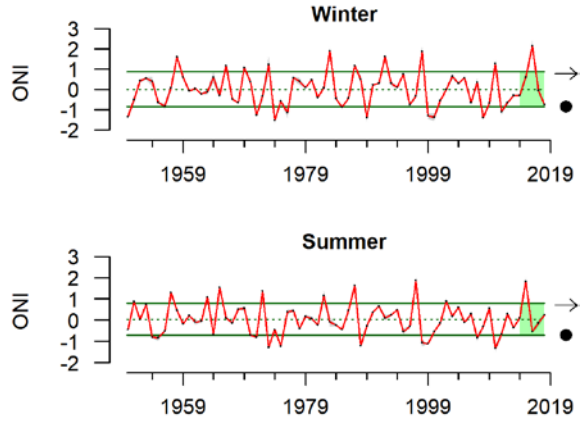

Figure D.1.1 Winter (top, Jan-Mar) and Summer (bottom, July-Sep) values of the Ocean Nino Index. Lines, colors, and symbols are as in Fig.1.

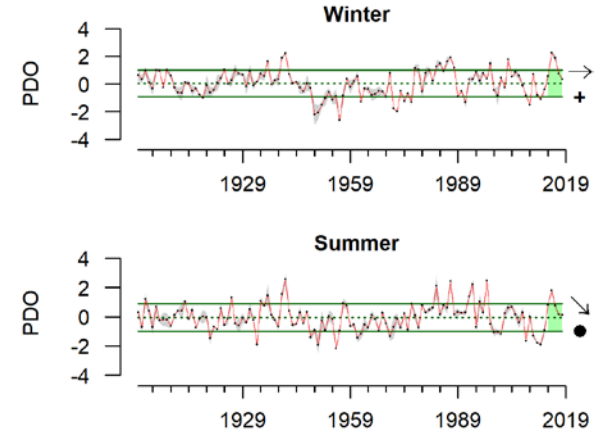

Figure D.1.2 Winter (top, Jan-Mar) and Summer (bottom, July-Sep) values of the Pacific Decadal Oscillation Index. Lines, colors, and symbols are as in Fig.1.

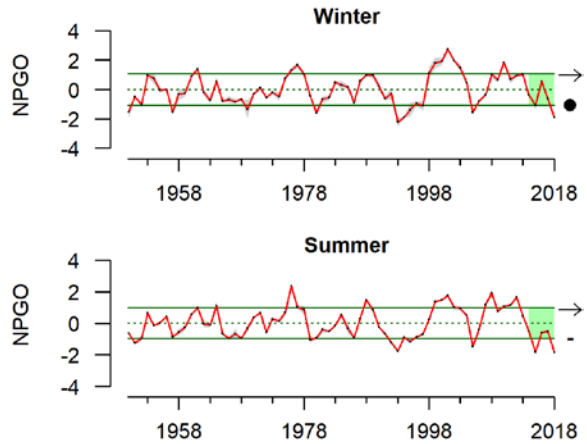

Figure D.1.3 Winter (top, Jan-Mar) and Summer (bottom, July-Sep) values of the North Pacific Gyre Oscillation Index. Lines, colors, and symbols are as in Fig.1.

D.2 ASSESSING THE OCCURRENCE OF MARINE HEATWAVES (MHWs)

Not all warm events in the ocean are marine heatwaves, and not all marine heatwaves in the North Pacific affect the CCE. In the Section 3.1 of the main body of the report, we described a warming event that occurred in the North Pacific in late 2018. Many news media outlets reported that this was a potential return of the "Blob," the popular name for the marine heatwave (MHW) of 2014-2015 that shifted distributions of marine life, altered food webs, and fueled blooms of toxic algae along the West Coast. In a retrospective analysis of SSTa from 1985-2016, Leising (in prep) concluded that a MHW should be defined as waters where the SSTa is >2 s.d. above 0 for the long-term SSTa time series at a particular location. Furthermore, for a MHW to affect coastal waters of the CCE in a similar way to that of the 2014-2015 event, the anomalous feature should be greater than 500,000 km^2 in area, and last for > 60 days. Although the feature in late 2018 surpassed the area threshold (the horizontal black line in Figure D.2.1), it did not surpass the duration threshold (i.e., it was below the shaded box in Figure D.2.2; see also the December 2018 map panel in Figure 3.1.3). Similarly, one of the warm features observed during 2017 surpassed the duration threshold but did not surpass the area threshold (Figure D.2.2).

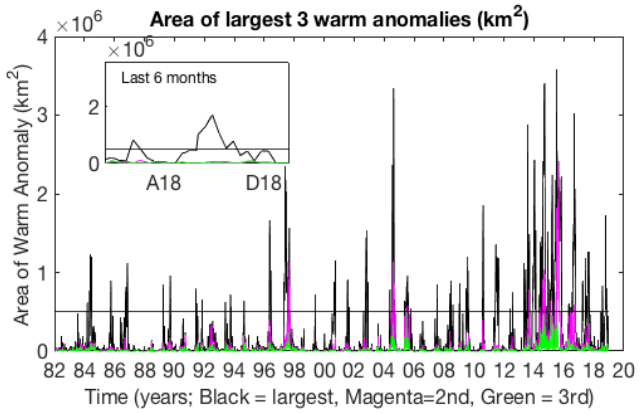

Figure D.2.1 Area of North Pacific warm SST anomalies >2 s.d. versus time. Because multiple anomalies can be present, black is the largest anomaly, magenta is the second largest and green is the third largest. The horizontal line represents 500,000 km^2, the area threshold for features likely to impact the coastal region of the CCE. The inset, showing the time period of June-December 2018, illustrates the increase and collapse of the warm area shown in Figure 3.1.3. Data courtesy of Dr. Andrew Leising (NOAA, SWFSC).

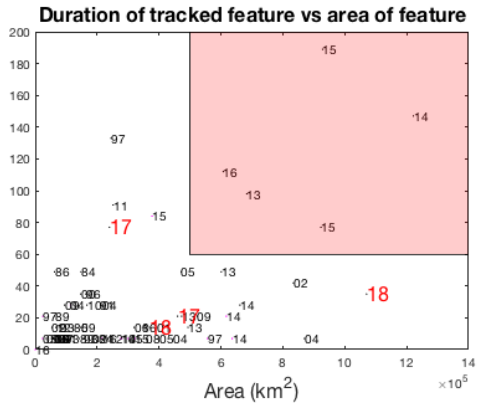

Figure D.2.2 Plot of MHW duration (days) vs area (km^2). The shaded area represents conditions that impacted the coastal region during the 2014-2016 event. Symbols represent the years in which an event occurred (e.g., "18" = 2018). Duplicate numbers may represent multiple distinct MHW areas in the same year, or the within-year evolution of a MHW in the same area. Data courtesy of Dr. Andrew Leising (NOAA, SWFSC).

D.3 SEASONAL TRENDS IN DISSOLVED OXYGEN AND OCEAN ACIDIFICATION INDICATORS

The first series of plots in this section shows time series of summer and winter averages for dissolved oxygen (DO) data off Newport, OR (stations NH05 and NH25) and in the Southern California Bight (stations CalCOFI 90.90 and CalCOFI 93.30). The second series shows summer and winter averages of aragonite saturation state (an ocean acidification indicator) off Newport.

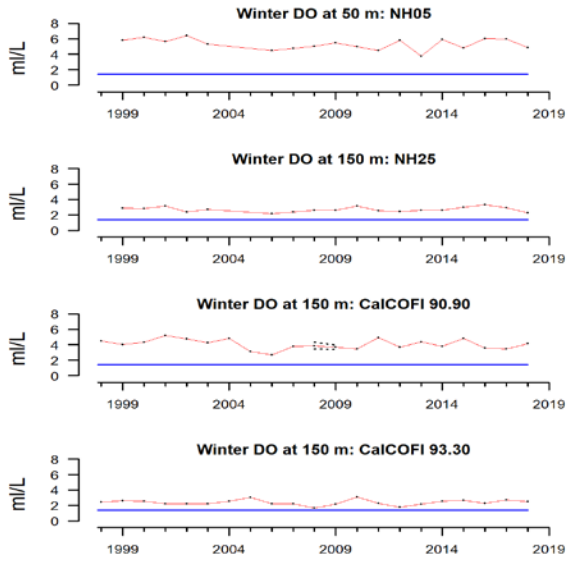

Figure D.3.1 Winter (top, Jan-Mar) dissolved oxygen (DO) at 150 m depth off of Oregon, 1999-2018 and southern California, 1998-2018. Stations NH25 and 93.30 are < 50 km from the shore; station 90.90 is >300 km from shore. Blue line indicates hypoxic threshold of 1.4 ml O2 per L. Lines, colors, and symbols are as in Fig.1.

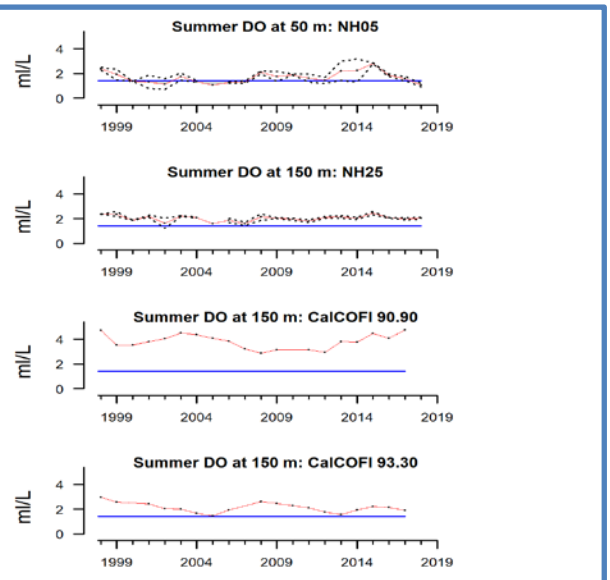

Figure D.3.2 Summer (Jul-Sep) dissolved oxygen (DO) at 50-m and 150 m depth off of Oregon, 1999-2018 and southern California, 1998-2018. Stations NH05, NH25 and 93.30 are < 50 km from the shore; station 90.90 is >300 km from shore. Blue line indicates hypoxic threshold of 1.4 ml O2 per L. Lines, colors, and symbols are as in Fig.1.

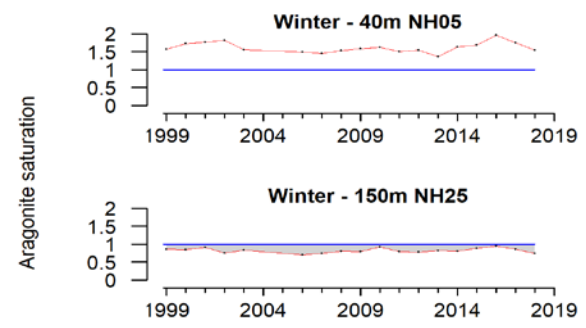

Figure D.3.3 Winter (Jan-Mar) aragonite saturation values at two stations off of Newport, OR, 1999-2018. Blue line indicates saturation state of omega = 1. Dotted lines indicate +/- 1.0 s.e. Lines, colors, and symbols are as in Fig.1.

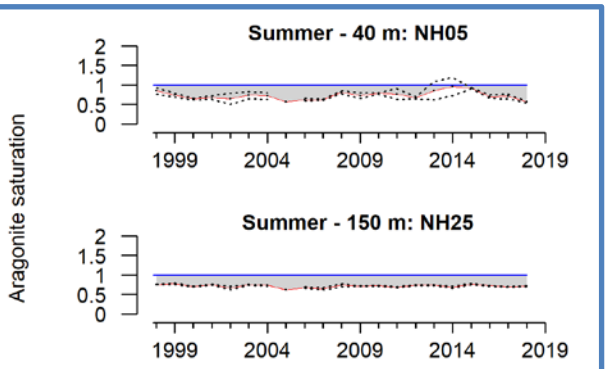

Figure D.3.4 Summer aragonite saturation values at two stations off of Newport, OR, 1998,2018. Blue line indicates saturation state of omega = 1. Dotted lines indicate +/- 1.0 s.e. Lines, colors, and symbols are as in Fig.1.

Appendix E DOMOIC ACID ON THE WASHINGTON COAST

Domoic acid is a toxin produced by several species of the cosmopolitan diatom genus *Pseudo-nitzschia.* Because domoic acid can cause amnesic shellfish poisoning in humans, shellfish fisheries (including the recreational razor clam and commercial Dungeness crab fisheries) are closed when concentrations exceed regulatory thresholds for human consumption. Razor clams can accumulate and retain domoic acid for up to a year following harmful algal blooms (HABs) of *Pseudo-nitzschia* and they are good indicators of HAB dynamics in the coastal ocean, providing an accurate record the arrival and intensity of HAB events on beaches. Related annual losses to Washington coastal economies have reached $24.4 million (Dyson and Huppert 2010).

Averaged monthly domoic acid values in razor clams from six sites along the Washington coast from 1991 through 2018 are shown in Figure E.1. The concentrations of domoic acid at the central Washington (Quinault) versus southern Washington (Long Beach) sites can be influenced by the transport of *Pseudo-nitzschia* and domoic acid from different offshore retention sites, including the Juan de Fuca eddy (at the border of US and Canada) and Heceta Bank (off Newport, Oregon) (Trainer et al. 2002; Hickey et al. 2013). The level of toxicity can also be influenced by the directional flow of the Columbia River plume that can help transport *Pseudo-nitzschia* and domoic acid from the south, northward along the Washington coast. The plume can also serve as a protective barrier by preventing offshore toxins from reaching beaches.

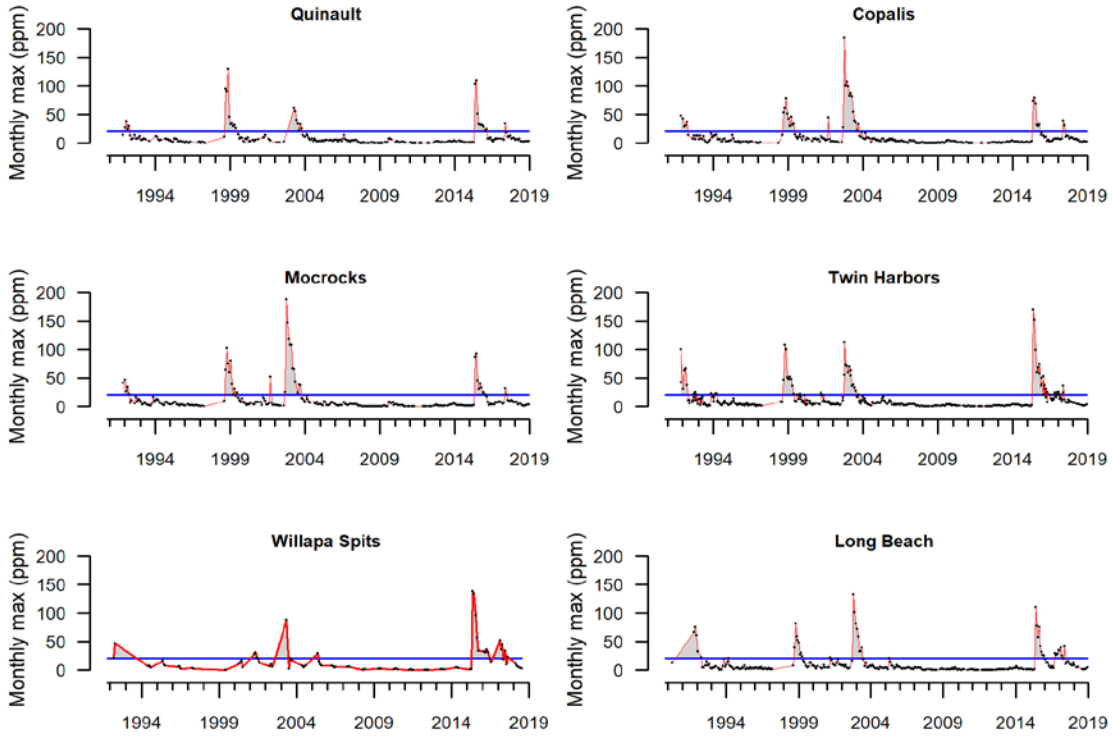

Figure E.1 Monthly maximum domoic acid concentration (ppm) in razor clams through 2018. The blue line is the managment threshhold of 20 ppm. Lines, colors, and symbols are as in Fig.1.

Off Washington and Oregon, extremely toxic HABs of *Pseudo-nitzschia* coincide with or closely follow El Niño events or positive PDO regimes and track regional anomalies in southern copepod species (Fisher et al., 2015; McCabe et al. 2016; McKibben et al. 2017). Such events can be seen to have occurred in 1991, 1998, 1999, 2002, 2003, 2015, 2016 and 2017. The 2015 event was the most toxic ever recorded and coincided with the north Pacific marine heatwave.

Appendix F SNOW-WATER EQUIVALENT, STREAMFLOW, AND STREAM TEMPERATURE

Development of habitat indicators in the CCIEA has focused on freshwater habitats. All habitat indicators are reported based on a hierarchical spatial framework. This spatial framework facilitates comparisons of data at the right spatial scale for particular users, whether this be the entire California Current, ecoregions within these units, or smaller spatial units. The framework we use divides the region encompassed by the California Current ecosystem into ecoregions (Figure 2.1b), and ecoregions into smaller physiographic units. Freshwater ecoregions are based on the biogeographic delineations in Abell et al. (2008; see also www.feow.org), who define six ecoregions for watersheds entering the California Current, three of which comprise the two largest watersheds directly entering the California Current (the Columbia and the Sacramento-San Joaquin Rivers). Within ecoregions, we summarized data using evolutionary significant units and 8-field hydrologic unit classifications (HUC-8). Status and trends for all freshwater indicators are estimated using space-time models (Lindgren and Rue 2015), which account for temporal and spatial autocorrelation.

Snow-water equivalent (SWE) is measured using two data sources: a California Department of Water Resources snow survey program (data from the California Data Exchange Center http://cdec.water.ca.gov/) and The Natural Resources Conservation Service's SNOTEL sites across Washington, Idaho, Oregon, and California (http://www.wcc.nrcs.usda.gov/snow/). Snow data (Figure F.1) are converted into SWEs based on the weight of samples collected at regular intervals using a standardized protocol. Measurements at April 1 are considered the best indicator of maximum extent of SWE; thereafter snow tends to melt rather than accumulate. Data for each freshwater ecoregion are presented in Section 3.5 of the main report.

The outlook for snowpack in 2019 is limited to examination of current SWE, an imperfect correlate of SWE in April due to variable atmospheric temperature and precipitation patterns. SWE as of February 1, 2019 was below the long-term median throughout much of Washington, Oregon and Idaho, but at or slightly above the median in the Sierra Nevadas (Figure F.1).

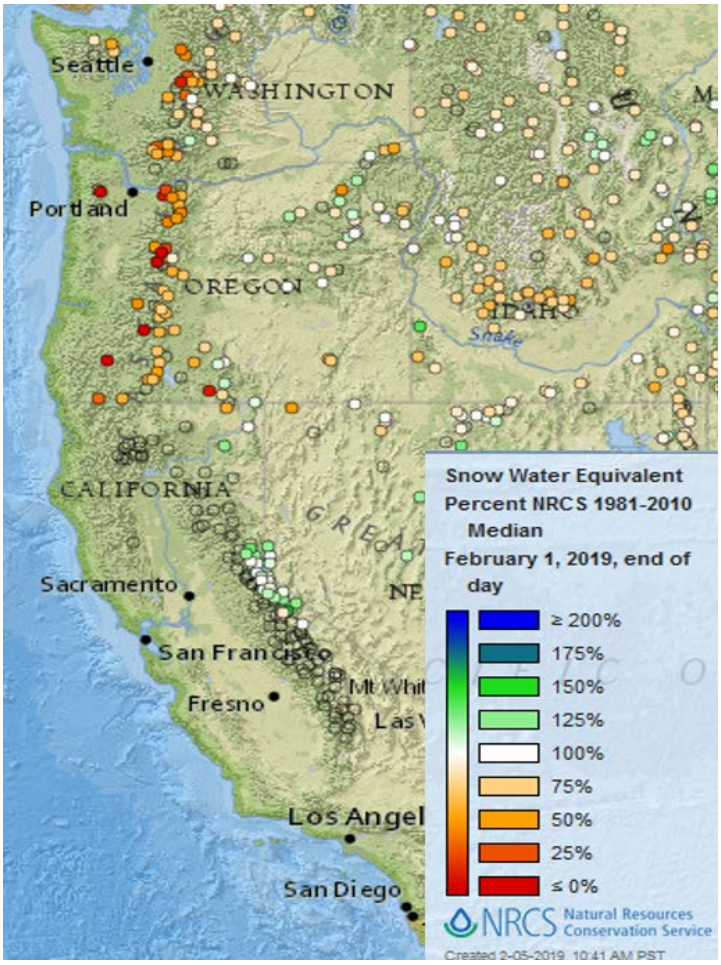

Figure F.1 Mountain snowpack as of February 1, 2019.

Mean maximum temperatures in August were determined from 446 USGS gages with temperature monitoring capability. While these gages did not necessarily operate simultaneously throughout the period of record, at least two gages provided data each year in all ecoregions. Stream temperature records are limited in California, so two ecoregions were combined. Maximum temperatures continued to exhibit strong ecoregional differences (for example, the Salish Sea / Washington Coast streams were much cooler on average than California streams), but the recent 5 years have been marked by largely average values region-wide. The exception is the Salish Sea and Washington Coast, which has much higher temperatures in the last five years compared to the period of record (Figure F.2). Most ecoregions exhibit long-term increasing trends in maximum temperature going back to the 1980's and 1990's.

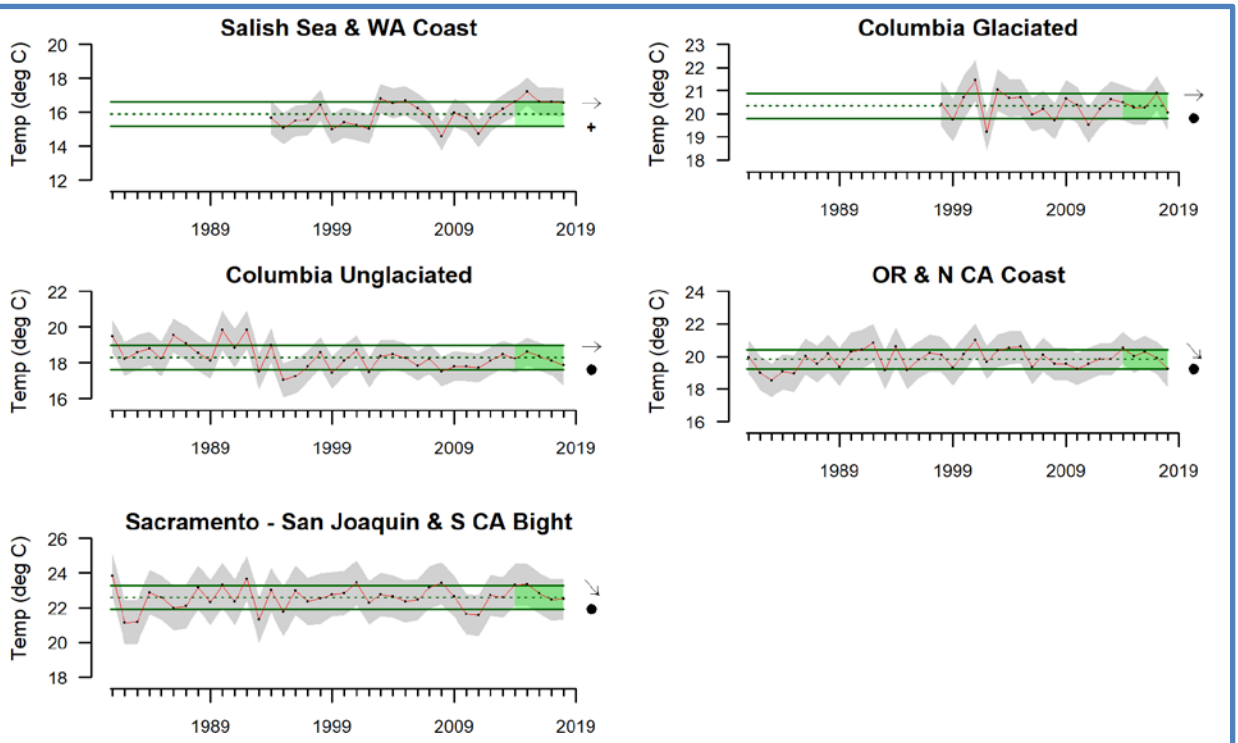

Figure F.2 Mean maximum stream temperature in August measured at 466 USGS gauges in six ecoregions from 1981-2018. Gages include both regulated (subject to hydropower operations) and unregulated systems, although trends were similar when these systems were examined separately. Lines, colors, and symbols are as in Fig.1.

Streamflow is measured using active USGS gages (http://waterdata.usgs.gov/nwis/sw) with records that meet or exceed 30 years in duration. Average daily values from 213 gages were used to calculate both annual 1-day maximum and 7-day minimum flows. These indicators correspond to flow parameters to which salmon populations are most sensitive. We use standardized anomalies of streamflow time series from individual gages.

Across ecoregions of the California Current, both minimum and maximum streamflow anomalies have exhibited some variability in the most recent five years. Minimum stream flows have exhibited fairly consistent patterns across all ecoregions (Figure F.3, see Figure F.5 for flows by ESU). Most all ecoregions demonstrated a decline in low flows over the last 5-8 years with an uptick in 2017 and average or below-average minimum flows in 2018. Little variation exists for rivers in the Southern California Bight, and their minimum flows have been among the ecoregion's lowest on record for many years. For maximum stream flows (Figure F.4 see Figure F.6 for flows by ESU), most ecoregions except the Salish Sea / Washington Coast and the Columbia Glaciated experienced declines in 2018 relative to 2017. Due to high short-term variability, most ecoregions had no significant trends in the past 5 years; the exception was

the Columbia Glaciated ecoregion, which has seen an increase in maximum flows although its recent 5-year average remains within 1 s.d. of the long-term average.

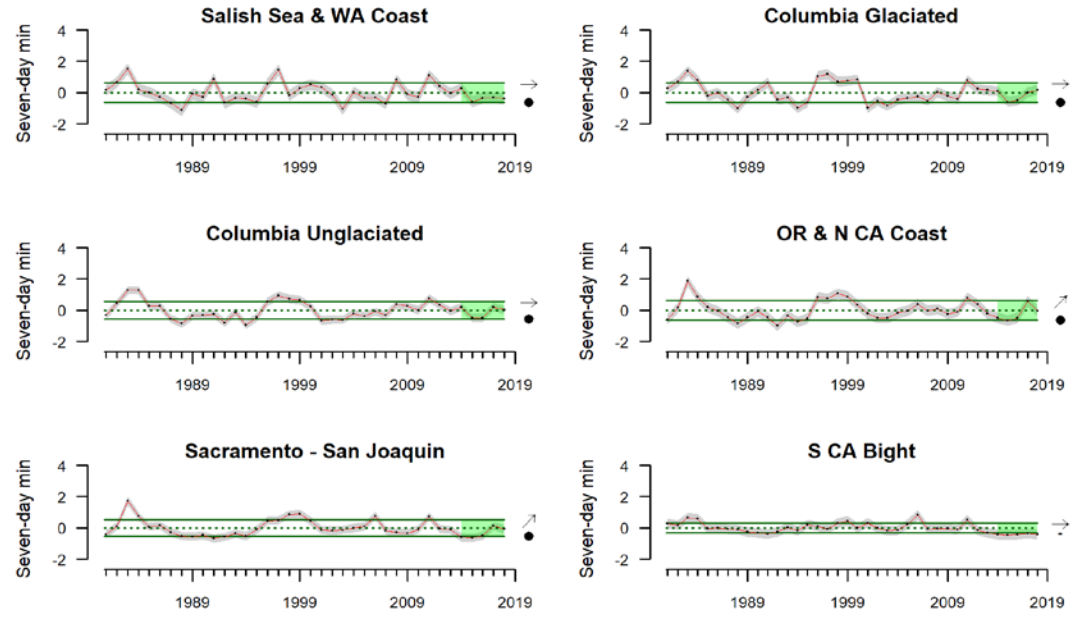

Figure F.3 Anomalies of the 7-day minimum streamflow measured at 213 gauges in six ecoregions. Gages include both regulated (subject to hydropower operations) and unregulated systems, although trends were similar when these systems were examined separately. Lines, colors, and symbols are as in Fig.1.

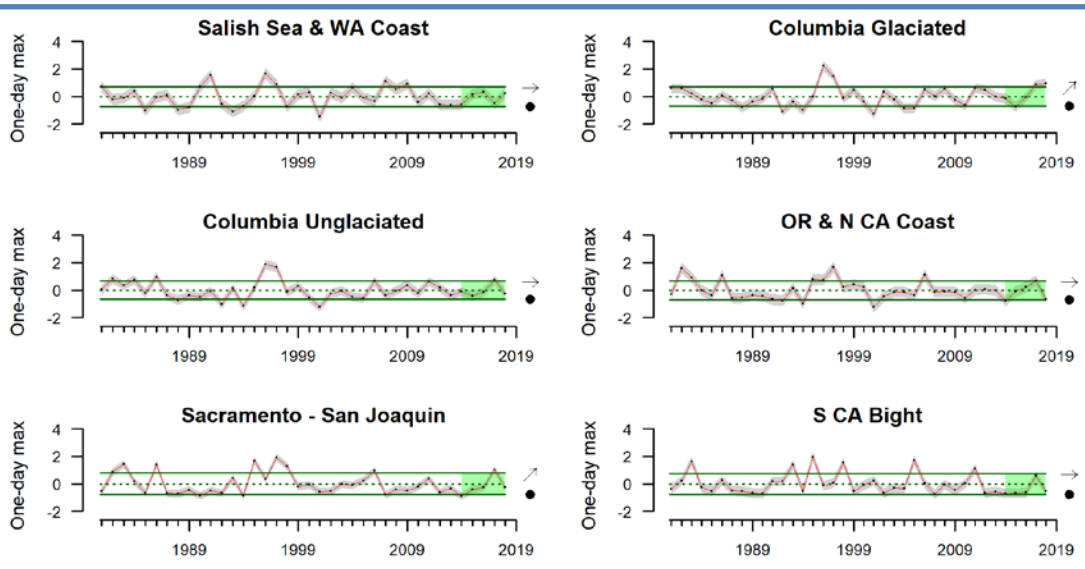

Figure F.4 Anomalies of the 1-day maximum streamflow measured at 213 gauges in six ecoregions. Gages include both regulated (subject to hydropower operations) and unregulated systems, although trends were similar when these systems were examined separately. Lines, colors, and symbols are as in Fig.1.

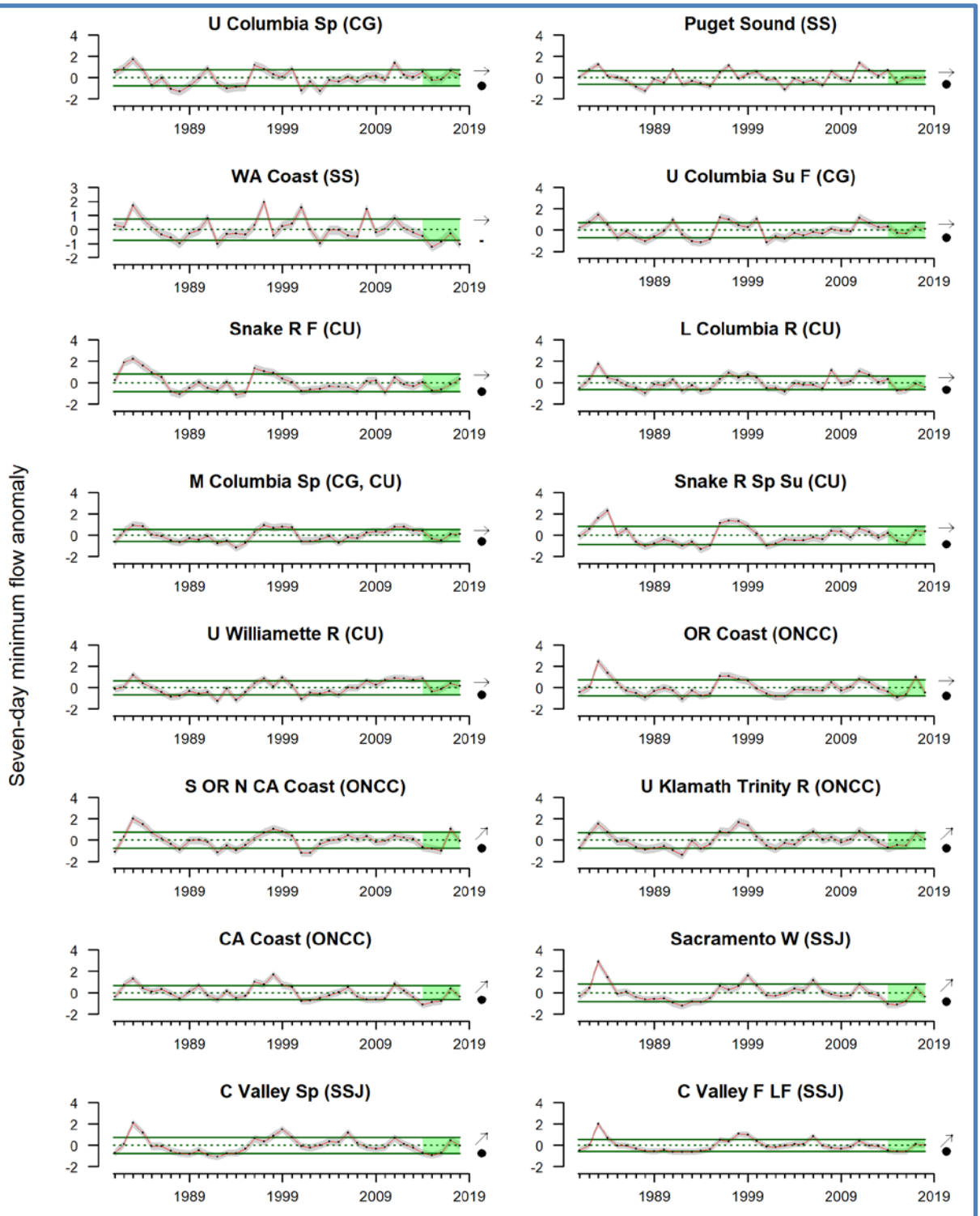

Figure F.5 Anomalies of the 7-day minimum streamflow measured at 213 gauges in 22 Chinook salmon ESUs. Gages include both regulated (subject to hydropower operations) and unregulated systems, although trends were similar when these systems were examined separately. Lines, colors, and symbols are as in Fig.1.

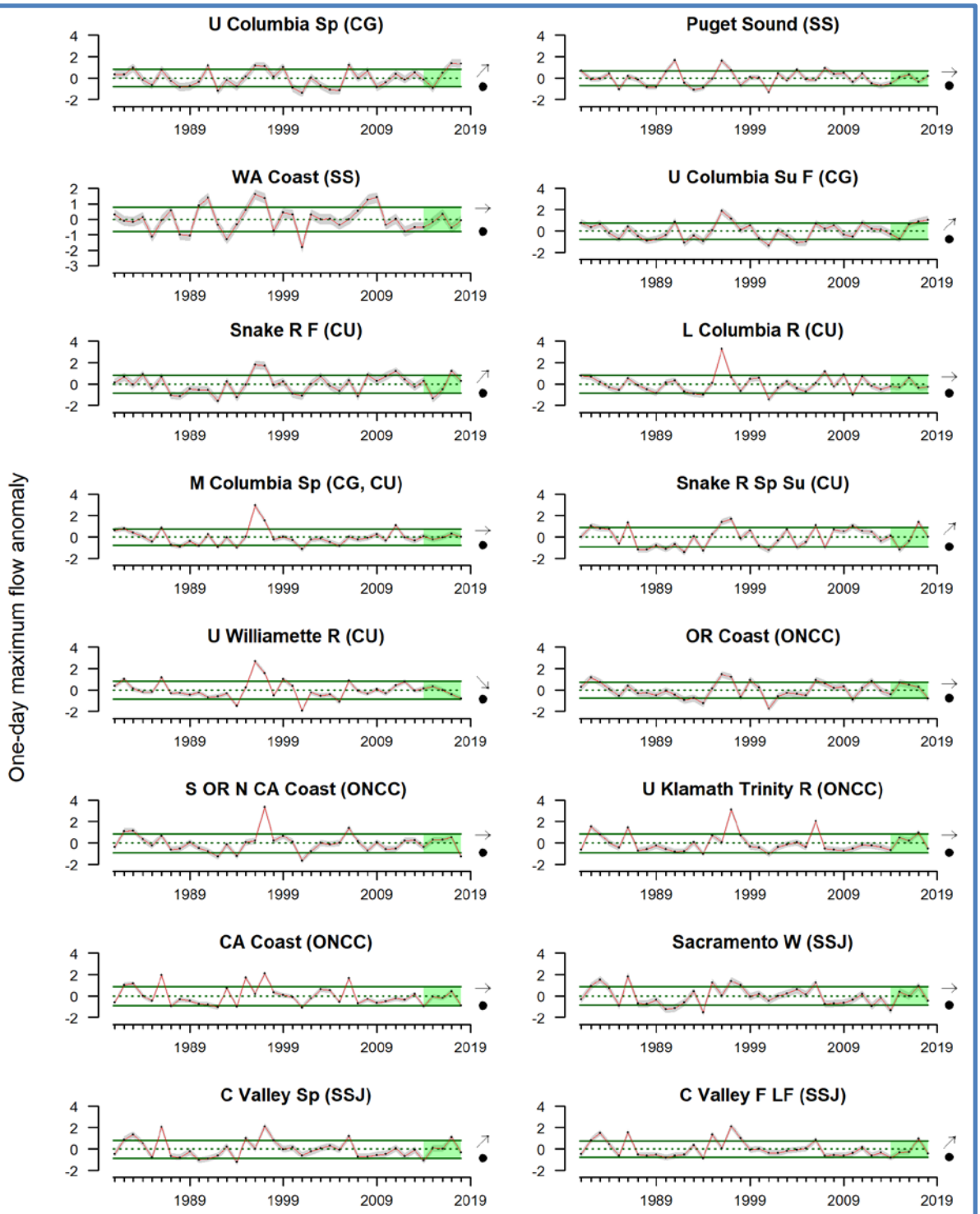

Figure F.6 Anomalies of the 1-day maximum streamflow measured at 213 gauges in 22 Chinook salmon ESUs. Gages include both regulated (subject to hydropower operations) and unregulated systems, although trends were similar when these systems were examined separately. Lines, colors, and symbols are as in Fig.1.

Appendix G REGIONAL FORAGE AVAILABILITY

Species-specific trends in forage availability are based on research cruises in the northern, central, and southern portions of the CCE (Figure 2.1). Section 4.2 of the main body of this report describes forage community dynamics using a new cluster analysis method that we implemented this year. There are some differences in which species were used in those analyses and which species appear in this Appendix, plotted in time series. This discrepancy is because we did not have time to fully update this Appendix due to the recent federal government shutdown. There will be better correspondence between the main body and these time series in the future.

G.1 NORTHERN CALIFORNIA CURRENT FORAGE

The Northern CCE survey (known as the "Juvenile Salmon Ocean Ecology Survey") occurs in June and targets juvenile salmon in surface waters off Oregon and Washington, but also collects adult and juvenile (age 1+) pelagic forage fishes, market squid, and gelatinous zooplankton (*Aequorea* sp., *Chrysaora* sp.) with regularity. In 2018, catches of juvenile salmon generally increased from lows in previous years, particularly the very poor catches of 2017 (Figure G.1.1). Catches of market squid and jellyfish also increased. Catches of jack mackerel declined after several years of increases.

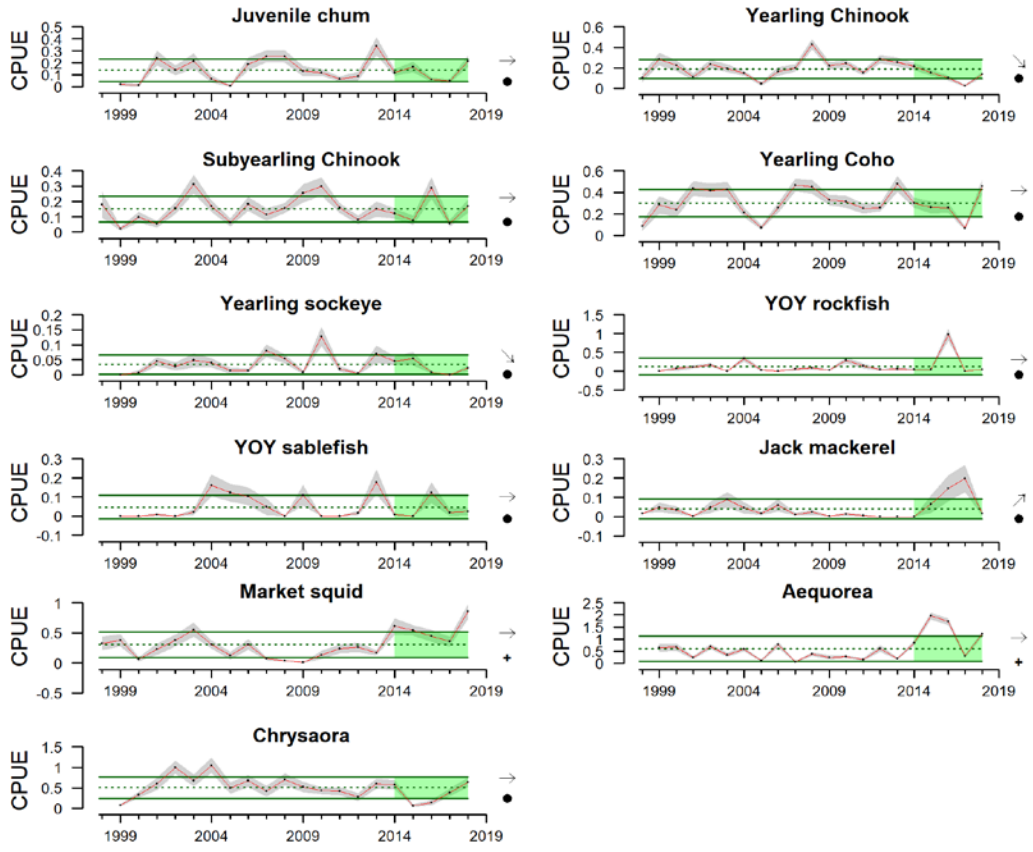

Figure G.1.1 Geometric mean CPUEs (Log10(no. km-1+ 1)) of key forage groups in the Northern CCE, from surface trawls conducted as part of the BPA Plume Survey, 1998 - 2018 . Lines, colors, and symbols are as in Fig.1.

G.2 CENTRAL CALIFORNIA CURRENT FORAGE

The Central CCE forage survey (known as the "Juvenile Rockfish Survey") samples this region using midwater trawls, which not only collect young-of-the-year (YOY) rockfish species, but also a variety of other YOY and adult forage species, market squid, adult krill, and gelatinous zooplankton. Time series presented here are from the "Core Area" of that survey (see Figure 2.1c in the Main Report). In 2018, catches of adult anchovy increased remarkably (Figure G.2.1). and there were also increases in YOY anchovy, YOY sardine and discernible catches of adult sardine for the first time in many years. Other notable results were large catches of krill and market squid, dramatic increases in jellyfish (*Aurelia* sp., *Chrysaora*), and a decline in catches of pyrosomes.

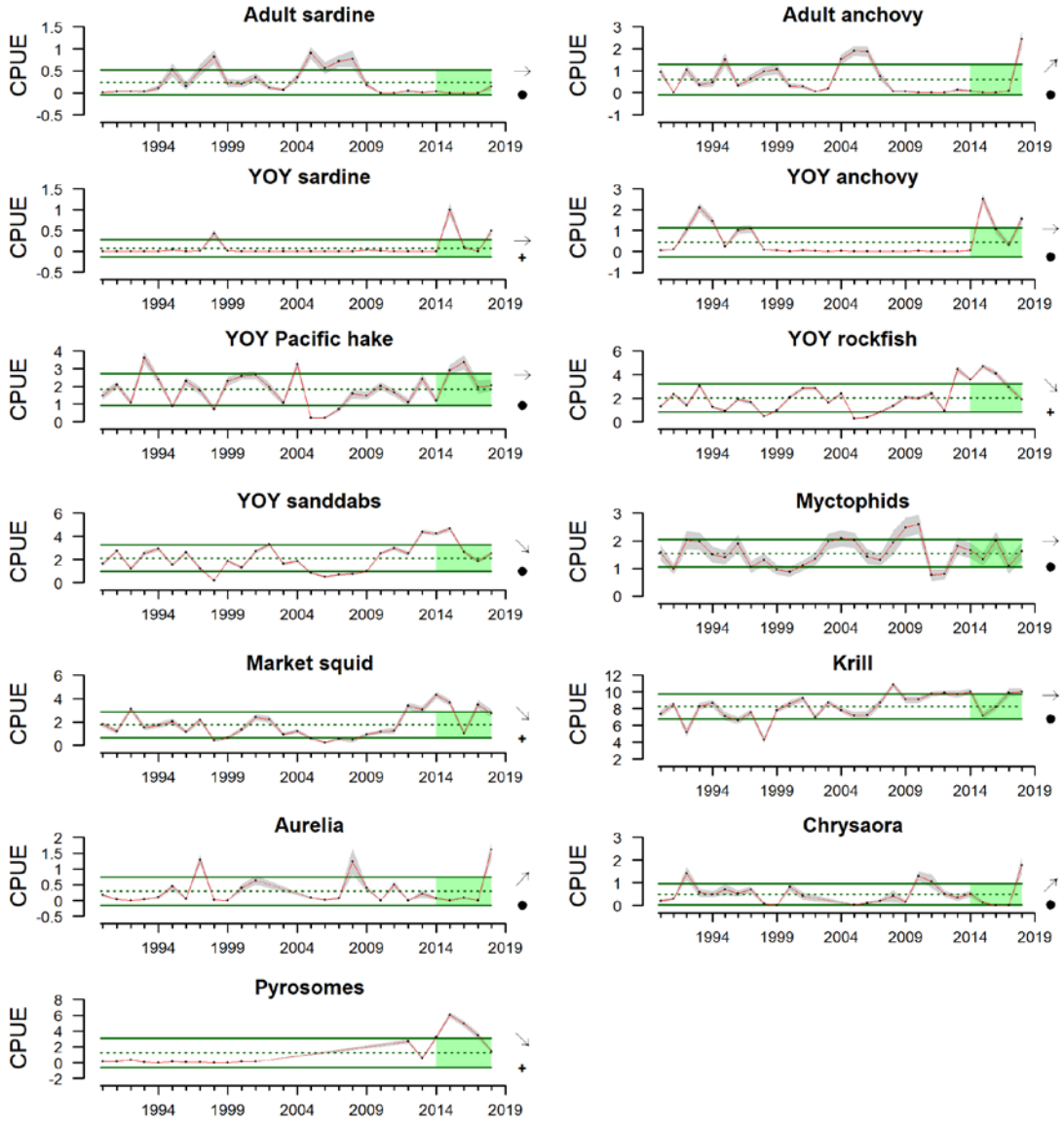

Figure G.2.1 Geometric mean CPUEs (mean (ln catch+1)) of key forage groups in the Central CCE, from the SWFSC Rockfish Recruitment and Ecosystem Assessment during 1990-2018. Lines, colors, and symbols are as in Fig.1., with the exception that shaded errors in these figures represent standard deviations of log transformed catches.

G.3 SOUTHERN CALIFORNIA CURRENT FORAGE

The abundance indicators for forage in the Southern CCE come from fish and squid larvae collected in the spring across all core stations of the CalCOFI survey using oblique vertical tows of fine mesh Bongo nets to 212 m depth. The survey collects a variety of fish and invertebrate larvae (<5 d old) from several taxonomic and functional groups. Larval data are indicators of the relative regional abundances of adult forage fish, such as sardines and anchovy, and other species, including certain groundfish, market squid, and mesopelagic fishes. Noteworthy observations from 2018 surveys include the ongoing increase in relative abundance of anchovy, and an increase in market squid after many years of poor catches (Figure G.3.1). There were also clear declines in larval shortbelly rockfish and jack mackerel.

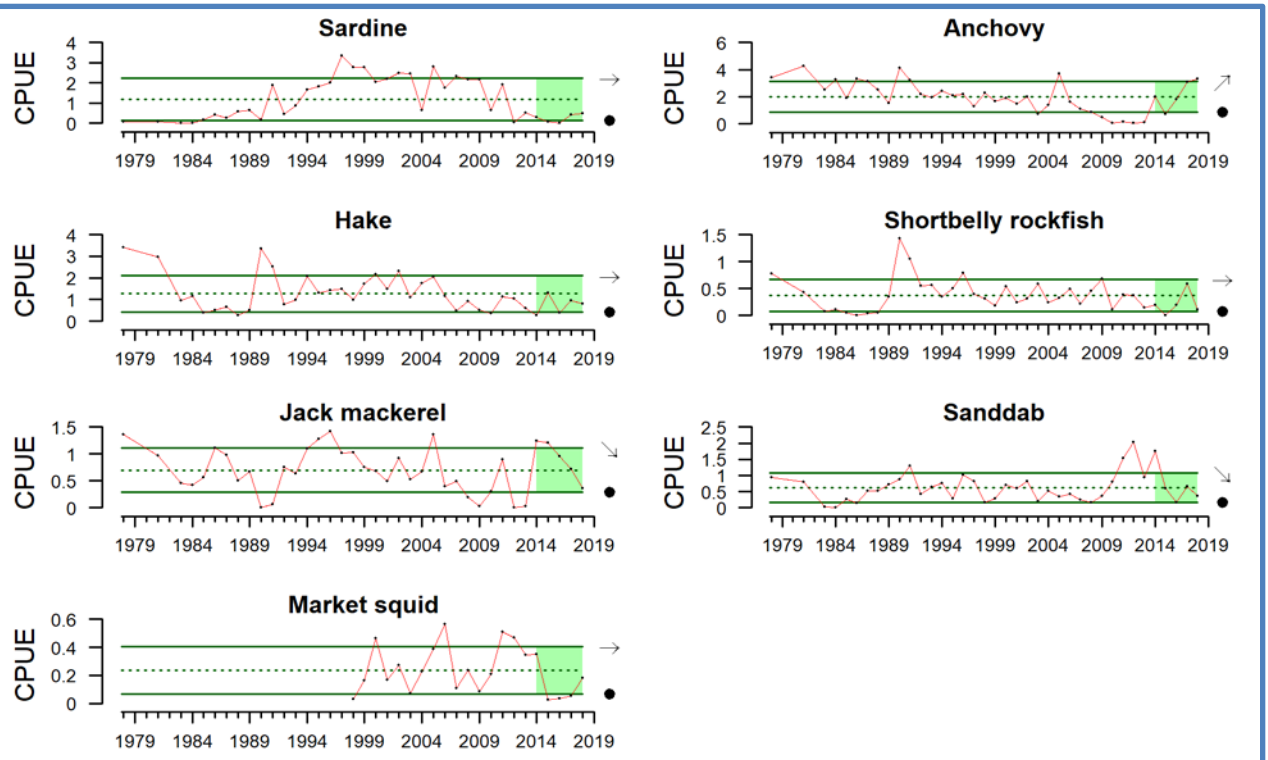

Figure G.3.1 Mean abundance (ln(abundance+1)) of the larvae of key forage species in the southern CCE, from spring CalCOFI surveys during 1978-2018. Lines, colors, and symbols are as in Fig.1.

Appendix H CHINOOK SALMON ESCAPEMENT INDICATORS

Population-specific status and trends in Chinook salmon escapement are provided in Section 4.3 of the Main Report. Figure 4.3.1 uses a quad plot to summarize recent escapement status and trends relative to full time series. These plots are useful for summarizing large amounts of data, but they may hide informative short-term variability in these dynamic species. The full time series for all populations are therefore presented here. We note again that these are escapement numbers, not run-size estimates, which take many years to develop. Status and trends are estimated for the most recent 10 years of data (unlike 5 years for all other time series in this Report) in order to account for the spatial segregation of successive year classes of salmon.

H.1 CALIFORNIA CHINOOK SALMON ESCAPEMENTS

The Chinook salmon escapement time series from California include data from as recent as 2017 extending back over 20 years, with records for some populations (Central Valley Late Fall; Southern Oregon/Northern California Coastal; Klamath Fall) stretching back to the 1970s. No population showed near-term trends (Figure H.1.1), but escapement estimates for several populations in 2017 were >1 s.d. below the long-term mean for their respective time series. Many populations have experienced decreasing escapements from 2013-2017 after some increases in the preceding years.

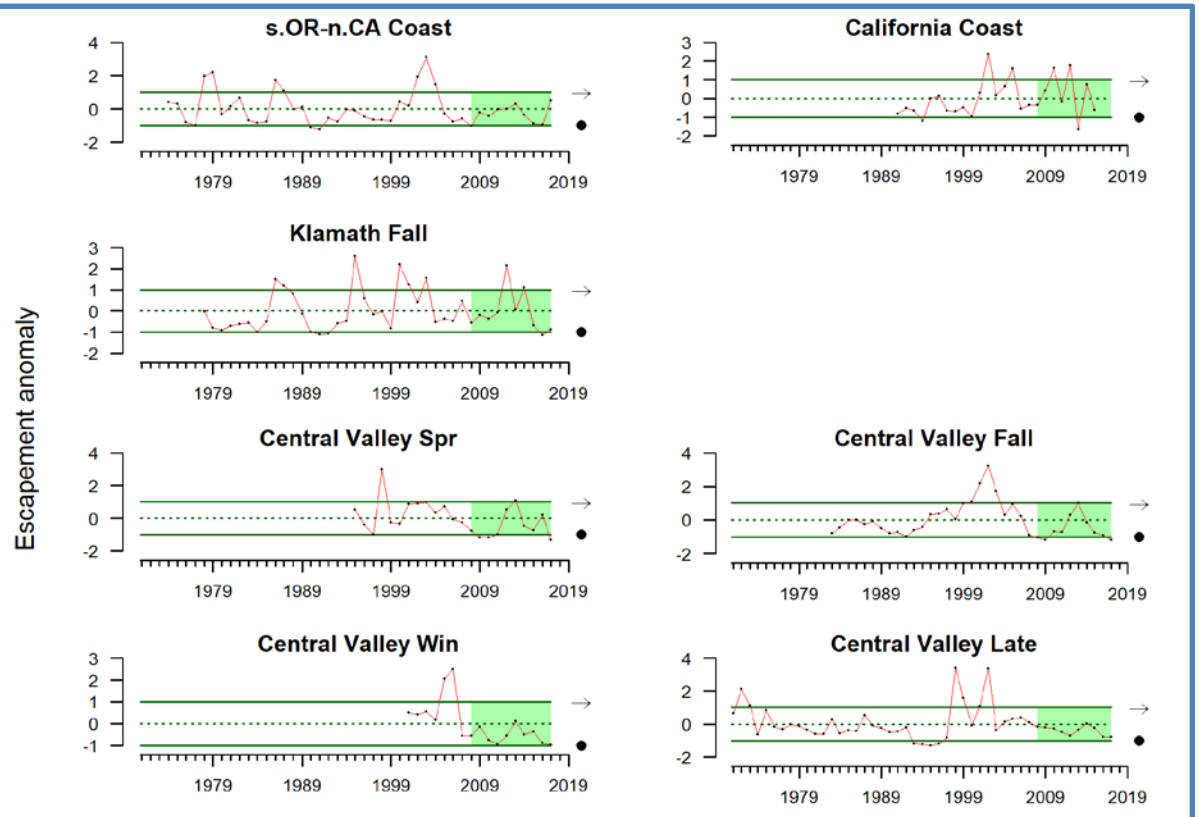

Figure H.1.1 Anomalies of escapement of wild Chinook salmon in California watersheds through 2017. Lines, colors, and symbols are as in Fig.1.

H.2 WASHINGTON/OREGON/IDAHO CHINOOK SALMON ESCAPEMENTS

The escapement time series used for Chinook salmon populations from Washington, Idaho, and Oregon extend back for up to 40+ years, and the most recent data currently available are through 2017 (Figure H.2.1). Stocks are often co-managed and surveyed by a variety of state and tribal agencies. Snake River Fall Chinook in 2017 were above the long-term mean for the eighth year in a row, and the 10-year average is >1 s.d. greater than the long-term mean. Other populations' recent averages are within 1 s.d. of the long-term mean. The Snake River Fall and Willamette Spring ESUs have shown improving escapement trends in the last ten years.

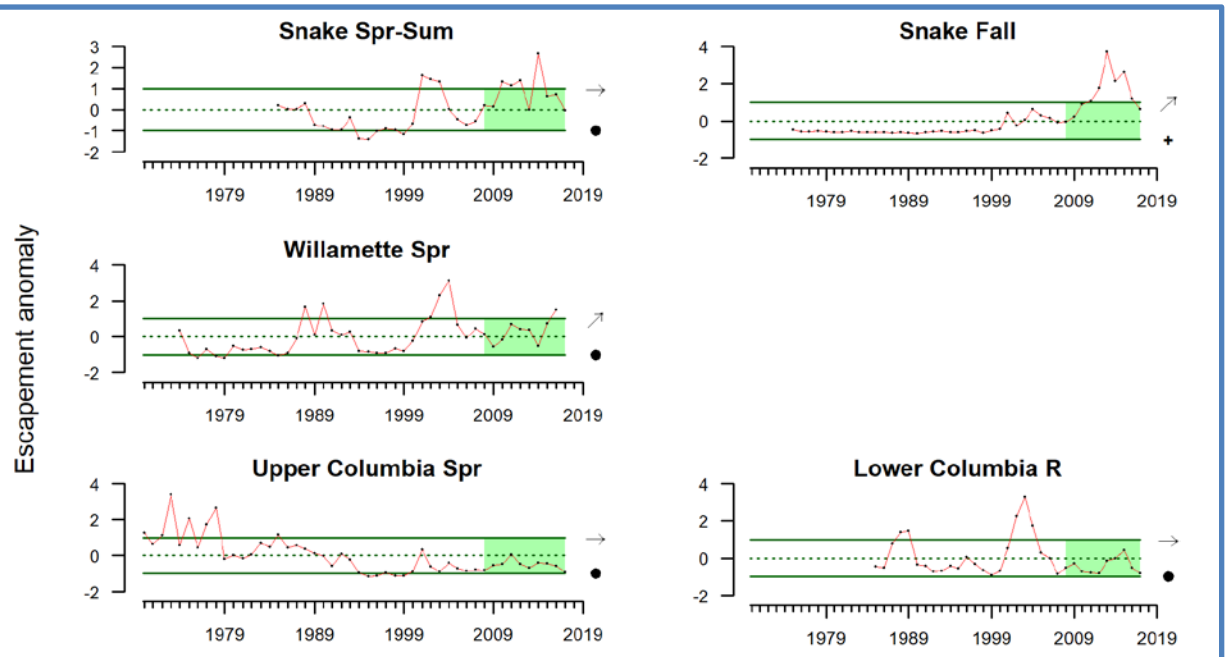

Figure H.2.1 Anomalies of escapement of wild Chinook salmon in Washington, Oregon, and Idaho watersheds through 2017. Lines, colors, and symbols are as in Fig.1.

H.3 FORECASTS OF 2019 SALMON RETURNS TO THE COLUMBIA AND OREGON PRODUCTION INDEX AREA

The main body of the report features the "stoplight" table (Table 4.3.1) that shows a ranking of indicators of conditions affecting marine growth and survival of Chinook salmon returning to the Columbia Basin, and coho salmon returning to streams in the Oregon Production Index (OPI) area. The stoplight table provides a qualitative perspective on the likely relative run sizes of salmon in the current year, based on indicator measures in the years since returning salmon originally went to sea as smolts. A somewhat more quantitative analysis based on the stoplight table analysis is depicted at the right. Here, annual Chinook salmon counts at Bonneville Dam (Figure H.3.1, top and middle) and OPI coho smolt-to-adult survival (Figure H.3.1, bottom) over the last two decades are plotted against the aggregate mean ranking of indicators in the stoplight table, with 1-year lag for coho and 2-year lag for Chinook. The highest ranking years at the left tend to produce the highest returns and survival. The 2017 stoplight indicators had a relatively low mean rank of 14.5, which would predict relatively low counts of 101,500 Spring and 277,400 Fall Chinook salmon at Bonneville Dam in 2019 (solid arrow, Figure H.3.1, top and middle panels, solid arrows). The 2018 stoplight indicators had a higher mean rank of 11.6, which would predict smolt-to-adult survival of 2.2% for OPI coho in 2019 (Figure H.3.1, bottom, solid arrow). A stoplight indicator ranking of 11.6 in 2018 also corresponds to 2020 Bonneville counts of 127,100 Spring Chinook and 356,800 Fall Chinook (Figure H.3.1, top and middle, dashed arrows). The relationships of past salmon returns to stoplight means explain between 32% (coho) and 55% (Fall Chinook) of variance. This is a fairly simple analysis, however, given that each indicator in the stoplight table is given equal weight.

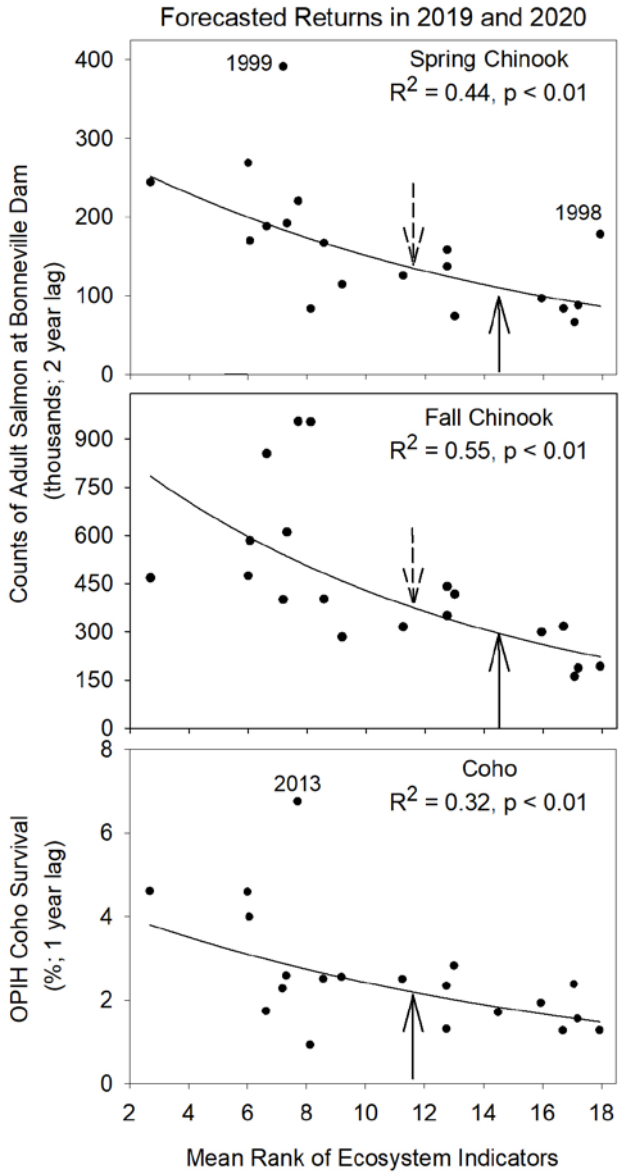

Figure H.3.1. Salmon returns versus the mean rank of ecosystem "stoplight" indicators from Table 4.3.1. Arrows show the forecasted returns of Chinook salmon to Bonneville Dam in 2019 (solid) and 2020 (dashed), and of coho salmon to Oregon coast streams in 2019 (solid). Data courtesy of Dr. Brian Burke (NOAA NWFSC).

A more robust quantitative analysis uses an expanded set of ocean indicators plus principal components analysis and dynamic linear modeling to produce salmon forecasts for the same systems. The principal components analysis essentially is used for weighted averaging of the ocean indicators, reducing the total

number of indicators while retaining the bulk of the information from them. The dynamic linear modeling technique relates salmon returns to the principal components of the indicator data, and the approach used here also incorporates dynamic information from sibling regression modeling. The model fits very well to data for Spring Chinook, Fall Chinook and coho salmon at the broad scales of the Columbia River and the OPI area (Figure H.3.2). Forecasts with 95% confidence intervals suggest 2019 Bonneville counts of Spring Chinook salmon that are similar to 2018 (Figure H.3.2, top), and potential increases of Fall Chinook at Bonneville and coho in the OPI area (Figure H.3.2, middle and bottom). Although these analyses represent a general description of ocean conditions, we must acknowledge that the importance of any particular indicator will vary among salmon species/runs. NOAA scientists and partners are working towards stock-specific salmon forecasts by using methods that can optimally weight the indicators for each response variable in which we are interested (Burke et al. 2013).

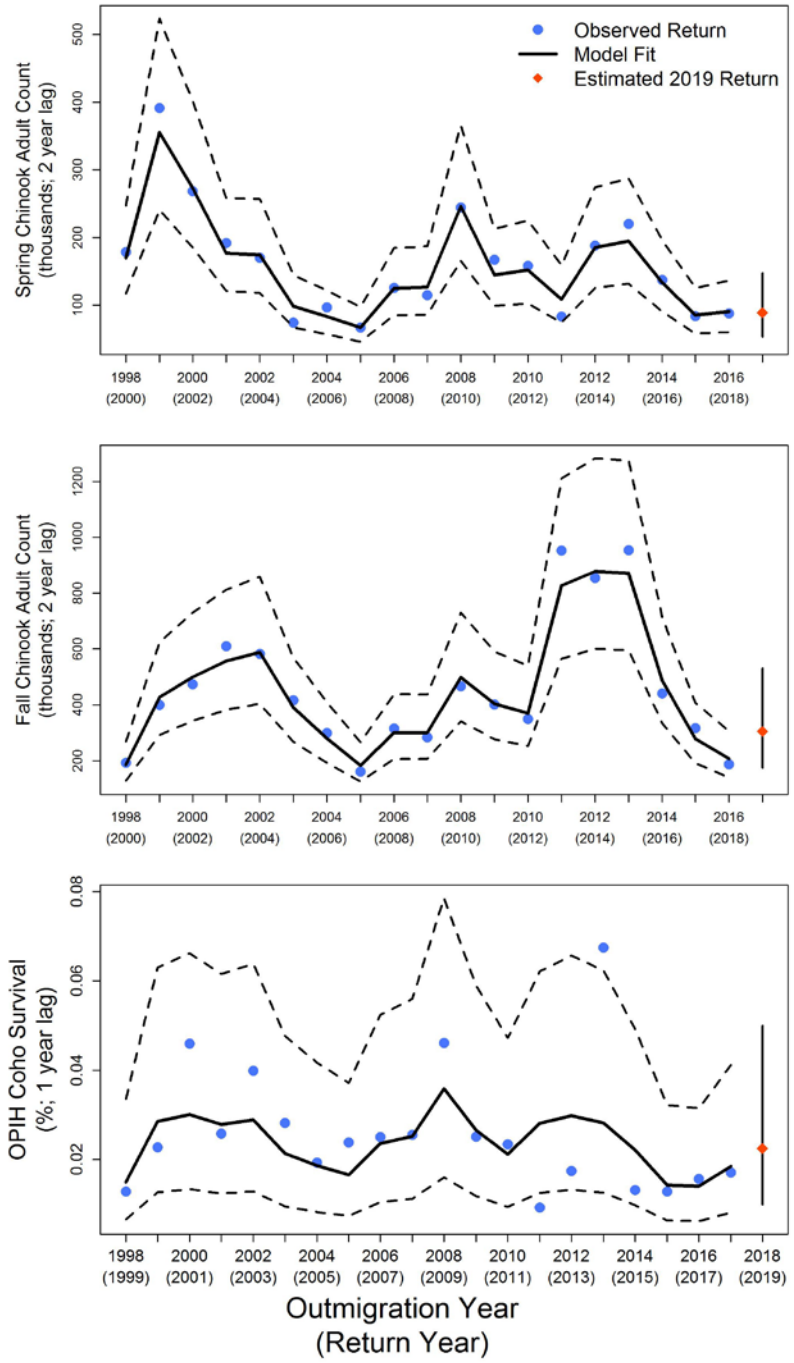

Figure H.3.2. Time series of observed spring Chinook salmon adult counts (top), fall Chinook salmon adult counts (middle), and coho salmon smolt-to-adult survival (bottom) by out-migration year. In each plot, the dark line represents the model fit and lighter lines represent 95% confidence intervals. Forecasts were created from a DLM (Dynamic Linear Models) with log of sibling counts (for the Chinook models only) and first principal component of ocean indicators as predictor variables. Courtesy of Dr. Brian Burke (NOAA, NWFSC).

Appendix I HIGHLY MIGRATORY SPECIES

Highly migratory species are discussed Section 4 of the main document (Figure 4.5.1). The time series for abundance (Figure I.1) and recruitment (Figure I.2) are plotted here for reference. Additional information on how these estimates were derived is provided below the figures.

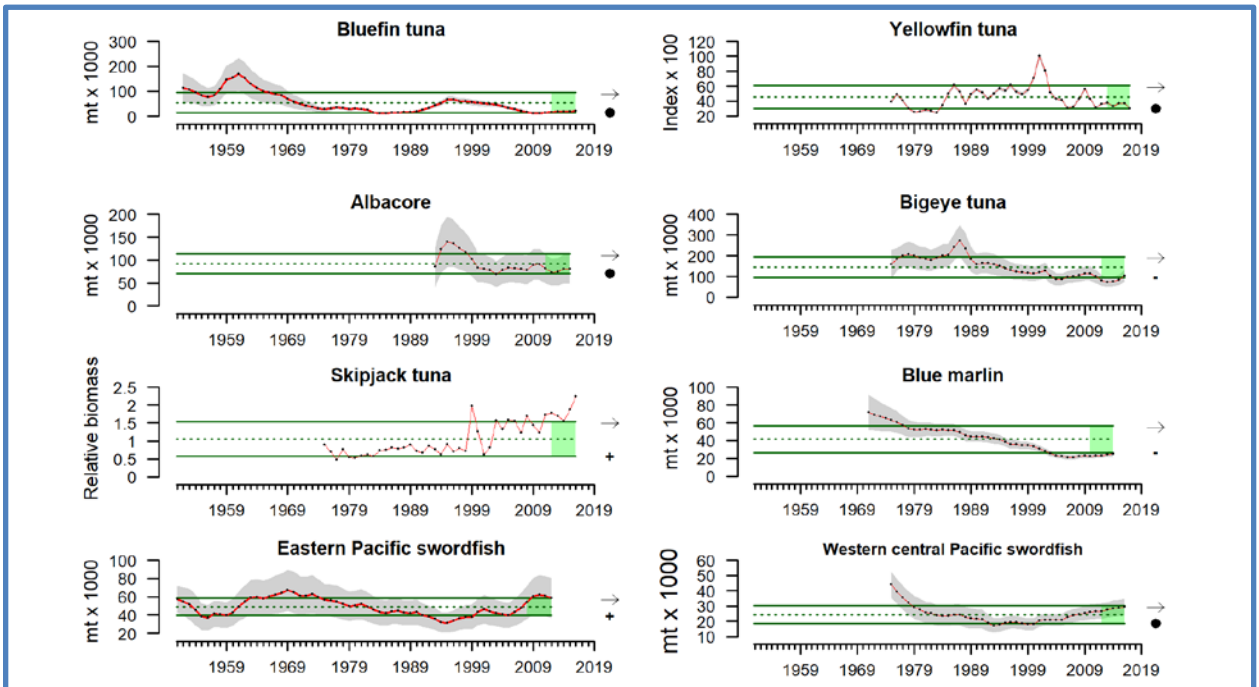

Figure I.1 Biomass for highly migratory species (HMS) in the California current to 2017. Lines, colors, and symbols are as in Fig.1.

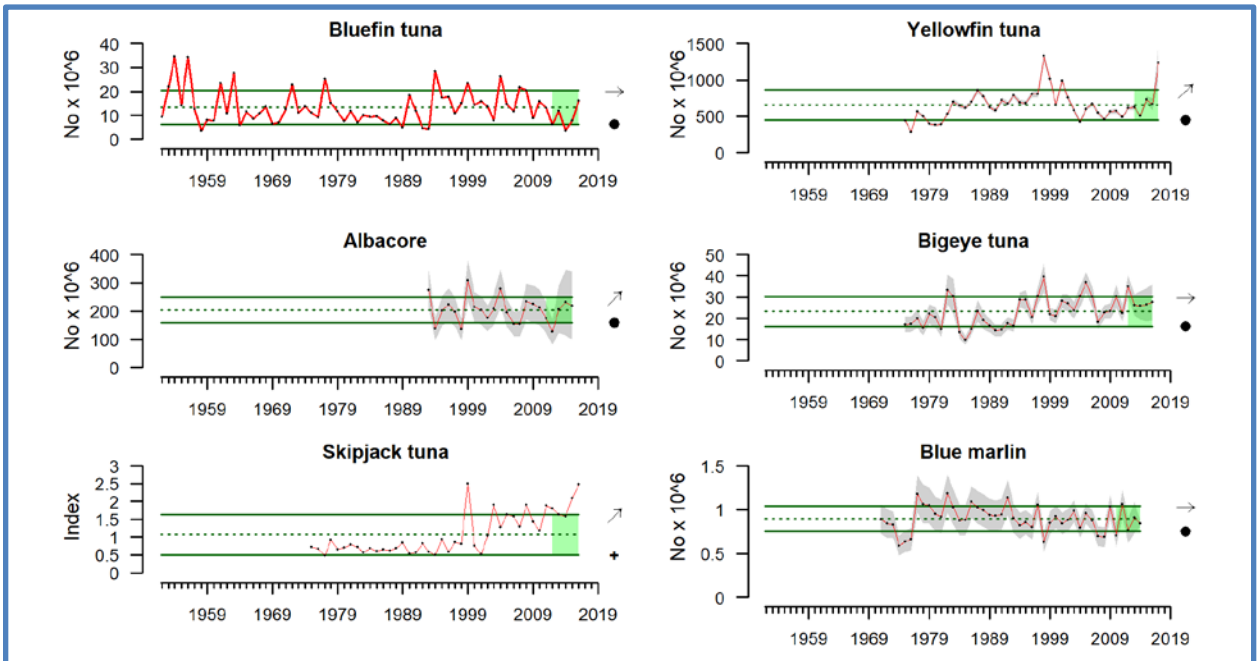

Figure I.2 Recruitment for highly migratory species (HMS) in the California current through 2017. Lines, colors, and symbols are as in Fig.1.

Pacific bluefin tuna

Spawning stock biomass: This index represents modeled spawning stock biomass from the latest (2018) stock assessment report, completed through the International Scientific Committee for Tuna and Tuna-like Species in the North Pacific Ocean (ISC). Pacific bluefin are considered to be one stock throughout the Pacific Ocean, and are fished throughout their range by multiple countries and fishing gears. At present, the majority are caught by purse seine gear. Their population dynamics are assessed using a fully integrated age-structured model (Stock Synthesis v3). The 2018 base-case model was constructed with minimal modifications relative the 2016. The full assessment is available from http://isc.fra.go.jp/reports/stock_assessments.html.

Recruitment: Annual recruitment is derived from the stock assessment model, and is primarily indexed by catches from troll fisheries on age-0 juvenile fish near Japan.

Implications: Declines in spawning stock biomass appeared to cease in 2010, however the stock remains at near-historic low levels (around 3.3% of unfished biomass). While no reference points have been agreed upon, the stock is likely to be overfished, and overfishing may be occurring. Recent recruitment estimates suggest below-average recruitment from 2010-2015, with some increase in 2016. Although recent recruitment estimates are uncertain, due to being informed only by data from the age-0 troll fishery, this CPUE series has been shown to be a good predictor of recruitment in the past.

North Pacific albacore

Spawning stock biomass: This index represents modeled spawning potential biomass from the latest (2017) stock assessment report, completed through the International Scientific Committee for Tuna and Tuna-like Species in the North Pacific Ocean (ISC). North Pacific albacore are considered to be one stock throughout the North Pacific Ocean, although some studies have suggested that a northern and southern stock may be present within the assessment area. They are fished throughout their range by multiple countries, mostly using surface gear (troll and pole and line), as well as pelagic longlines and other gears. Their population dynamics are assessed using an age-, length- and sex-structured model (Stock Synthesis v3). The full assessment is available from http://isc.fra.go.jp/reports/stock_assessments.html.

Recruitment: Estimates of annual recruitment are derived from the stock assessment model.

Implications: Spawning stock biomass has increased slightly in the past few years. The stock is not considered likely to be overfished, and it is not likely that overfishing is currently occurring. Recent recruitment estimates suggest near-average recruitment in the past 5 years, however it should be noted that estimates from terminal model years are highly uncertain.

Swordfish

Spawning biomass: This index represents modeled spawning biomass for the western central Pacific swordfish stocks from the latest (2018) stock assessment report, completed through the International Scientific Committee for Tuna and Tuna-like Species in the North Pacific Ocean (ISC). Swordfish are considered to comprise two stocks in the North Pacific. The western and central Pacific stock is located throughout the entire North Pacific, except for waters off Baja California and Central and South America, which are occupied by the eastern Pacific stock. However, recent electronic tagging of swordfish off the Southern California coast suggests that there may be more mixing of fish between northern and southern regions of the EPO than previously thought. The highest catches of swordfish in the North Pacific are from pelagic longline gears. In 2018, only the western and central North Pacific stock assessment was updated. The assessment is available from http://isc.fra.go.jp/reports/stock_assessments.html.

Implications: Estimates of total stock biomass show a relatively stable population, with a slight decline until the mid-1990s followed by a slight increase since 2000. The base case model indicated that the

WCNPO swordfish stock is not likely overfished and is not likely experiencing overfishing relative to MSY-based or 20% of unfished spawning biomass-based reference points. No long term trend in recruitment is apparent, and recruitment estimates from recent years are around average.

Blue marlin

Spawning stock biomass: This index represents modeled spawning stock biomass from the latest (2016) stock assessment report, completed through the International Scientific Committee for Tuna and Tuna-like Species in the North Pacific Ocean (ISC). Blue marlin are considered to be one stock throughout the Pacific Ocean, and the majority of catch is from pelagic longlines. Their population dynamics are assessed using an age-, length- and sex-structured model (Stock Synthesis v3). The full assessment is available from http://isc.fra.go.jp/reports/stock_assessments.html.

Recruitment: Estimates of annual recruitment are derived from the stock assessment model.

Implications: Spawning stock biomass has been largely stable in the past 5 years, at historically low levels (around 21% of unfished biomass). Despite this, the stock is currently considered to be not overfished, and overfishing is not likely to be occurring. However, the stock is near fully exploited. In recent years, recruitment has been variable around historical mean levels, however it should be noted that estimates from terminal model years are highly uncertain.

Yellowfin tuna

Spawning stock biomass: This series shows the modeled spawning stock biomass index from the 2018 stock assessment, which was an update of the 2017 assessment. Yellowfin tuna are assessed through the Inter-American Tropical Tuna Commission (IATTC), using Stock Synthesis V3.23b. They are assumed to comprise one stock throughout the Pacific, although tagging data suggest considerable regional fidelity. In the eastern Pacific, they are primarily fished in tropical waters, from Baja California south. Indices were provided by C. Minte-Vera (IATTC).

Recruitment: Estimates of recruitment are derived from the assessment model.

Implications: Recruitment has been mostly average or below average until 2014. The most recent annual recruitments (2015-2017) were estimated to be at or above average, but these estimates are highly uncertain. The recruitment estimates for 2017 might be upwardly biased, because of a retrospective pattern already noticed in previous assessments. Spawning stock biomass has been near average or below average since 2003, except during 2008-2010. However, this may increase in the next two years, due to the above-average recruitments of 2015 and 2016, which coincided with the 2014-2016 marine heat wave and El Niño event.

The recent fishing mortality is slightly above the MSY level, however the current spawning biomass is estimated to be above that level. The stock assessment report notes that recent biomass of fish aged 3 quarters and older is also higher than that corresponding to the MSY level, because of the large recent recruitments. The catches are predicted to increase in the near future. However, these interpretations are uncertain, and highly sensitive to the assumptions made about the steepness parameter of the stock-recruitment relationship, the average size of the oldest fish, and the assumed levels of natural mortality.

Bigeye tuna

Spawning stock biomass: This index shows modeled spawning stock biomass of bigeye tuna from the 2017 stock assessment report, which was completed through the Inter-American Tropical Tuna Commission (IATTC), using Stock Synthesis V3. The assessment assumes that there is one stock of bigeye in the eastern Pacific. However, the assessment report acknowledges that recent tagging research

suggests that bigeye undertake extensive longitudinal movements, which may be at odds with this assumption. Indices were provided by C. Minte-Vera (IATTC).

Recruitment: Estimates of recruitment are derived from the assessment model.

Implications: The results of the 2018 stock assessment of bigeye tuna in the eastern Pacific Ocean using the same methodology as in previous years revealed several uncertainties which led assessment scientists to question its use as a basis for management advice. The 2018 assessment was therefore not accepted for use in management. Indices from the 2017 assessment are therefore shown here, and will be updated when the uncertainties in the stock assessment have been resolved.

The 2017 biomass indices showed that the stock biomass ratio (compared to estimated unfished biomass) declined to a historically low level of 0.16 in 2013. This may have been partially due to below-average recruitment in 2007 – 2008, coincident with strong La Nina events. Spawning biomass may have increased in recent years, indicated by increases in CPUE of adult fish on pelagic longlines. These trends may be a result of strong recruitment in 2012. The 2017 base-case stock assessment model suggested that the stock was not overfished, or undergoing overfishing, but there is high uncertainty associated with these results. There is some suggestion that recruitment may be higher during El Nino events, thus environmental variability may influence stock productivity in this species.

Skipjack tuna

Relative biomass: Skipjack tuna are assumed to comprise one contiguous stock throughout the Pacific ocean. In the eastern Pacific, they are primarily fished in tropical waters, using purse seine gear. Skipjack are difficult to assess with standard stock assessment methods, due to high and variable productivity, and uncertainties in natural mortality and growth. This species is thus assessed using a simple model which generates indicators of biomass, recruitment and exploitation rate, and compares these to historically observed values (Maunder & Deriso 2007). The stock assessment is completed through the Inter-American Tropical Tuna Commission (IATTC). The relative biomass index shown is from the 2017 update assessment, including data up to 2016. Indices were provided by M. Maunder (IATTC).

Recruitment: Estimates of recruitment are derived from the assessment model.

Implications: The relative biomass and recruitment indices have been increasing since the mid-2000s, and appear to have been above average in recent years. While no traditional reference points are available for skipjack in the north Pacific, results suggest that the stock is likely not overfished, and overfishing is likely not occurring. The fishery for skipjack tuna in the eastern Pacific is constrained by effort restrictions implemented for the conservation of bigeye tuna. As skipjack tuna are much more productive than bigeye, there was found to be no evidence for concern about the status of the skipjack stock. Biological data suggest that abundance of larval skipjack tends to increase with water temperature, at least up to ~29°C. However, catches of adults by surface gears tend to be reduced during warmer periods (such as El Nino), as fish spend less time near the surface, possibly due to deepening thermoclines. Environmentally variability may therefore influence stock productivity and availability to fisheries.

Appendix J SEABIRD DENSITY AND MORTALITY

J.1 SEABIRD AT-SEA DENSITIES

Sooty shearwaters migrate from the southern hemisphere in spring and summer to prey on small fish and squid on the shelf and near the shelf break. Common murres and Cassin's auklets are resident, colony-forming species that feed over the shelf; Cassin's auklets mostly prey on zooplankton, while common murres target small fish and squid.

At-sea densities of these three seabirds in the northern, central and southern CCE (NCC, CCC and SCC respectively) are discussed in the main report. Figure 4.7.1 shows the trends in a quad plot. In Figure J.1.1 we replot the trends in standard time-series figures for more complete reference.

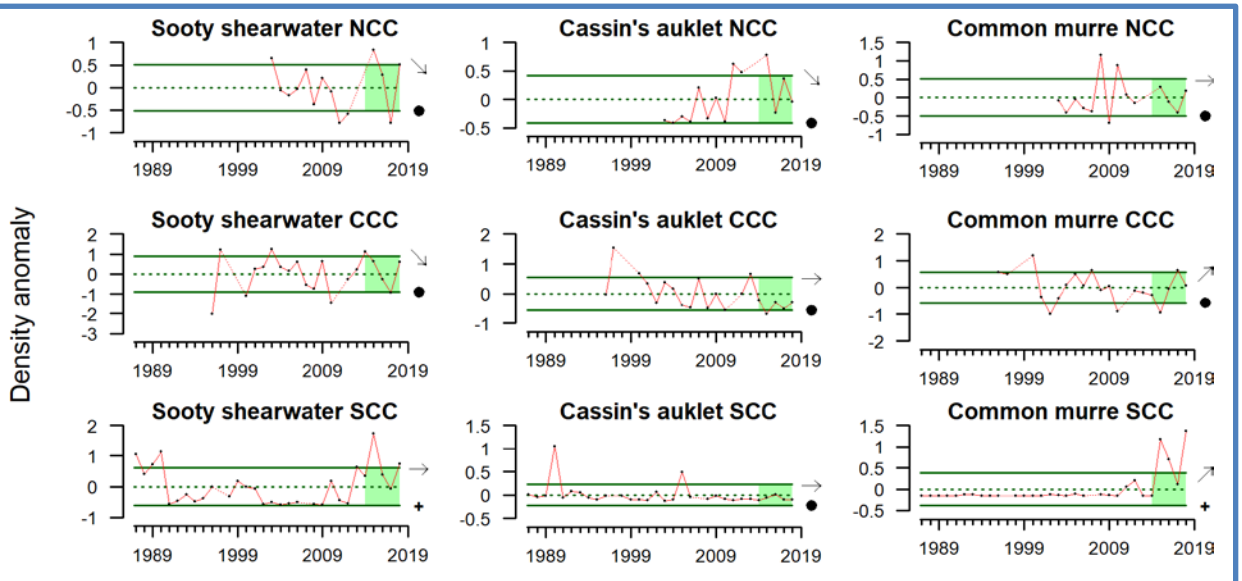

Figure J.1.1 Recent (5-year) trend and average of seabird at-sea densities during the spring in the California Current in three regions through 2018. Lines, colors, and symbols are as in Fig.1.

J.2 SEABIRD MORTALITY

The Coastal Observation and Seabird Survey Team (COASST) documented average to below-average numbers of beached birds for four indicator species in their most recent data (Figure J.2.1). The encounter rate of Cassin's auklet in the fall/winter of 2017–18 remained near baseline levels, where it has been since the large die-off in 2014. The encounter rate of sooty shearwaters in 2018 was low relative to the long-term mean and has had no significant short-term trend since a spike in mortality in 2011–13. The encounter rate of northern fulmars in fall/winter 2017–18 was below the long-term mean, with no significant short-term trend. The encounter rate of common murres in 2018 was unavailable as this report went to press.

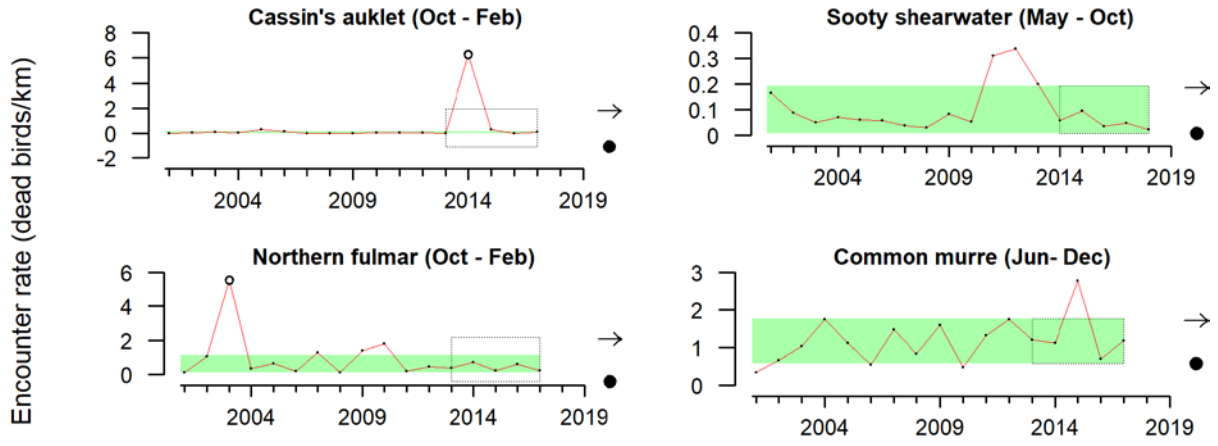

Figure J.2.1 Encounter rate of dead birds on west coast beaches through 2018. The mean and trend of the last five years is evaluated versus the mean and s.d. of the full time series but with the outliers removed. Open circles indicate outliers. The green box indicates the upper and lower s.d. of the full time series with outliers removed. Dotted lines indicate the evaluation period and the upper an lower s.d. of the full time series with the outliers included. Note variability was low for Cassin's auklet and the s.d. range is very small. Data provided by the Coastal Observation and Seabird Survey Team (https://depts.washington.edu/coasst/).

Appendix K STATE-BY-STATE FISHERY LANDINGS AND REVENUES

State-by-state landings and revenues from fisheries are presented here. Data come from the Pacific Fisheries Information Network (PacFIN, http://pacfin.psmfc.org) for commercial landings and by the Recreational Fisheries Information Network (RecFIN, http://www.recfin.org) for recreational landings. Landings provide the best long-term indicator of fisheries removals. Revenue was calculated based on consumer price indices for 2016.

K.1 STATE-BY-STATE LANDINGS

Total landings in California decreased to historically low levels in recent years, primarily due to steep decreases in landings of market squid in 2015 and 2016 (Figure K.1.1). Commercial landings of shrimp and salmon also decreased over the last five years, and landings of CPS were consistently below average from 2013-2017. Groundfish, hake, HMS and Other species were relatively unchanged. Crab landings varied around historical averages over the last 5 years. Methods for sampling and calculating total mortality in recreational fisheries changed recently, leading to shorter comparable time series than shown in previous reports. Recreational landings in California (excluding salmon and Pacific halibut) increased from 2008 to 2015, but a 70-80% decrease in yellowfin tuna and yellowtail landings in 2016 brought recreational landings within historical averages over the last 5 years (Figure K.1.1). Recreational salmon landings were relatively unchanged and near the lower bounds of the long-term average.

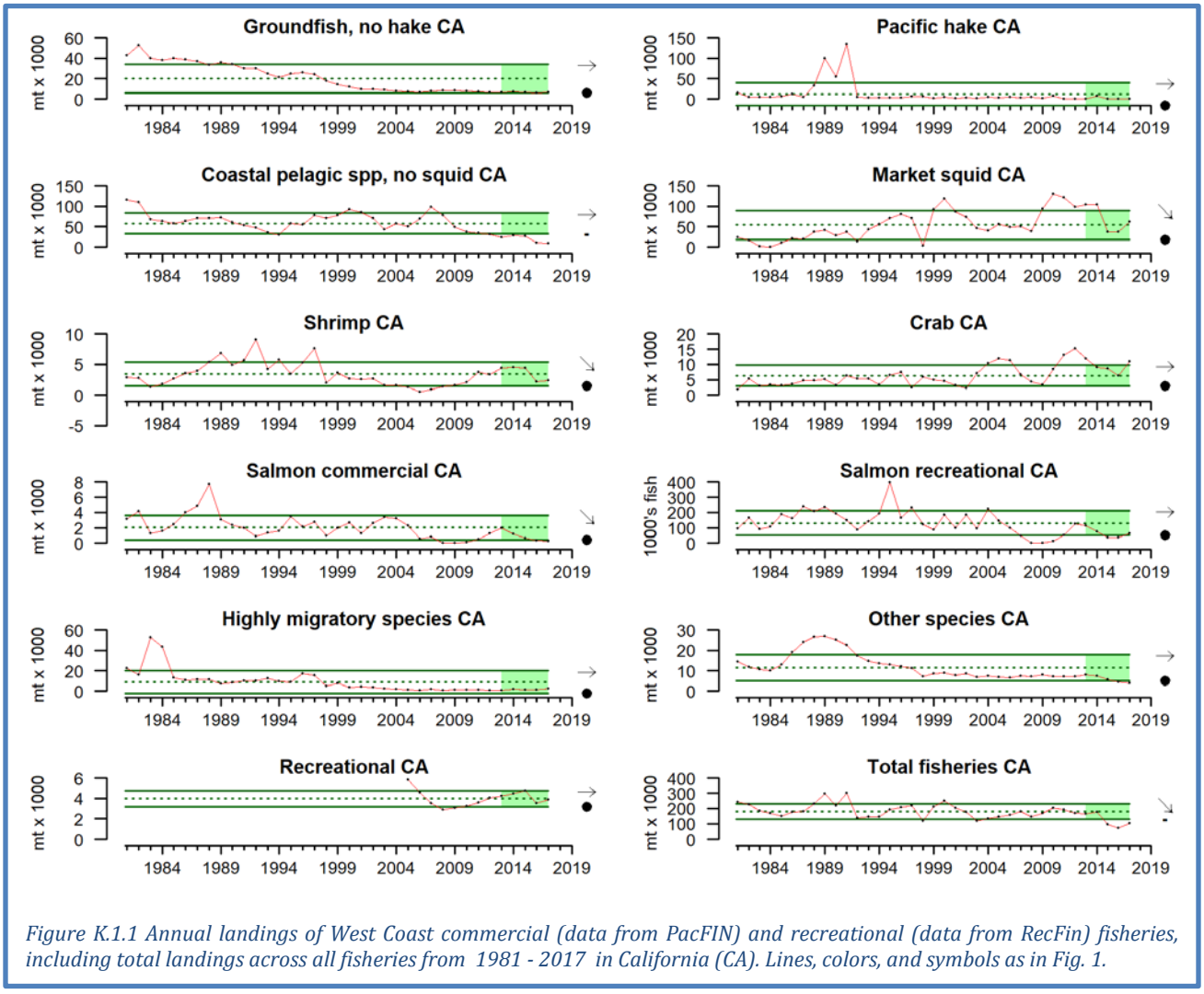

Figure K.1.1 Annual landings of West Coast commercial (data from PacFIN) and recreational (data from RecFin) fisheries, including total landings across all fisheries from 1981 - 2017 in California (CA). Lines, colors, and symbols as in Fig. 1.

Total fisheries landings in Oregon have varied but were above historical levels from 2013-2017. (Figure K.1.2). These patterns were primarily driven by historically high landings of hake over the last 5 years. Commercial landings of other groundfish, crab, salmon and Other species showed no trends and within historical averages from 2013-2017. CPS (excluding squid), shrimp and HMS landings all decreased over the last 5 years in Oregon, although recent average shrimp landings were still historically high due to high landings from 2013 to 2015. Landings of market squid have been at or near 0 across the time series, but landings over 1200 tons in 2016 caused this indicator to show an increasing recent trend.

Methods for sampling and calculating total mortality in recreational fisheries changed recently, leading to shorter comparable time series than shown in previous reports. Recreational fisheries landings (excluding salmon and Pacific halibut) in Oregon showed a decreasing trend from 2013-2017 relative to the long-term average (Figure K.1.2). Salmon recreational landings showed no recent trends and were within, but near the lower limits of, the historical range over the last 5 years.

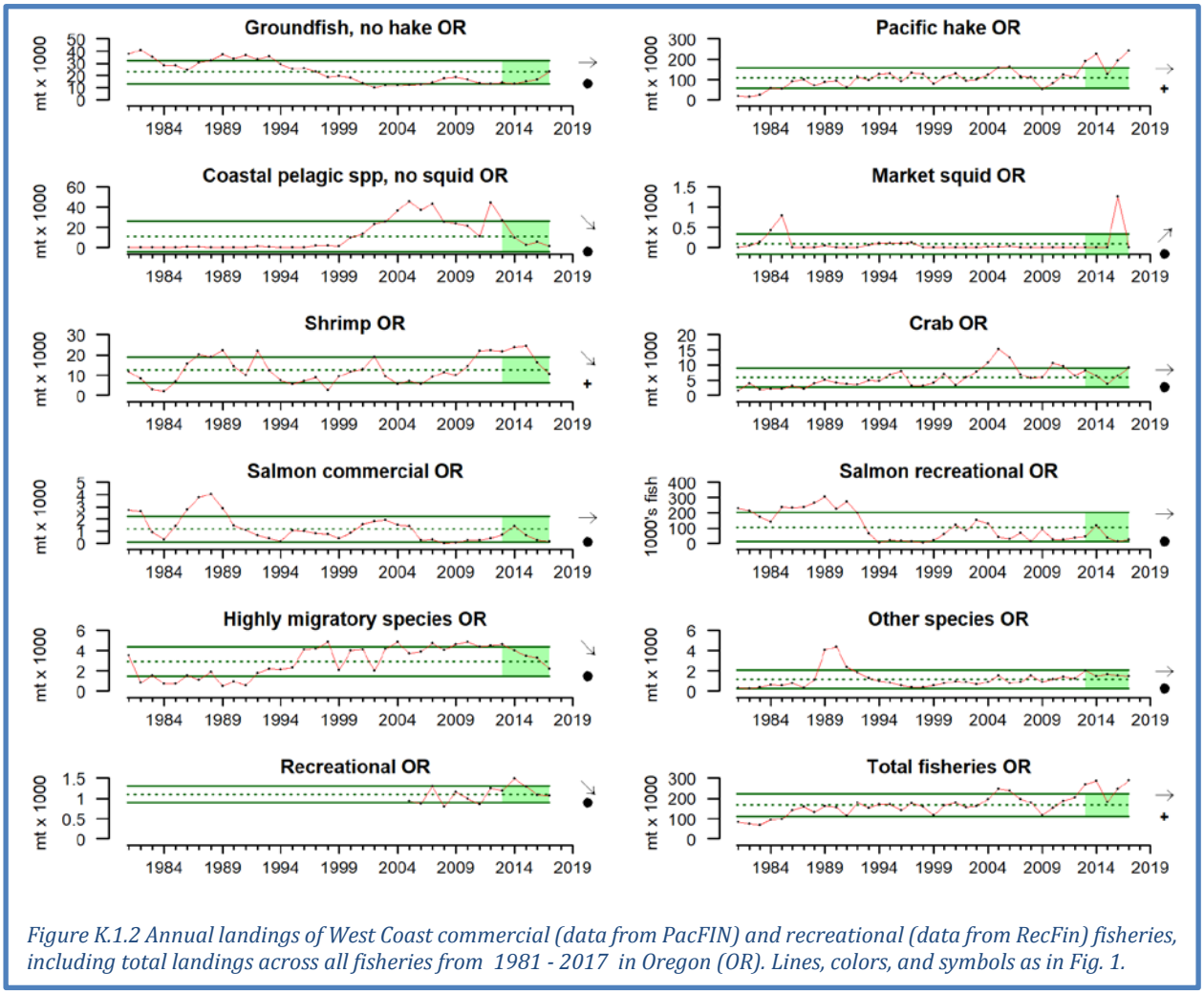

Figure K.1.2 Annual landings of West Coast commercial (data from PacFIN) and recreational (data from RecFin) fisheries, including total landings across all fisheries from 1981 - 2017 in Oregon (OR). Lines, colors, and symbols as in Fig. 1.

Total fisheries landings in Washington were highly variable from 2013-2017, with particularly low landings in 2015 and a large increase in 2017 (Figure K.1.3). These patterns were driven primarily by large increases in hake landings from 2015 to 2017 and large decreases in the landings of CPS (excluding squid), shrimp and commercial salmon over the same period. Landings of groundfish (excluding hake) were consistently below historical averages from 2013-2017, while landings of crab, Other species and HMS showed no current trends and were within 1 s.d. of historical averages over the last 5 years.

Methods for sampling and calculating total mortality in recreational fisheries changed recently, leading to shorter comparable time series than shown in previous reports. Total landings of recreational catch (excluding salmon and halibut) in Washington state decreased, but remained within 1 s.d. of the average from 2013-2017 (Figure K.1.3). Recreational salmon landings showed no trends and were within 1 s.d. of the average over the last 5 years; however, recreational salmon landings have been close to 1 s.d. below average for the past 2 years of available data.

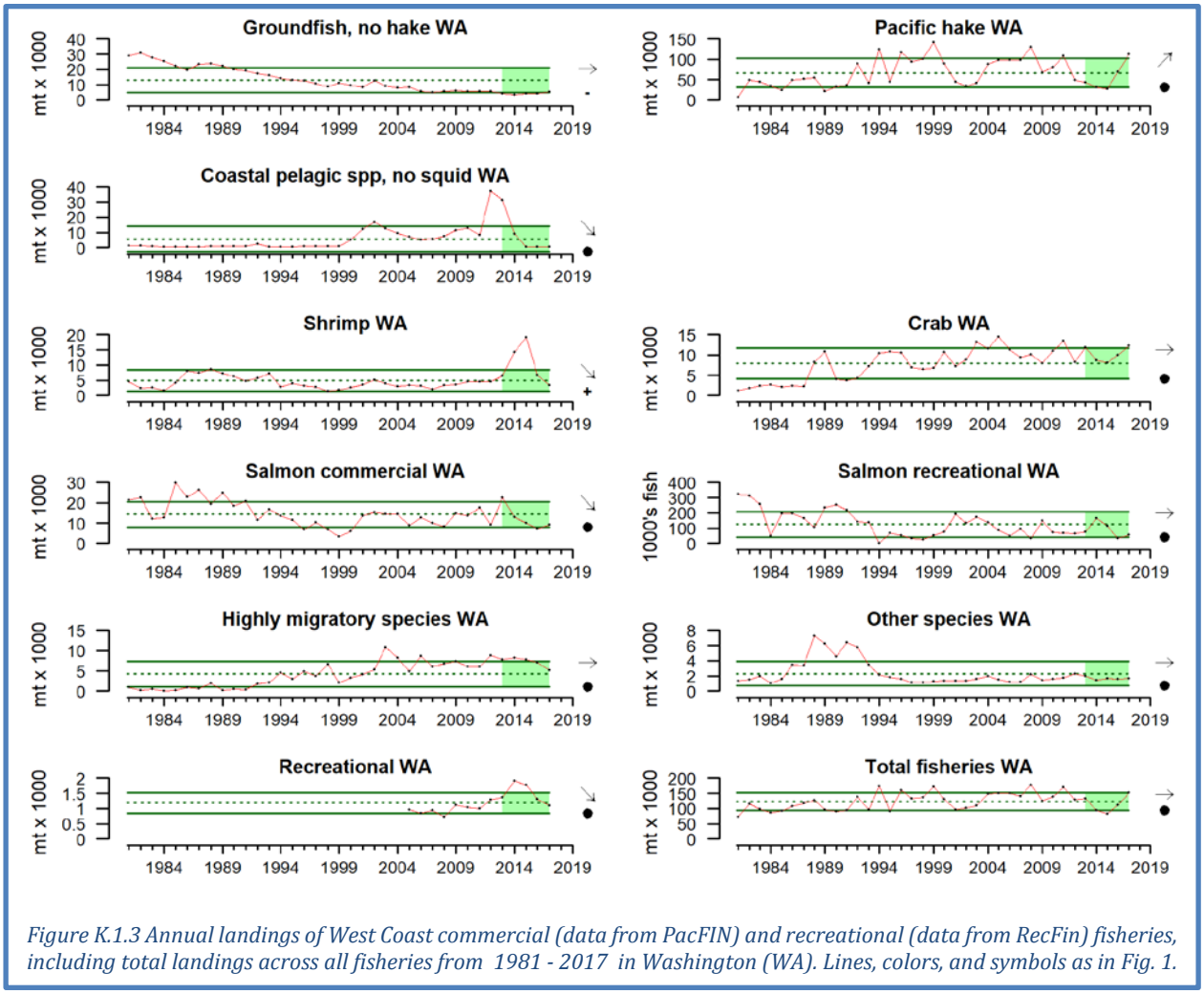

Figure K.1.3 Annual landings of West Coast commercial (data from PacFIN) and recreational (data from RecFin) fisheries, including total landings across all fisheries from 1981 - 2017 in Washington (WA). Lines, colors, and symbols as in Fig. 1.

K.2 COMMERCIAL FISHERY REVENUES

Total revenue across US West Coast commercial fisheries has varied near upper historical averages from 2013–2017 (Figure K.2.1). This pattern was driven primarily by interactions between historically high revenue from Pacific hake, market squid and crab fisheries and historically low and decreasing revenue in the CPS fisheries over the last 5 years. Revenue of groundfish (excluding hake) showed gradual increases that brought the fishery back to within 1 s.d. of the long-term average from 2013-2017. Shrimp fishery revenue varied over the last 5 years, with an average within 1 s.d. of the long-term average and no clear trend. Revenues from commercial salmon, HMS and Other species were relatively unchanged and within 1 s.d. of long-term averages over the last 5 years.

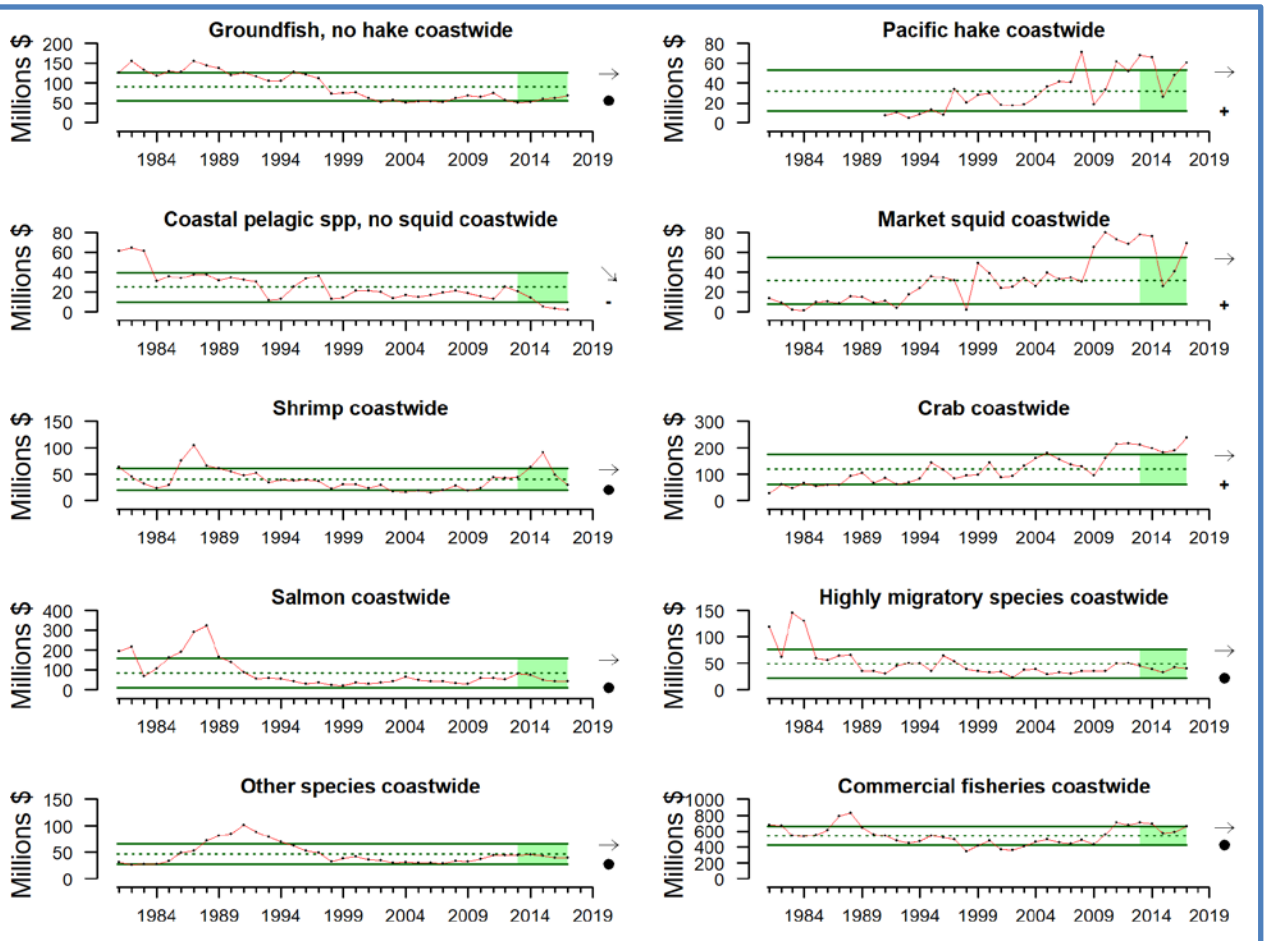

Figure K.2.1 Annual revenue (Ex-vessel value in 2015 dollars) of West Coast commercial fisheries (data from PacFin) from 1981-2017. Pacific hake revenue includes shore-side and at-sea hake revenue values from PacFIN, NORPAC (North Pacific Groundfish Observer Program) and NMFS Office of Science & Technology. Lines, colors, and symbols are as in Fig.1.

Total revenue across commercial fisheries in California varied from 2013–2017 (Figure K.2.2). This pattern was primarily driven by changes in market squid and crab revenue, which were >1 s.d. above long-term averages but experienced drops and rebounds from 2015 to 2017. Revenue from CPS fisheries were >1 s.d. below historical averages over the last 5 years. There were no fisheries that had increasing trends for revenue over the last 5 years, however revenue from Pacific hake and commercial salmon decreased from 2013-2017. Revenue of groundfish (excluding hake) and HMS remained consistently near historically low levels over the last 5 years, while revenue from shrimp and Other species showed no consistent trends and varied within 1 s.d. of long-term averages over the last 5 years.

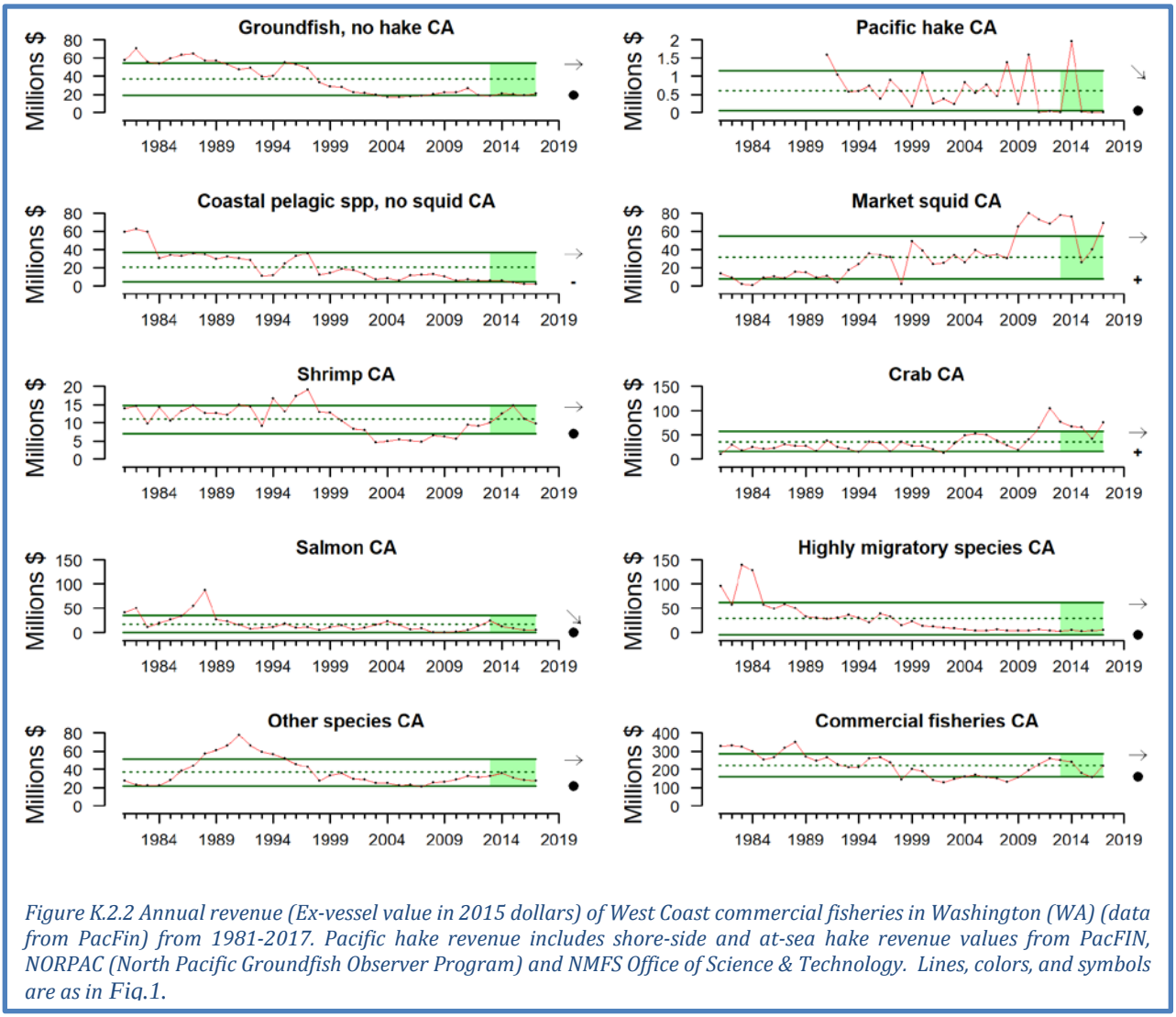

Figure K.2.2 Annual revenue (Ex-vessel value in 2015 dollars) of West Coast commercial fisheries in Washington (WA) (data from PacFin) from 1981-2017. Pacific hake revenue includes shore-side and at-sea hake revenue values from PacFIN, NORPAC (North Pacific Groundfish Observer Program) and NMFS Office of Science & Technology. Lines, colors, and symbols are as in Fig.1.

Total revenue across commercial fisheries in Oregon was at historically high annual averages from 2013–2017 (Figure K.2.3). This was driven by higher than average revenues for Pacific hake and crab, along with increases in revenue from groundfish fisheries. CPS fishery revenue declined over the last 5 years. Market squid showed an abnormally large and apparently short-lived increase in revenue in 2016 that may be related to the unusual oceanographic conditions of the marine heat wave and major El Niño. With increasing variation in oceanographic conditions, this pattern should be monitored for potential changes in the distribution of market squid revenue among west coast states. All other fisheries showed no trends and were within 1 s.d. of long-term averages in revenue over the last 5 years.

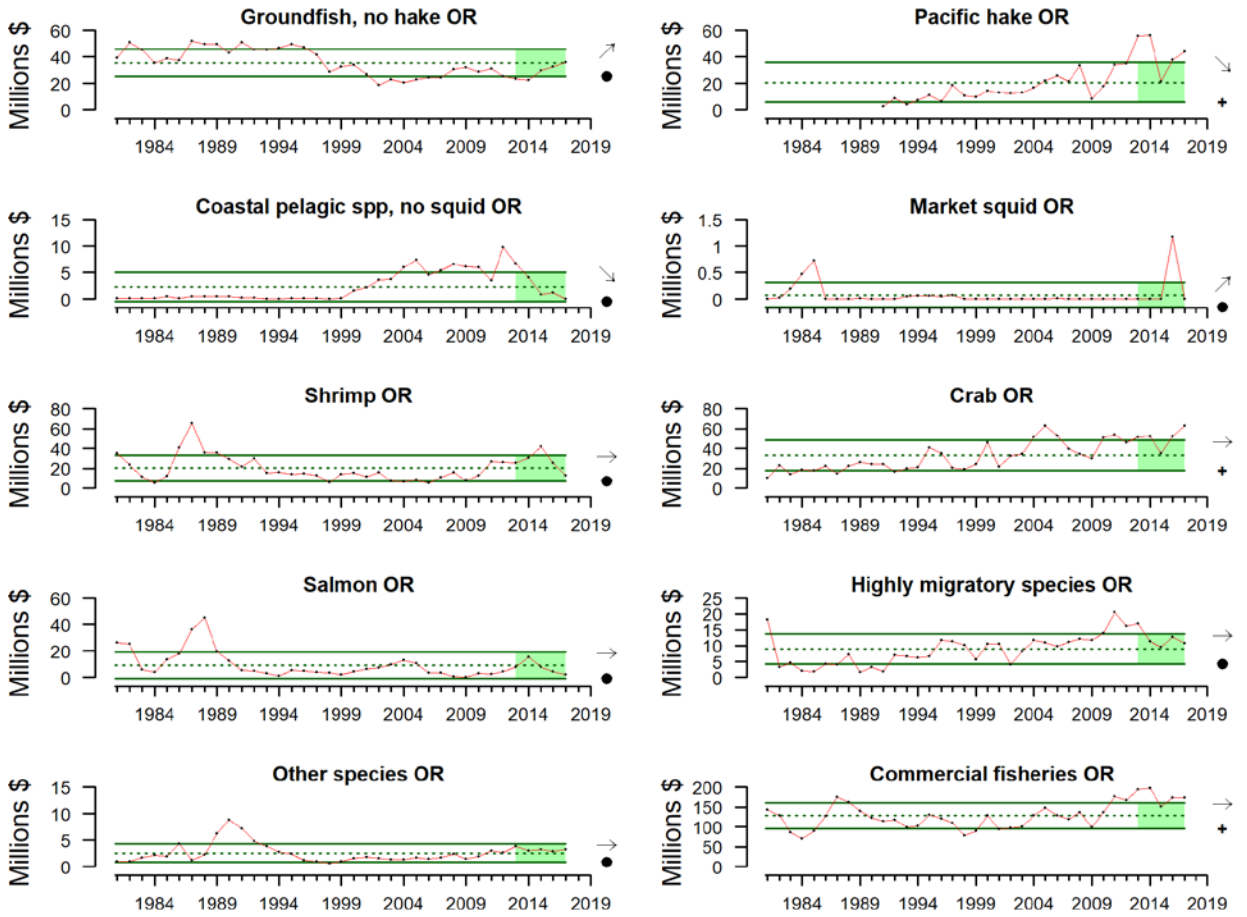

Figure K.2.3 Annual revenue (Ex-vessel value in 2015 dollars) of West Coast commercial fisheries in Oregon (OR) (data from PacFin) from 1981-2017. Pacific hake revenue includes shore-side and at-sea hake revenue values from PacFIN, NORPAC (North Pacific Groundfish Observer Program) and NMFS Office of Science & Technology. Lines, colors, and symbols are as in Fig.1.

Total revenue across commercial fisheries in Washington remained relatively unchanged and above the long-term average from 2013–2017 (Figure K.2.4). This was a similar pattern to that observed in Oregon over the same time period (Figure K.2.3). This pattern in Washington is primarily driven by the relatively consistent and above-average levels of revenue for crab and HMS and the peak in revenue in the shrimp fisheries observed in 2015. Revenue for CPS fisheries decreased from 2013-2017, while all other fisheries showed no recent trends in revenue. Revenue of groundfish (excluding hake) remained consistently below historic averages from 2013-2017, while revenue from Pacific hake, salmon and Other species showed no significant trends and were within 1 s.d. of long-term averages over the last 5 years.

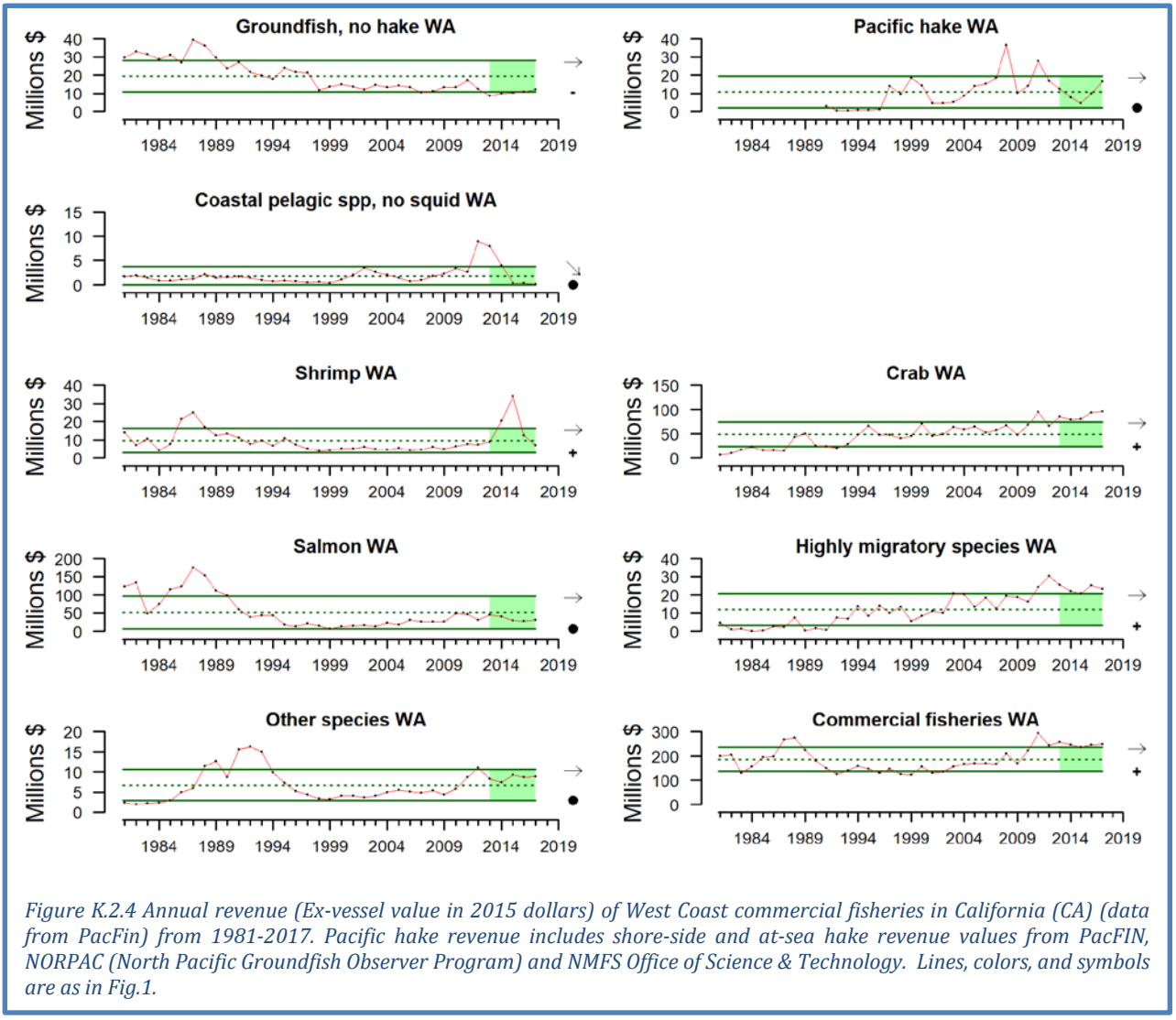

Figure K.2.4 Annual revenue (Ex-vessel value in 2015 dollars) of West Coast commercial fisheries in California (CA) (data from PacFin) from 1981-2017. Pacific hake revenue includes shore-side and at-sea hake revenue values from PacFIN, NORPAC (North Pacific Groundfish Observer Program) and NMFS Office of Science & Technology. Lines, colors, and symbols are as in Fig.1.

Appendix L FISHING GEAR CONTACT WITH SEAFLOOR HABITAT

In Section 5.2 of the report, we presented a spatial representation of the status and trends of gear contact with the seafloor as a function of distances trawled. We used estimates of coastwide distances exposed to bottom trawl fishing gear along the ocean bottom from 1999–2016. We calculated trawling distances based on set and haul-back locations. We weighted distances by fishing habitat according to sensitivity values described in Table A3a.2 of the 2013 Groundfish EFH Synthesis Report to PFMC. Data come from logbooks analyzed by the Northwest Fisheries Science Center's West Coast Groundfish Observer Program. Here, we present time series of the data at a coastwide scale and broken out by ecoregion (Northern, north of Cape Mendocino; Central, Cape Mendocino to Point Conception; and Southern, south of Point Conception), substrate type (hard, mixed, soft) and depth zone (shelf, upper slope, lower slope).

At the scale of the entire coast, bottom trawl gear contact with seafloor habitat remained consistently at historically low levels from 2012–2016 (Figure L.1, top). During this period, the vast majority of bottom trawl gear contact occurred in soft upper slope and soft shelf habitats (Figure L.1, bottom). The Northern ecoregion also has seen the most bottom trawl fishing gear contact with seafloor habitat with nearly four times the magnitude as observed in the central ecoregion. Very little to no bottom trawling has occurred in the Southern ecoregion within the time series. A shift in trawling effort from shelf to upper slope habitats was observed during the mid-2000's, which in part corresponded to depth-related spatial closures implemented by the Council. With new regulations beginning, this indicator will be of interest to monitor over the next few years for changes in bottom trawl fishing effort. Reduced bottom trawl gear contact may not coincide with recovery times of habitat depending on how fast recovery happens, which is likely to differ among habitat types (e.g., hard and mixed habitats will take longer to recover than soft habitat).

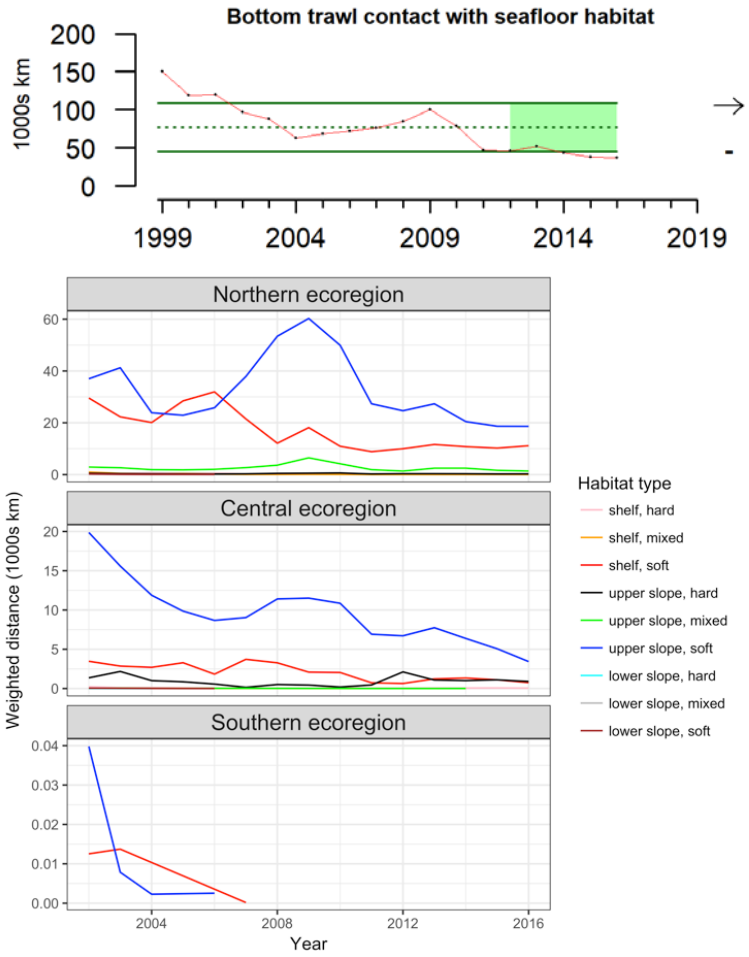

Figure L.1 Weighted distance (1000s km) of fishing gear contact with seafloor habitat across the entire CCE (top; 1999-2016) and within each ecoregion (bottom three panels; 2002-2016). Lines, colors and symbols in top panel are as in Fig. 1.

Appendix M SOCIAL VULNERABILITY OF FISHING-DEPENDENT COMMUNITIES

In Section 6.1 of the main report, we present information on the Community Social Vulnerability Index (CSVI) as an indicator of social vulnerability in coastal communities that are dependent upon commercial fishing. Fishery *dependence* can be expressed by two terms, or by a composite of both. Those terms are engagement and reliance. *Engagement* refers to the total extent of fishing activity in a community; engagement can be expressed in terms of commercial activity (e.g., landings, revenues, permits, processing, etc.) or recreational activity (e.g., number of boat launches, number of charter boat and fishing guide license holders, number of charter boat trips, number of bait and tackle shops, etc.). *Reliance* is the per capita engagement of a community; thus, in two communities with equal engagement, the community with the smaller population would have a higher reliance on its fisheries activities.

In the main body of the report, Figure 6.1.1 and Figure 6.1.2 plot CSVI in 2016 against commercial and recreational fishing reliance, respectively, for the five most dependent communities in each sector from each of five regions of the CCE. Here, we present similar plots of CSVI relative to commercial and recreational fishing engagement scores. We then compare communities based on their relative commercial:recreational fishing reliance and engagement.

Figure M.1 shows commercial fishing-engaged communities and their corresponding social vulnerability results. Communities above and to the right of the dashed lines are at least 1 s.d. above the coastwide averages of both indices. Of note are communities like Westport, Crescent City, and Port Orford, which have relatively high commercial fishing engagement results and also a high CSVI composite result.

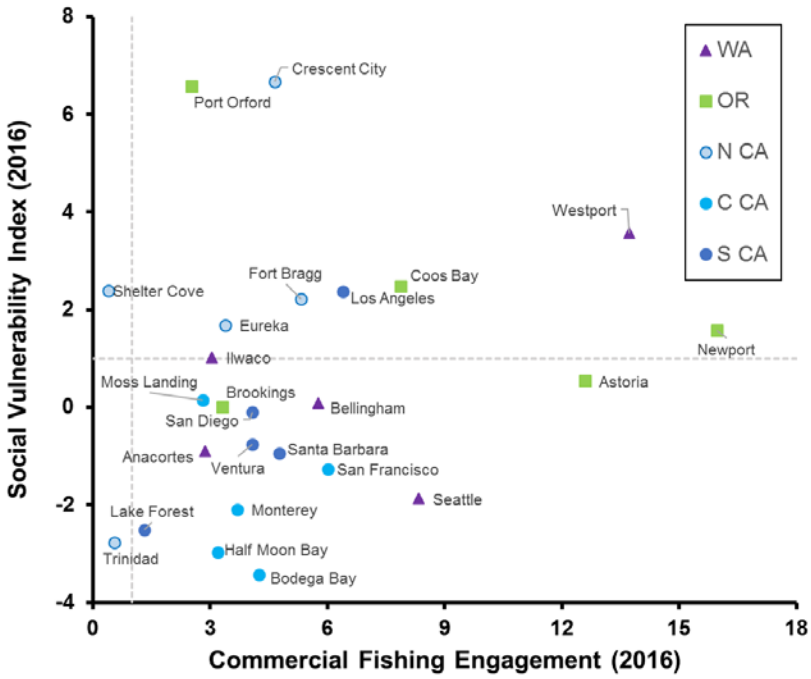

Figure M.1 Commercial fishing engagement and social vulnerability scores plotted for twenty-five communities from each of the 5 regions of the California Current: WA, OR, Northern, Central, and Southern California. The top five highest scoring communities for fishing engagement were selected from each region.

Figure M.2 shows recreational fishing-engaged communities with their corresponding social vulnerability results. Of note are communities like Los Angeles and Westport, which have relatively high recreational fishing reliance results and also high CSVI composite results. In contrast, San Diego has very high recreational fishing engagement, but relatively low social vulnerability. It is also notable that many (but not all) of the communities in Figures M.1 and M.2 are different from those in Figures 6.1.1 and 6.1.2, because these are total community engagement plots, not per capita reliance plots.

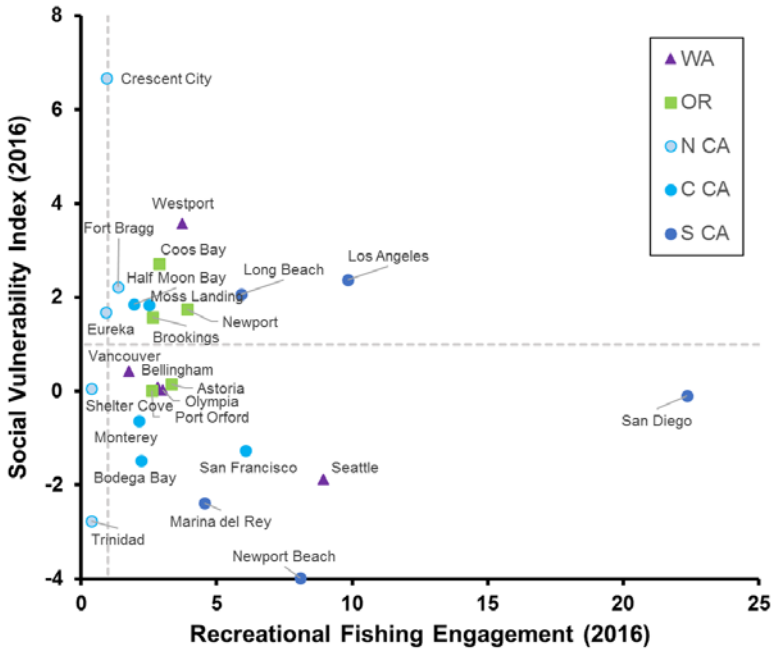

Figure M.2 Recreational fishing engagement and social vulnerability scores plotted for twenty-five communities from each of the 5 regions of the California Current: WA, OR, Northern, Central, and Southern California. The top five highest scoring communities for fishing engagement were selected from each region.

Figures Figure M.3 and M.4 are intended to show that some communities are more dependent upon one sector (commercial or recreational) than the other, while also accounting for CSVI. Figure M.3 plots each community's recreational fishing engagement level against its commercial fishing engagement. The size of the plot point for each community is scaled to approximate the level of social vulnerability for each community. All of the communities from Figures 6.1.1., 6.1.2, Figure M.3 and M.4 are included here; it is thus possible for regions to have more than five communities in these plots. San Diego demonstrates a disproportionately high level of engagement in recreational fishing relative to commercial fishing engagement, while Westport, Newport, and Astoria demonstrate a similarly high level of engagement with commercial fishing relative to recreational engagement.

Similarly, Figure M.4 plots each community's results for recreational fishing reliance against each community's results for commercial fishing reliance. Of particular note are the communities of Westport, Winchester Bay and Ilwaco, which exhibit relatively high levels of commercial fishing reliance, recreational fishing reliance and general social vulnerability. Moss Landing and Elkton both present relatively high social vulnerability, and appear as examples of communities that are both outliers in terms of their degrees of reliance on commercial fishing (Moss Landing) and recreational fishing (Elkton).

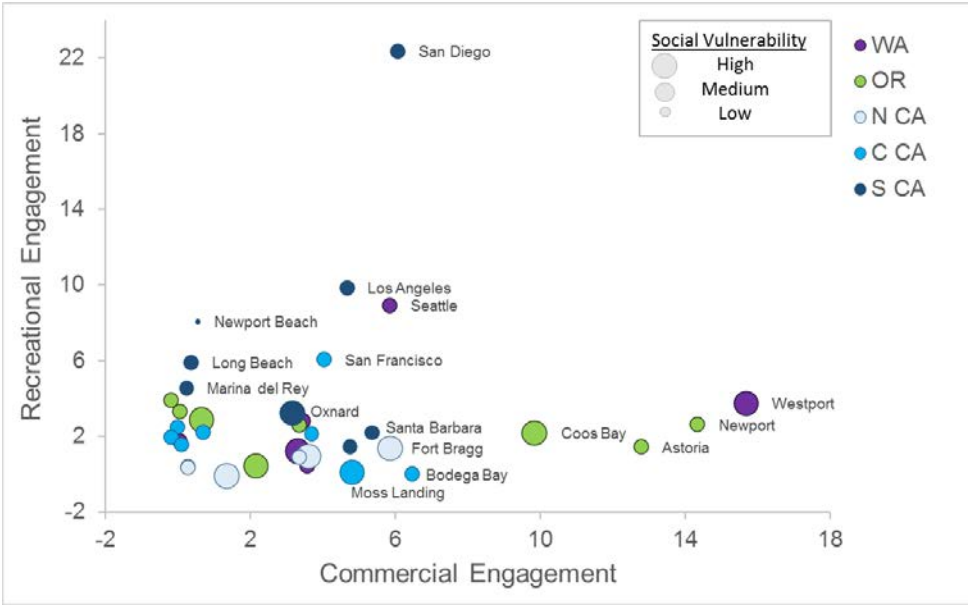

Figure M.3 Communities with the top five highest scores for commercial fishing and recreational fishing engagement from each of the five regions of the California Current are plotted. Bubble size indicates a high, moderate, or low social vulnerability score.

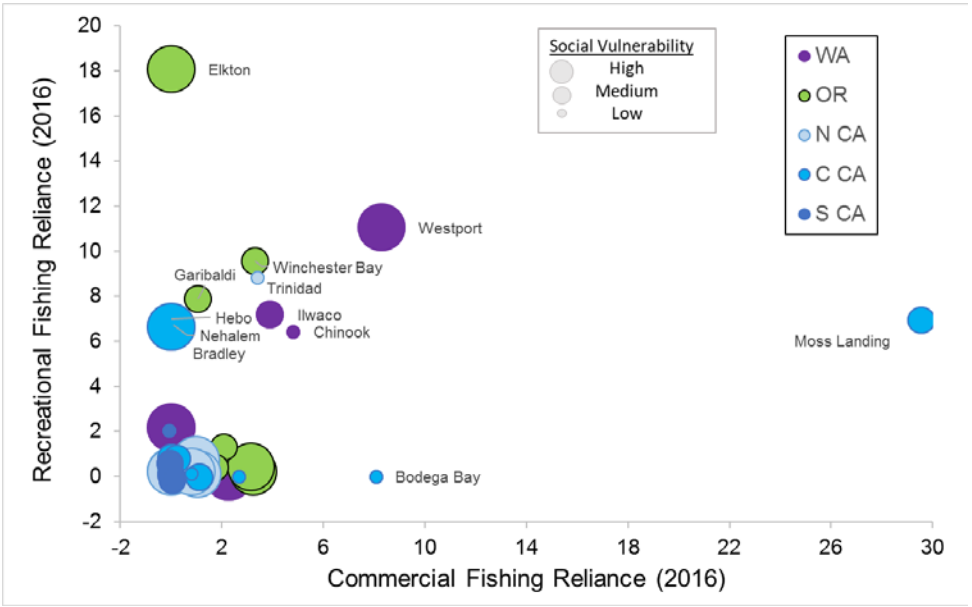

Figure M.4 Communities with the top five highest scores for commercial fishing and recreational fishing reliance from each of the five regions of the California Current are plotted. Bubble size indicates a high, moderate, or low social vulnerability score.

Appendix N FLEET DIVERSIFICATION INDICATORS FOR MAJOR WEST COAST PORTS

Catches and prices from many fisheries exhibit high inter-annual variability leading to high variability in fishermen's revenue, but variability can be reduced by diversifying fishing activities across multiple fisheries or regions (Kasperski and Holland 2013). We use the effective Shannon index (ESI) to measure fishing vessel diversification. ESI increases as revenues are spread across *more* fisheries, and as revenues are spread more *evenly* across fisheries; ESI = 1 when a vessel's revenues are from a single species group and region; ESI = 2 if revenues are spread evenly across 2 fisheries; and so on. If revenue is not evenly distributed across fisheries, then the ESI value is lower than the number of fisheries a vessel enters.

As is true with individual vessels, the variability of landed value at the port level is reduced with greater diversification of landings. Diversification of fishing revenue has declined over the last several decades for some ports (Figure N.1). Examples include Seattle and most, though not all, of the ports in Southern Oregon and California. However, a few ports have become more diversified, such as Bellingham Bay. Diversification scores are highly variable year-to-year for some ports, particularly those in Southern Oregon and Northern California that depend heavily on the Dungeness crab fishery, which has highly variable landings. Many major ports saw a decrease in diversification between 2016 and 2017, but others saw an increase. No clear recent trends are apparent.

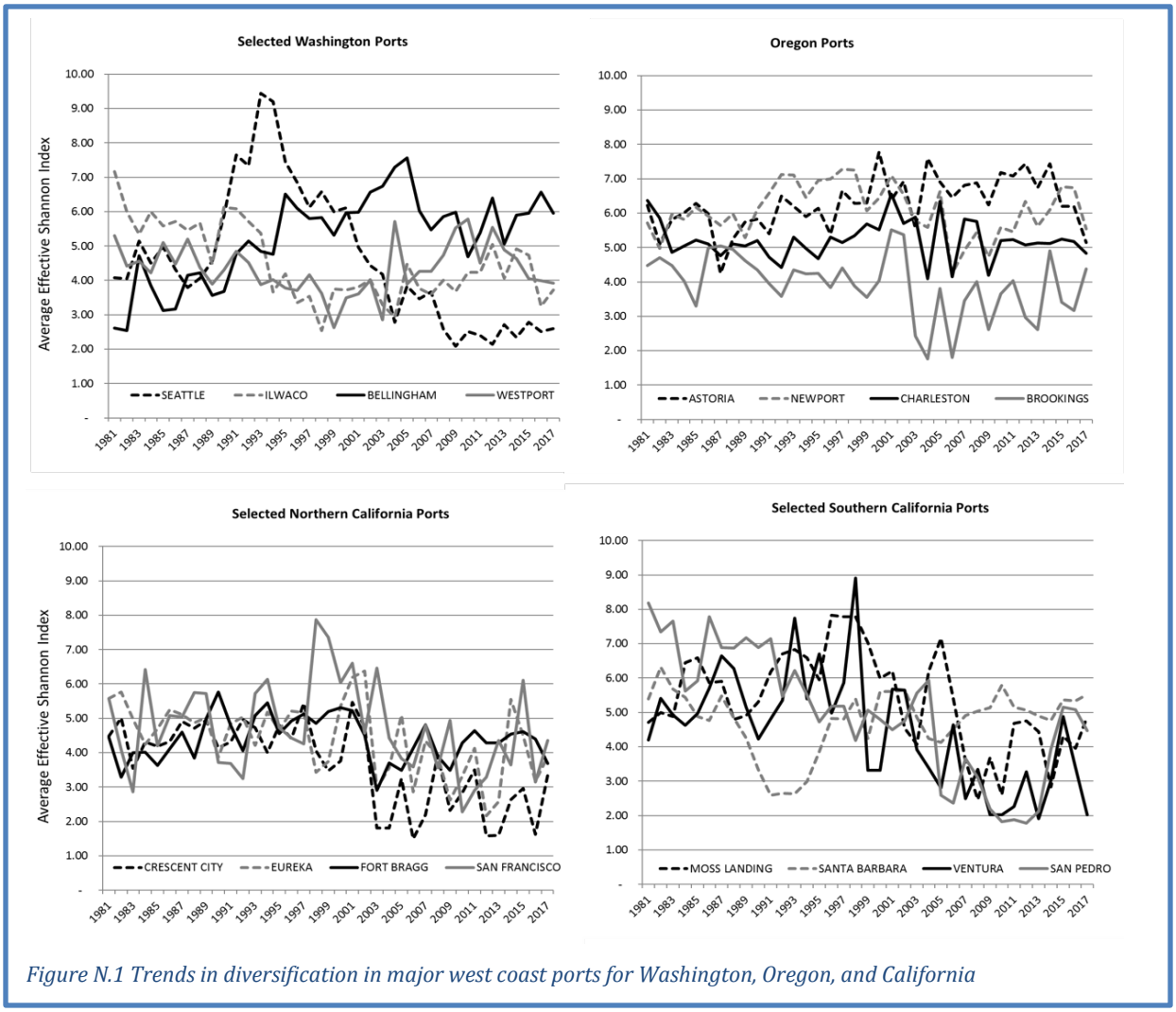

Figure N.1 Trends in diversification in major west coast ports for Washington, Oregon, and California

Appendix O METHODS FOR ESTIMATING GROUNDFISH STOCK AVAILABILITY TO WEST COAST FISHING PORTS

In section 6.3, we introduced an analysis describing shifts in availability of petrale sole and sablefish to the ports of Astoria, Coos Bay, Fort Bragg, and Morro Bay, as a function of changing stock abundance (derived from stock assessments) and spatial distribution (derived from VAST analysis of fishery-independent groundfish survey data).

We estimated stock biomass *b(s,t)* for each species at each location within the spatial sampling domain of the NWFSC West Coast Groundfish Bottom Trawl Survey and any year t from 1977-2017. To do so, we combined two sources of information:

1. Stock assessment estimate of total population biomass *B(t)*, developed based on many different data sources. The estimates account for age- and length-based selectivity and catchability within available survey data. By doing so, the assessment also estimates the proportion of total abundance that is not vulnerable to a given survey gear.

2. Spatio-temporal estimates of biomass-density *d(s,t)* at each location, where each location is associated with area *a(s)* within the sampling domain. These estimates are obtained from available survey data from two different survey sampling designs: the triennial bottom trawl survey (operating 1977-2004) and the annual bottom trawl survey (operating 2003-present). Spatio-temporal analysis (VAST; reviewed by the SSC-ES in September 2018) allows us to estimate the spatial distribution of biomass vulnerable to each sampling gear.

These two data sources predict total biomass (biomass both vulnerable and invulnerable to the trawl survey) at each location using the following equation:

$$b(s,t) = B(t)\frac{a(s)d(s,t)}{\sum_{s=1}^{n} a(s)d(s,t)}$$

Estimates of biomass density *d(s,t)* (in units kg/km^2) associated with each spatial location *s* were multiplied by the area *a(s)* associated with each location (km^2) to generate a location-specific biomass estimate (in units kg). Relative biomass in each location was calculated by dividing the area-level biomass (kg) by the region-wide biomass (kg). Total stock biomass (mt) associated with each location *b(s,t)* was computed by multiplying the relative biomass in each location by the total stock-level spawning biomass (mt).

This calculation implicitly assumes that the ratio of vulnerable and invulnerable biomass is constant across space within each year. Future research could develop a spatio-temporal assessment model to estimate spatial variation in catchability, but the current effort is the first to correct estimates of spatial distribution from a spatio-temporal model to account for vulnerability estimates from a stock assessment model (arising from the net effect of catchability and selectivity-at-age estimates).

An index of port-specific stock availability for each species *A(p,t)* was created from the log of the average stock biomass (metrics tons) weighted by the inverse distance (*D*) of the location to a port (km):

$$A_{p,t} = \sum_{s=1}^{n} b(s,t)\frac{1}{D(s,p)}$$

Appendix P REFERENCES

Abell, R., *et al.* 2008. Freshwater ecoregions of the world: A new map of biogeographic units for freshwater biodiversity conservation. *BioScience* 58:403-414.

Bond, N. A., *et al.* 2015. Causes and impacts of the 2014 warm anomaly in the NE Pacific. *Geophysical Research Letters* 42:3414-3420.

Brodeur, R., *et al.* 2018. An unusual gelatinous plankton event in the NE Pacific: the great pyrosome bloom of 2017. *PICES Press* 26:22-27.

Burke, B. J., *et al.* 2013. Multivariate models of adult Pacific salmon returns. *PLoS One* 8:e54134.

Chan, F., *et al.* 2008. Emergence of anoxia in the California current large marine ecosystem. *Science* 319:920-920.

Dyson, K., Huppert, D.D. 2010. Regional economic impacts of razor clam beach closures due to harmful algal blooms (HABs) on the Pacific coast of Washington. *Harmful Algae* 9: 264-271.

Feely, R. A., *et al.* 2008. Evidence for upwelling of corrosive "acidified" water onto the continental shelf. *Science* 320:1490-1492.

Fisher, J. L., *et al.* 2015. The impact of El Niño events on the pelagic food chain in the northern California Current. *Global Change Biology* 21:4401-4414.

Hickey, B.M., *et al.* 2013. A springtime source of toxic *Pseudo-nitzschia* on razor clam beaches in the Pacific Northwest. *Harmful Algae* 25;1-14.

Jacox, M. G., *et al.* 2016. Impacts of the 2015–16 El Niño on the California Current System: Early assessments and comparison to past events. *Geophysical Research Letters* 43:7072–7080.

Jacox, M. G., et al. 2018. Coastal upwelling revisited: Ekman, Bakun, and improved upwelling indices for the U.S. west coast. *Journal of Geophysical Research: Oceans* 123:7332-7350.

Jepson, M. and L. L. Colburn. 2013. Development of social indicators of fishing community vulnerability and resilience in the U.S. Southeast and Northeast Regions. NOAA Tech. Memo. NMFS-F/SPO-129.

Kaplan, I.C., *et al.* 2016. Cloudy with a chance of sardines: forecasting sardine distributions using regional climate models. *Fisheries Oceanography* 25:15-27.

Kasperski, S., and D. S. Holland. 2013. Income diversification and risk for fishermen. *Proceedings of the National Academy of Sciences of the United States of America* 110:2076-2081.

Keister, J. E., *et al.* 2011. Zooplankton species composition is linked to ocean transport in the Northern California Current. *Global Change Biology* 17:2498-2511.

Leising, A.W., in prep. Just how unusual was the large marine heatwave of 2014-2015: A retrospective analysis of SSTa across the NEP. For submission to *Journal of Geophysical Research: Oceans*.

Lindgren, F., and H. Rue. 2015. Bayesian spatial modelling with R-INLA. *Journal of Statistical Software* 63(19):1-25.

McCabe, R.M., *et al.* 2016. An unprecedented coastwide toxic algal bloom linked to anomalous ocean conditions. *Geophysical Research Letters* 43:10366-10376.

McKibben, M., *et al.* 2017. Climatic regulation of the neurotoxin domoic acid. *Proceedings of the National Academy of Sciences* 114:239-244.

Melin, S. R., *et al.* 2012. California sea lions: an indicator for integrated ecosystem assessment of the California Current system. *CalCOFI Reports* 53:140-152.

Peterson, W. T., *et al.* 2014. Applied fisheries oceanography ecosystem indicators of ocean condition inform fisheries management in the California Current. *Oceanography* 27:80-89.

Reynolds, R. W., *et al.* 2007. Daily high-resolution-blended analyses for sea surface temperature. *Journal of Climate* 20:5473–5496.

Siedlecki, S.A., *et al.* 2016. Experiments with seasonal forecasts of ocean conditions for the northern region of the California Current upwelling system. *Scientific Reports* 6:27203.

Thompson, A.R. *et al.* 2018. State of the California Current 2017-18: still not quite normal in the north and getting interesting in the south. *CalCOFI Reports* 59:1-66.

Trainer, V.L., *et al.* 2002. Biological and physical dynamics of domoic acid production off the Washington U.S.A. coast. *Limnology and Oceanography* 47:1438-1446.
Waples, R. S. 1995. Evolutionarily significant units and the conservation of biological diversity under the Endangered Species Act. *American Fisheries Science Symposium* 17:8-27.